SAND89-2270
Unlimited Release
Printed January, 1991

Estimates of Spatial Correlation in Volcanic Tuff Yucca Mountain, Nevada

C. A. Rautman
Geoscience Analysis Division
Sandia National Laboratories

ABSTRACT

The spatial correlation structure of volcanic tuffs at and near the site of the proposed high-level nuclear waste repository at Yucca Mountain, Nevada, is estimated using samples obtained from surface outcrops and drill holes. Data are examined for four rock properties: porosity, air permeability, saturated hydraulic conductivity, and dry bulk density. Spatial continuity patterns are identified in both lateral and vertical (stratigraphic) dimensions. The data are examined for the Calico Hills tuff stratigraphic unit and also without regard for stratigraphy.

Variogram models fitted to the sample data from the tuffs of Calico Hills indicate that porosity is correlated laterally over distances of up to 3,000 feet. Spatial continuity in the vertical (cross-stratigraphy) direction within the Calico Hills units is limited to approximately 200 feet. These distances imply a horizontal-to-vertical anisotropy ratio of roughly 15 to 1. If air permeability and saturated conductivity values are viewed as semi-interchangeable for purposes of identifying spatial structure, the data suggest a maximum range of correlation of 300 to 500 feet without any obvious horizontal to vertical anisotropy. Data for dry bulk density exist only for the vertical dimension. These results are similar to those for porosity. Continuity exists over vertical distances of roughly 200 feet. Similar variogram models fitted to sample data taken from vertical drill holes without regard for stratigraphy suggest that correlation exists over distances of 500 to 800 feet for each rock property examined.

Spatial correlation of rock properties violates the sample-independence assumptions of classical statistics to a degree not usually acknowledged. In effect, the existence of spatial structure reduces the "equivalent" number of samples below the number of physical samples. This reduction in the effective sampling density has important implications for site characterization for the Yucca Mountain Project.

The work described in this report was completed at Quality Assurance Level III and supports WBS Element 1.2.3.2.2.2.1.

DRAFT

Table of Contents

List of Figures

List of Tables

INTRODUCTION

The U. S. Department of Energy is considering construction of a geologic repository for high-level nuclear waste in volcanic tuffs at Yucca Mountain in southern Nevada. Designing the proposed repository and assessing the potential performance of such a facility for thousands of years into the future will require a thorough understanding of the site itself. This understanding is the goal of the site characterization process.

One of the objectives of site characterization is the measurement of physical rock properties at the site, and the modeling of these properties for use in engineering design and performance assessment studies. Because the number of locations at which the site may be sampled -- particularly at depth -- is limited, construction of rock properties models will involve interpolation of measured values. Numerous techniques exist for interpolation. If consideration is restricted to methods that are unbiased linear combinations of the available data, geostatistics provides an interpolation technique that provides minimum-variance estimates. The uncertainty associated with each estimate may be quantified as well. The essential concept of geostatistics is that the observed data are used to determine the spatial correlation structure of the variable of interest. This spatial correlation is quantified mathematically, and the mathematical representation is used to constrain the estimation of unsampled points.

This paper documents some preliminary work that attempts to determine approximately what spatial correlation structure might be expected at the Yucca Mountain site. Data are presented for several rock properties that may be representative of the suite of properties relevant to the overall site characterization and modeling efforts. The paper also discusses some of the implications of these results for site characterization.

GEOLOGY OF THE YUCCA MOUNTAIN REPOSITORY SITE

Yucca Mountain is located at the southwestern boundary of the Nevada Test Site in Nye County, Nevada (Figure 1). The area is underlain by several thousand feet of middle Tertiary welded and nonwelded ash flow tuffs, interspersed with a variety of air-fall tuffs and reworked tuffs. The volcanic sequence has been affected by typical Basin and Range deformation. Relatively intact and gently dipping blocks are separated from one another by generally north-trending, high-angle normal faults that typically dip to the west. Yucca Mountain itself is a major east-dipping fault block a few square miles in extent.

A representative stratigraphic section for the Yucca Mountain site is shown as Figure 2. The proposed location of the underground facilities of the repository is within the lower portion of the Topopah Spring welded tuff. The Topopah Spring varies in thickness across the region, but is approximately 1,000 feet thick at the site. The underlying unit, the tuffs of Calico Hills, has been designated by the primary barrier to migration of radionuclides (DOE, 1988, table 8.3.5.13-8, p. 8.3.5.13-90). This designation is a result of the expected long groundwater travel time through the unit because of limited fracturing, high porosity, and low saturated conductivity. An additional factor is that the Calico Hills tuffs typically contain substantial quantities of zeolite minerals that would tend to adsorb migrating radionuclide cations.

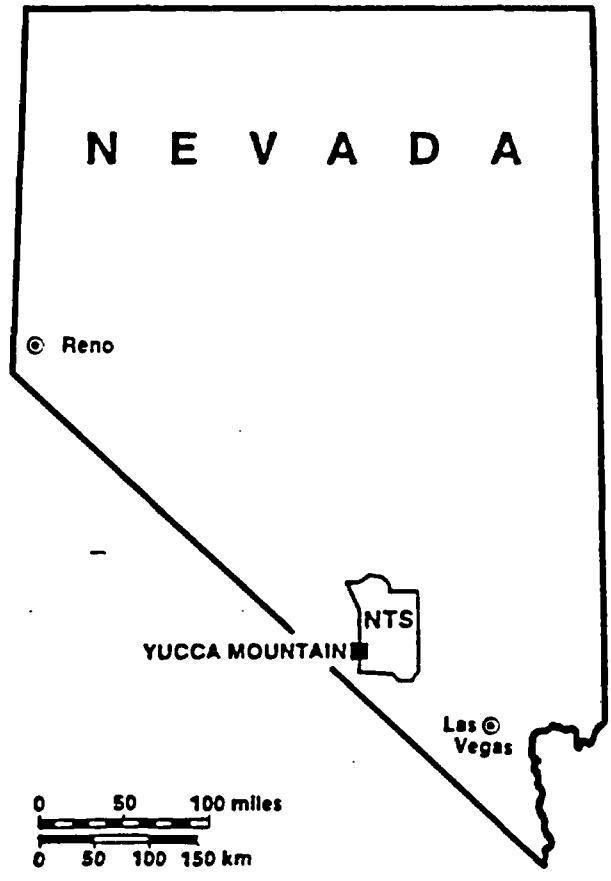

Figure 1. Index map showing location of the Yucca Mountain repository site and the Nevada Test Site (NTS) in southern Nevada.

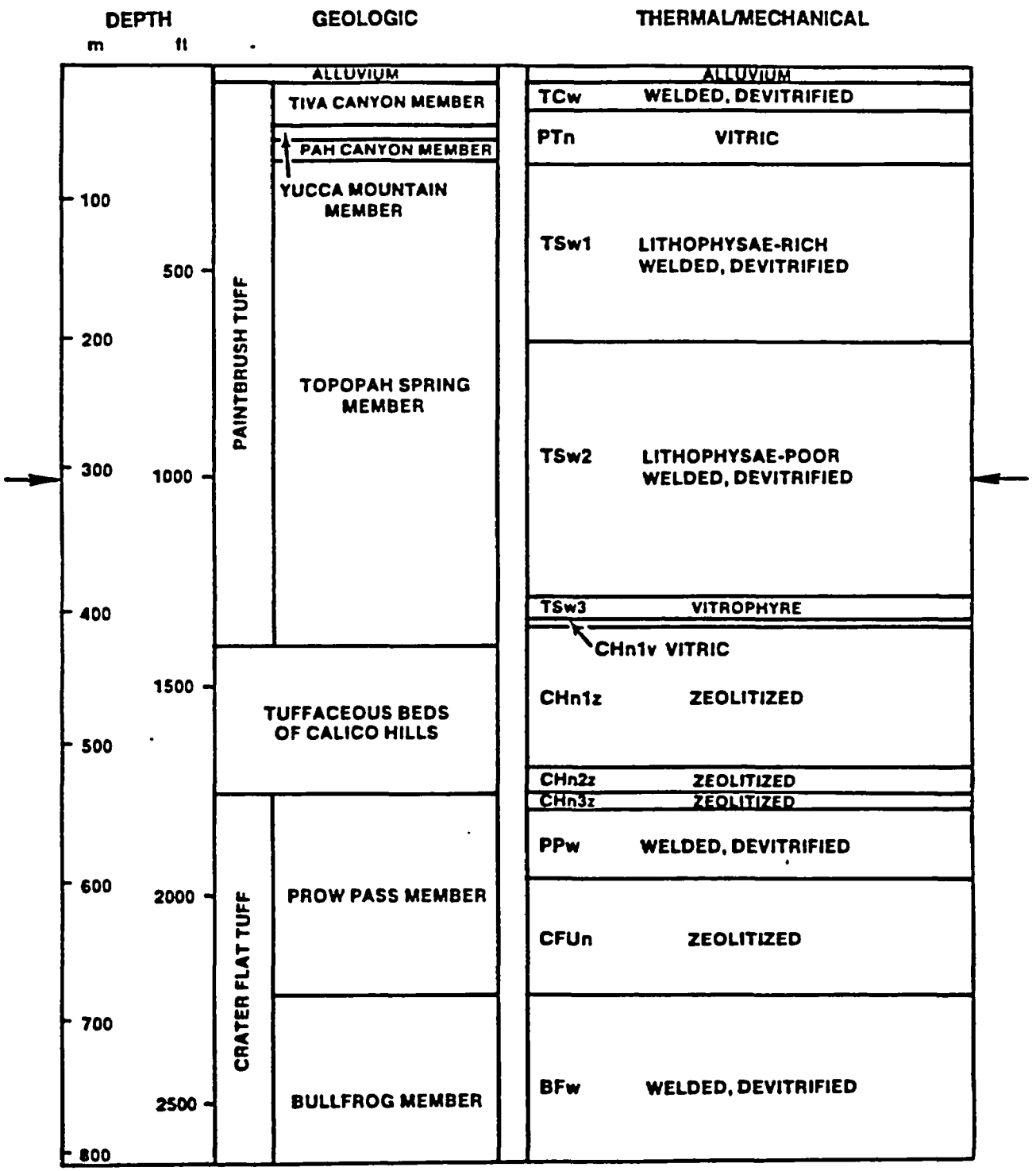

Figure 2. Representative stratigraphic section of Yucca Mountain showing lithologic terminology used in this report. Approximate stratigraphic location of repository underground facilities indicated by arrows.

SPATIAL CORRELATION

General Discussion

Characterization of rock properties at Yucca Mountain will involve statistical analyses of measured values. Construction of geometric and numerical models of the site will involve either the interpolation or the "expansion" (Journel and Alabert, 1989, p. 123) of data obtained from relatively small samples taken at various locations to construct a "solid-volume" representation of the mountain and environs. The question naturally arises as to how "representative" the samples and measured values are of the much larger volume of interest.

An assumption underlying much of classical statistical analysis (time-series analysis being a notable exception) is that one is dealing with independent samples. Even when "correlation" as a concept is introduced, the correlation considered is that between two variables measured on the same entity. An example is the correlation between porosity and permeability measured on the same specimen.

However, another type of correlation is of interest in sampling and analyzing geologic materials: that is, the correlation between a measurement of a variable at a given location and the measurement of the same variable at a location some distance from the first. It is this type of autocorrelation that is referred to as spatial correlation or spatial structure throughout this document.

Intuitively, one expects that if one measures a rock property at two locations separated by, say, one foot, the observed values will be rather similar. In like fashion, one expects the observed values for samples taken 10, 100, 1000, and 10,000 feet apart to be progressively less likely to resemble each other. At some distance, the samples will be essentially inde-

pendent of each other. The spatial structure described by this type of correlation may differ in different directions (anisotropic).

Part of the relevance of spatial correlation to site characterization is in determining the number of samples necessary for a given level of understanding of specific rock properties. For example, if every sampled location within a geologic unit of interest yielded a porosity value of 25 percent, one would be fairly confident that (1) 25-percent porosity is a representative value, and (2) the value at a given unsampled location is also 25 percent. In fact, a single sample would be "representative." Pursuing another extreme example, if porosity is completely uncorrelated and if measurements on a large number of samples vary between zero and (arbitrary value) 50 percent, then the expected value of porosity at any unsampled location is also 25 percent. However, the map appearance of posted values would be significantly different. The uncertainty associated with a given interpolated value in the second example is significantly higher than in the first case. The means or expected values of the two sets of samples each may be "representative" of the site, but the implications for a numerical model certainly differ.

Implications of Spatial Structure

There are a number of implications of spatial correlation to site characterization. The implications are different depending upon the perceived purpose of that characterization.

A common view of site characterization is that the objective is to predict the expected value of a rock property with some specific level of confidence. This concept corresponds to the "mean value plus-or-minus confidence limits" of classical statistics:

$$\bar{X} \pm t_{\alpha} \, s \, n^{-\frac{1}{2}} \quad , \qquad \text{(Eq. 1)}$$

where $\bar{X}$ is the sample mean; t_α is the Student t value for the desired confidence level, α; s is the sample standard deviation; and n is the number of samples. A restriction is that the distribution of values be approximately normal. Furthermore, the n samples are assumed to be independent.

An alternative view of site characterization is provided by Barnes (1988). In this view, the objective is not concerned so much with the expected or mean value, but with ensuring that enough sampling has been performed that one is reasonably confident that extreme values of the population have been sampled. Extreme values of some variable are more likely to be associated with some mode of "failure" of the site to meet regulatory or design criteria than is the mean value. Barnes presents a simple formula to calculate the required number of samples:

$$\Pr(\text{max of } N \text{ spls} \geq \beta \text{ percentile}) = 1 - \beta^N \quad . \qquad \text{(Eq. 2)}$$

The result is the probability that the maximum observed value from N samples exceeds the ß-percentile of the population. This probability function is plotted for several commonly used values of ß in Figure 3. The formula is independent of the underlying distribution shape, mean, and variance (Barnes, 1988, p. 479). However, direct application of the technique requires that the samples be independent of one another.

Spatial correlation introduces itself directly into both of these issues. For example, if principal concern is with the expected value, spatial correlation works to good advantage. Intuitively, the greater the degree of correlation, the fewer samples are required to estimate the mean with a given level of confidence (Equation 1), because each sample will "resemble" the others. More rigorously, the primary cause is that the standard deviation of the samples will decrease (to zero in the pathological case of "perfect" spatial correlation).

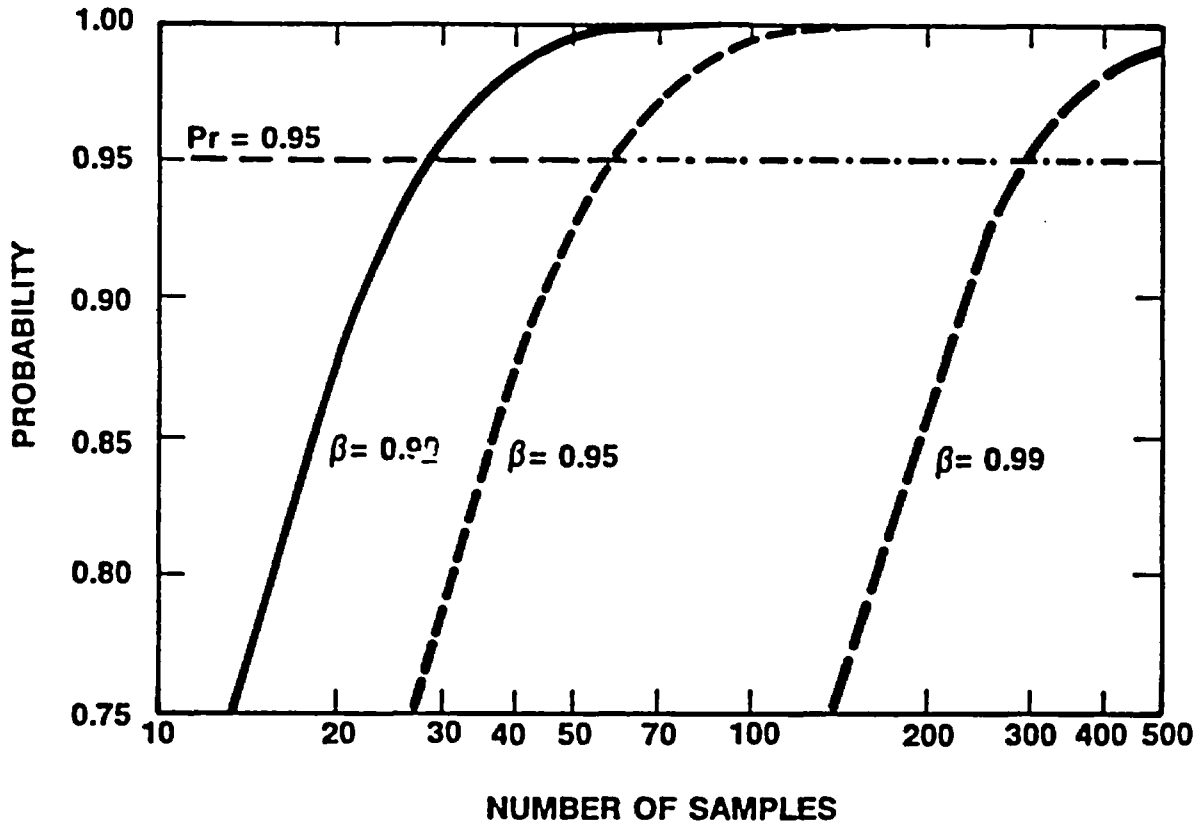

Figure 3. Graph of the function $Pr = 1 - \beta^N$ for selected, commonly used levels of ß. Refer to text for discussion.

However, if the concern is with sampling extreme values, this resemblance implies that N physical samples represent only some N_{eq} number of "equivalent" independent samples, where $N_{eq} \leq N$. Substituting N_{eq} into the formula of Barnes presented above (Equation 2) implies that the probability of having sampled a value greater than the ß-percentile is less for a given number of physical samples if spatial correlation is present. Calculating the equivalent number of uncorrelated samples, N_{eq}, requires a description of the degree of spatial correlation via geostatistics. It also requires a knowledge of the actual locations of the samples. Barnes provides such a method (1988, p. 483 and his Appendix B).

Another implication of spatial correlation, or alternatively the lack of such correlation, concerns the continuity of extreme values; this is the entropy concept discussed by Journel and Alabert (1989). Most geologic phenomena are interpreted to exhibit some degree of spatial continuity. Spatial correlation is, after all, the principle which allows geologic mapping in the absence of (literally) continuous exposures. Geologists continually make the (usually implicit) assumption of low entropy.

If there is no spatial correlation, samples are, by definition, independent one of another. This independence applies both to actual samples and to potential samples (i.e., those not "yet" collected and measured). Given independence, a measured extreme value is essentially an isolated occurrence. Surrounding values, measured or not, are just as likely to be much lower as they are to be additional extreme values. Thus, under a hypothesis of spatial independence, *there can be no general continuity of extreme values*. In other words, spatial independence implies a high degree of disorder, viz. high entropy, for extreme values or tails of the distribution. This is a statement with rather profound implications. In terms of site characterization, it means that under spatial

independence, there most likely will be (for example) no preferred paths of fluid transport because high values of hydraulic conductivity will tend not to link together to form conductive channels.

Because of the importance of assertions such as the above to characterization of the Yucca Mountain site and to performance assessment and design analyses that use site data, it is obviously imperative to identify and to describe the nature and extent of spatial structure for numerous rock properties. Conclusions based upon rock properties data using an incorrect description of spatial structure may be grossly in error. Of particular importance are interpretations based upon some type of assumed Gaussian behavior. The Gaussian distribution is explictly a maximum entropy model (Journel and Alabert, 1989, p. 130). Because failure of a nuclear waste repository is most likely to be associated with some type of "connected" behavior (read, flow path), maximum entropy assumptions may not be conservative for some purposes.

Approach to Determination of Spatial Structure

The purpose of this paper is to describe what can be learned about the spatial correlation structure of volcanic tuffs that may be relevant to a nuclear waste repository by examining samples of tuff taken from and near the Yucca Mountain site. The Calico Hills stratigraphic unit (Figure 2) was selected for initial study of spatial correlation structure because of its designation as the primary barrier to waste migration. Later, samples of rock units other than the Calico Hills were examined as well. Two separate sets of data were evaluated, collectively representing the best available data for the determination of spatial structure. The data consist of a set of surface samples and a set of samples obtained from drill holes.

The rock properties considered in this study are (1) porosity, (2) air

permeability, (3) saturated hydraulic conductivity, and (4) dry bulk density. The surface data set consists of porosity and air permeability values, whereas the drill hole data comprise measurements of porosity, conductivity, and density. Only porosity is common to both sets of values.

The air permeability data are presented in millidarcies (md) throughout this report. In comparison, data for saturated hydraulic conductivity are presented as reported by the Site and Engineering Properties Data Base in units of meters per day (m/day). Although the units nominally are convertible (1 md = 894.24 m/day), this distinction is maintained to emphasize the fact that two different rock properties have been measured: one for air and one for water. In concluding sections of this report, the fact that both air permeability and hydraulic conductivity are flow-related rock properties is used to speculate about comparability of the spatial structures deduced for each. However, the integrity of the descriptive portions of this report is enhanced by maintaining a clear distinction between the two data sets.

Surface Data and Lateral Variability

The surface samples were obtained for this report from excellent outcrops of the tuffs of Calico Hills located to the north of the site near Prow Pass and elsewhere within the Calico Hills (the topographic feature; Figure 4). Surface sampling was restricted to a narrow stratigraphic interval to reduce the effect of variability in the third dimension (stratigraphic vertical). The drill hole data are derived from samples taken from several drill holes that penetrate the repository block. These samples have been analyzed and reported in a number of publications. The values are also available from the Yucca Mountain Project Site and Engineering Properties Data Base (SEPDB, 1989). The broader relationship of the sampling localities to the volcanic source areas is

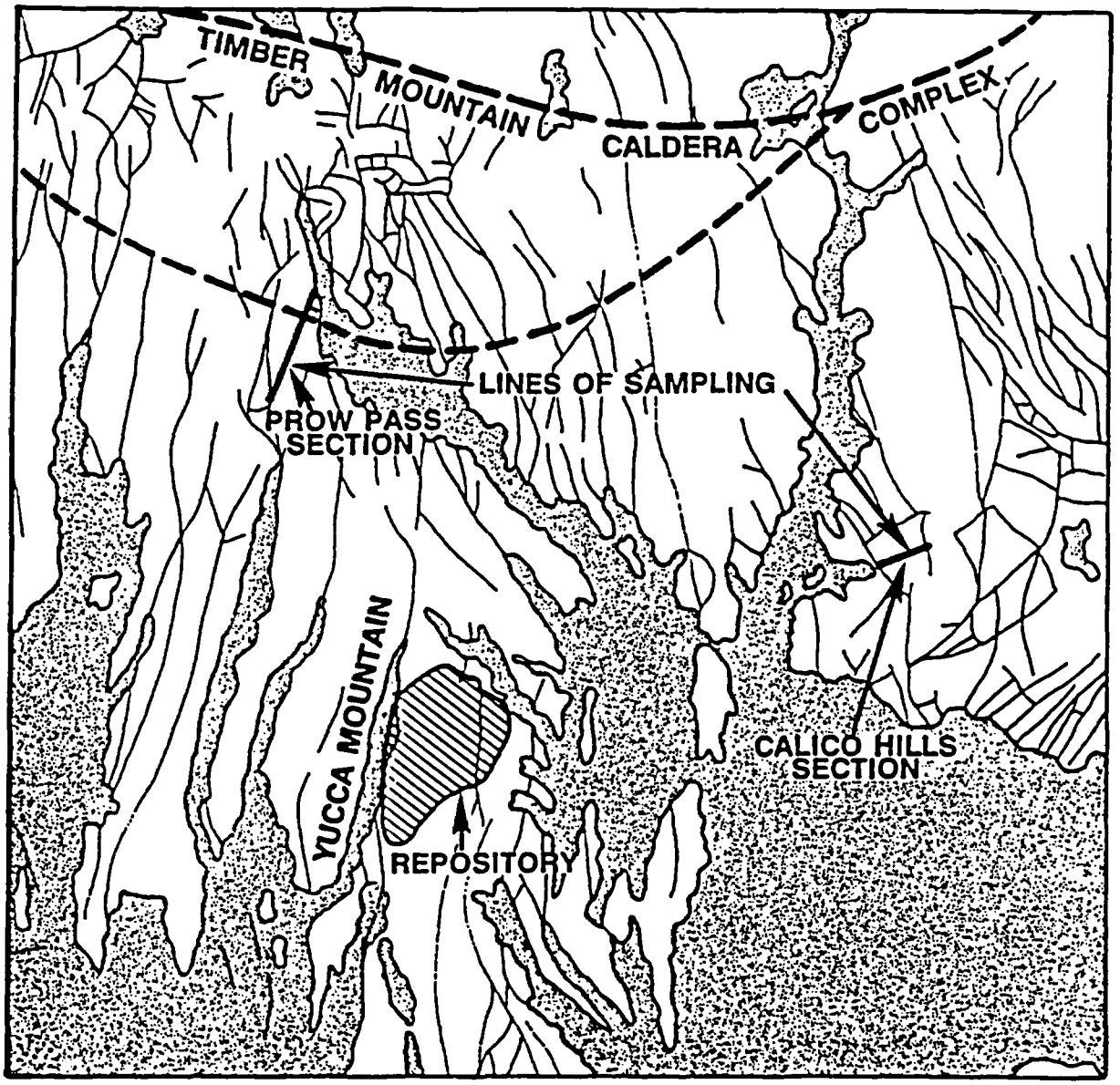

Figure 4. Map of the Yucca Mountain region showing location of the proposed repository and outcrops of the Calico Hills tuffs sampled for this study. Approximate lines of sampling traverses shown.

shown schematically in Figure 5.

The surface data were used to examine spatial structure in the lateral directions. Although the applicability of the outcrop values to the Yucca Mountain repository site located three miles or so distant is indirect, Borgman (1988, p. 383) advocates the use of variograms derived from "similar data collected elsewhere" in geostatistical studies when data from the area of interest are inadequate. In effect, the action is to establish a Bayesian prior distribution that will be modified later as data are obtained from the site.

Though direct evidence is lacking, the Prow Pass surface section in particular is believed to be fairly similar to the subsurface Calico tuffs beneath the repository block. The thickness of the unit appears comparable to that observed in the few drill holes located near the underground facilities,[1] and the geographic location of Prow Pass is approximately the same distance from the inferred eruptive source of the unit in the Forty-Mile Canyon area (Figure 5). Inferred similarity of the Prow Pass rocks to the Calico Hills underlying the proposed repository extends to the observation that the Prow Pass section is extensively zeolitized. Outcrops of this unit within the Calico Hills themselves, while extensive, are much closer to the source terrane and typically include abundant flow rocks, breccias, and hydrothermally altered tuffs.

Drill Hole Data and Vertical Variability

The drill hole data were used to examine stratigraphically vertical correlation structure. These data are all from the repository site itself

[1]Calculation of true stratigraphic thickness at Prow Pass based on the mapping of Scott and Bonk (1984) indicates the Calico Hills is roughly 450 feet thick. Compare this thickness to the approximately 350 feet reported in hole USW G-4 (near the proposed Exploratory Shaft location) by Spengler and Chornak (1984).

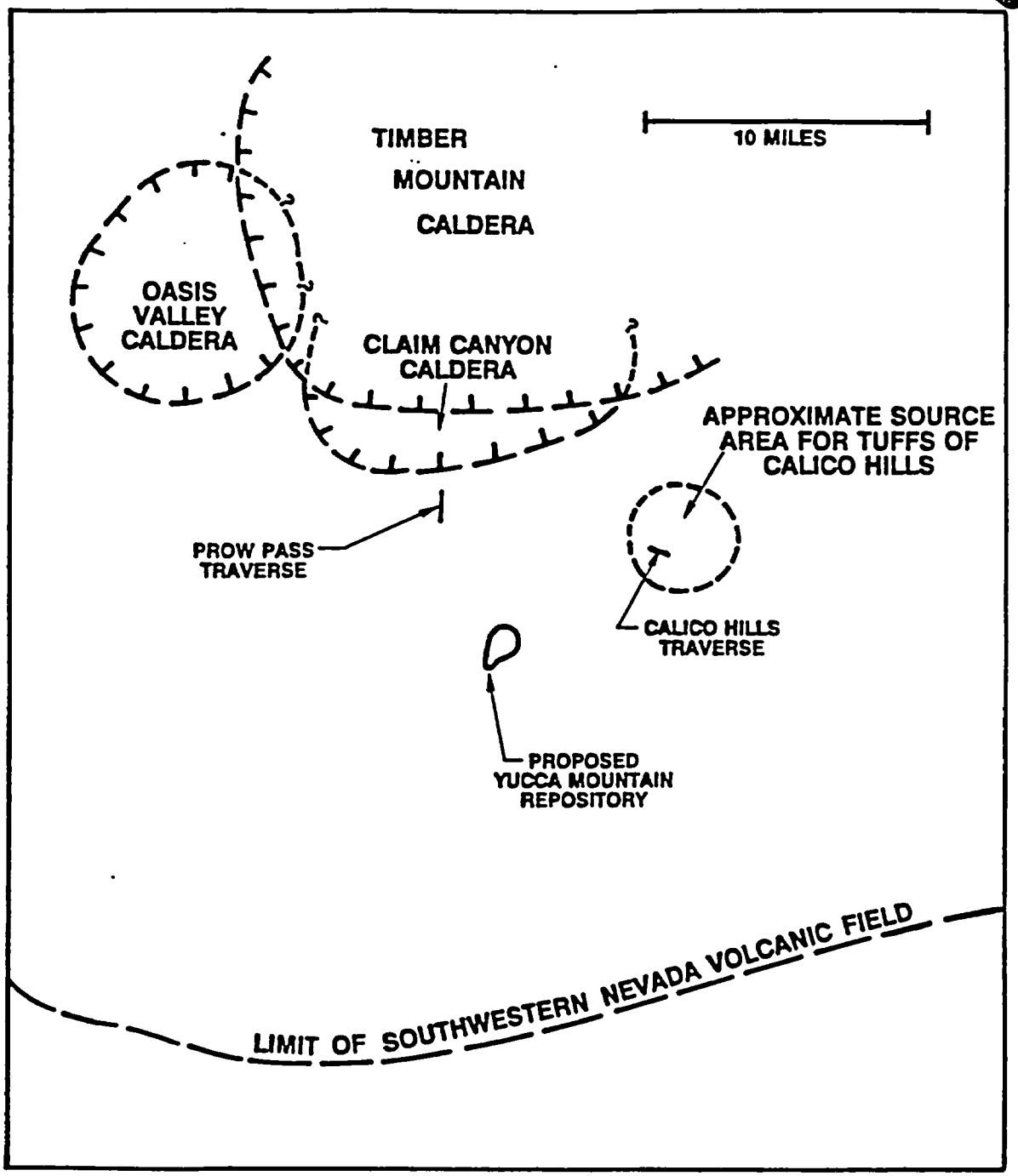

Figure 5. Sketch map showing the location of sampling localities (outcrops and repository area with several drill holes) in relationship to interpreted source areas. Correspondence between rock units and individual vent regions after Carr (1988, Table 4.1 and Figure 4.1).

(Figures 4 and 5), and they include samples of virtually all stratigraphic units shown in Figure 2. Many of these samples represent the Tiva Canyon and Topopah Spring units in addition to the tuffs of Calico Hills. Older units belonging to the Crater Flat Tuff are represented as well. Carr (1988, Table 4.1) describes the source of the Tiva Canyon Member as the Claim Canyon Caldera segment shown schematically in Figure 5. The Topopah Spring Member is inferred to have originated from the Timber Mountain-Oasis Valley caldera complex. The present margin of the Timber Moutain caldera (Figure 5) appears most directly related to the younger and overlying Timber Mountain Tuff. The relevance of the drill hole data to characterization of the site is direct.

Methodology

After preliminary statistical evaluation of the data sets, the spatial structure of data was investigated through the use of various geostatistical techniques. In general, a number of sample variograms were constructed to examine the degree and extent of spatial correlation. Various mathematical variogram models were then fitted to the sample plots to quantify the range and degree of spatial correlation.

To a large extent, the primary focus of this study is to determine the range of any spatial structure present. As a first approximation, the maximum variogram range can be used to assist in determining the maximum allowable spacing for sampling purposes. For example, sample spacings of more than about 85 percent of the range of correlation have been described as "sparse" (Yfantis and others (1987, p. 203).

Initial estimates of the range of correlation can be made by visual inspection of variograms without recourse to the fitting of a mathematical model. Nevertheless, the modeling exercise has been conducted for this report,

partly as a demonstration of the technique for an audience largely unfamiliar with the applications of geostatistics. A secondary reason for developing formal variogram models is that such mathematical representations of spatial structure can be used to simulate two- and three-dimensional fields of rock properties. These simulated fields may be used to impart a "real-life" character to preliminary (i.e., prior to the completion of site characterization) performance assessment and design activities within the Yucca Mountain Project. To the extent that the preliminary estimates of spatial structure place limits on the degree of spatial continuity or variability actually present in volcanic tuffs at Yucca Mountain, limits are also placed on the expected results of design and performance assessment calculations.

In accordance with the primary emphasis on identifying the range of spatial correlation, less emphasis has been placed on identifying the exact shape or form of the variogram. The feasibility of modeling a given set of data by different mathematical representations has been noted in most instances. In general, the data contained in this report are insufficient to distinguish among the alternatives presented. In some instances, geologic knowledge external to the numerical data may be used to suggest a preferred alternative. Another geostatistical aspect that has been slighted to some extent in this study is the determination of the nugget-sill ratio. Both the behavior of the variogram near the origin (variogram shape) and the nugget-to-sill ratio have greater bearing on interpolated values located near measured samples (and thus on the "smoothness" of the resulting estimate) than does the range. However, the range is of more importance in determining a sampling program for site characterization.

DATA ANALYSIS

Univariate Description.

The measured values of porosity and air permeability from the surface samples collected by this study are tabulated in Appendix A (Table A-1). Summary statistics for the measured data are given in Table 1. Histograms and cumulative probability plots of the data are shown in Figures 6 and 7.

Table 1. Descriptive Statistics for Surface Samples (Prow Pass, Calico Hills)

Statistic	Porosity (%)	Air Perm (md)
No. of Values	38.00	37.00
Maximum	40.90	1.80
Minimum	22.20	0.07
Mean	32.00	0.59
Median	33.30	0.49
Std.Dev.	5.32	0.42
Coef.Var.	0.17	0.71
Skewness	-0.43	0.99
Kurtosis	-1.07	0.70

Notes: Air permeability data exclude fractured sample CRPP-24-SNL

One prepared subcore exhibited a natural fracture that produces an apparent air permeability at least two orders of magnitude greater than that represented by the majority of the specimens. The permeability datum for this sample (CRPP-24-SNL, Table A-1) has been omitted from the analysis that follows. The porosity of this sample appears not to have been affected by the presence of the fracture.

The porosity data are notably bimodal (Figure 6), although the origin of this phenomenon is uncertain. The 38 porosity values appear unlikely to represent a normal distribution; a hypothesis of normality can be rejected at the 0.05 level of significance. The non-normal interpretation is probably directly attributable to the bimodality of this limited data set.

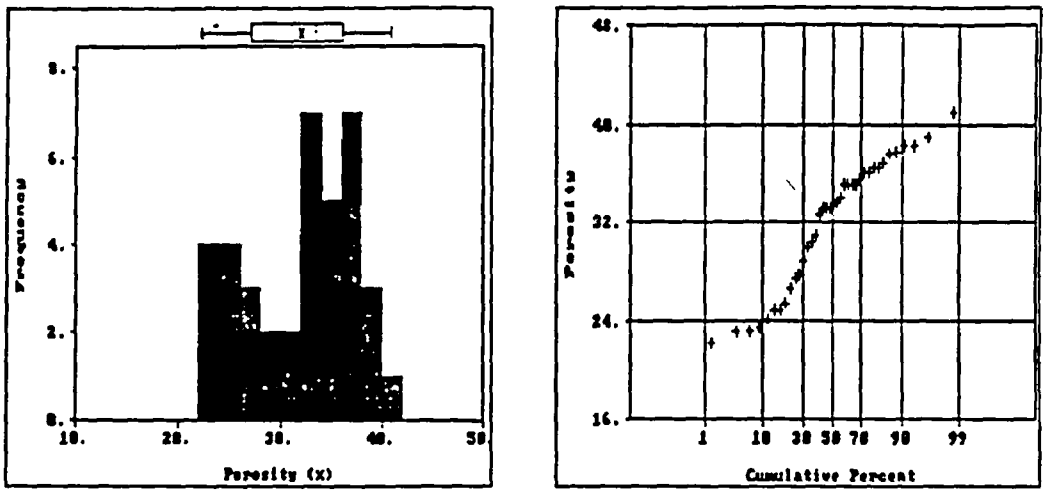

Figure 6. Histogram and cumulative probability plot of porosity values for surface samples reported in Table 1. Box plot key: "fingers" - minimum and maximum values, "box" - first and third quartiles, "bar" - median, "X" - mean. X-axis of cumulative probability plot utilizes a probability scale. A normally distributed population will plot as a straight line on this type of diagram.

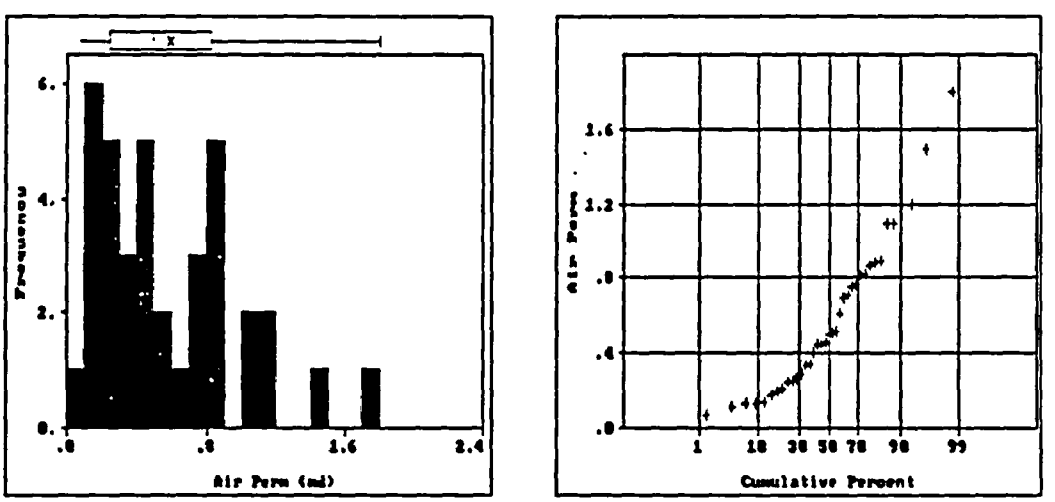

Figure 7. Histogram and cumulative probability plot of air permeability values for surface samples reported in Table 1.

The air permeability data (Figure 7) are similarly multimodal, although the separation of modes is much less obvious. A hypothesis of log-normality cannot be rejected at the 0.05 level of significance. For comparison with the hydraulic conductivity data discussed below, the air permeability data shown in Table 1 vary from 62.6 to 1,609.63 m/day.

Porosity and permeability are not correlated; correlation coefficients between porosity and simple permeability and between porosity and log permeability are less than 0.04. Spearman's rho (correlation coefficient for rank-order data) is only 0.09.

The drill hole sample data are also presented in Appendix A (Table A-2). Complete summary statistics for the porosity, hydraulic conductivity, and dry bulk density data from these drill hole samples are presented in Table 2 (all stratigraphic units) and Table 3 (Calico Hills unit only). Histograms and the corresponding cumulative probability plots of these data sets are shown in Figures 8, 9 and 10.

Table 2. Descriptive Statistics for Drill Hole Samples, All Stratigraphic Units

Statistic	Porosity (%)	Dry B.D. (Mg/m^3)	$\ln(k_{sat})$ (m/day)
No. of Values	308.00	284.00	42.00
Maximum	54.40	2.71	-5.52
Minimum	1.40	1.05	-15.02
Mean	19.62	2.00	-10.22
Median	17.80	2.08	-9.81
Std.Dev.	10.16	0.29	2.27
Coef.Var.	0.52	0.14	0.22
Skewness	0.86	-0.84	-0.49
Kurtosis	3.80	3.36	2.58

Dry B.D. = Dry Bulk Density
$\ln(k_{sat})$ = natural log of saturated conductivity

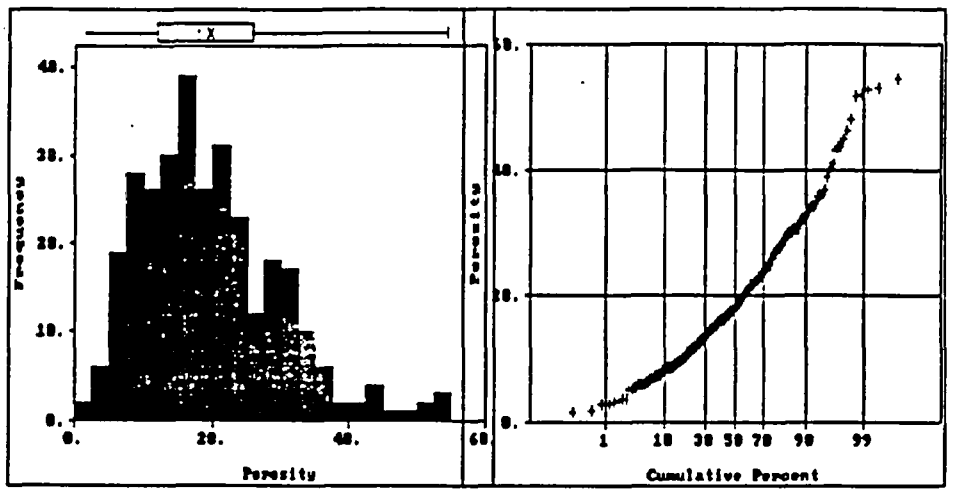

(a)

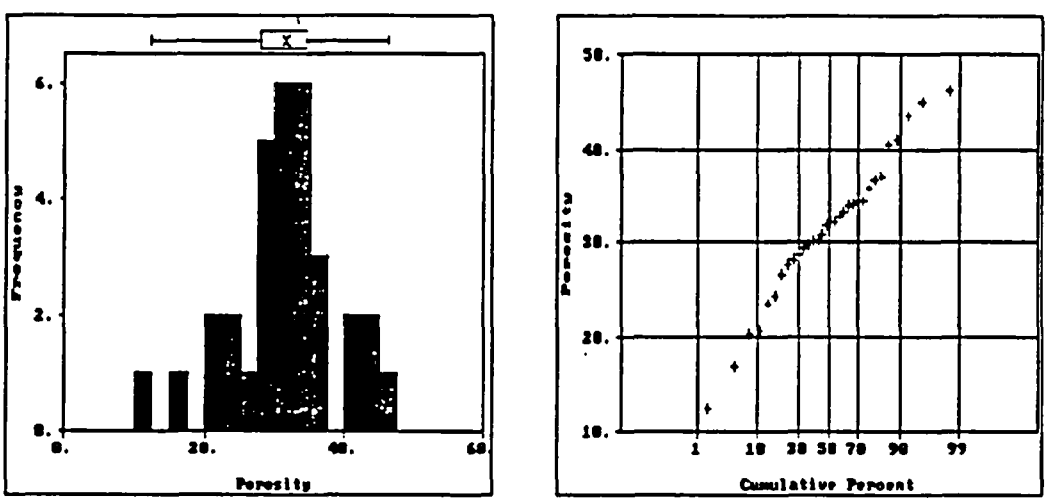

(b)

Figure 8. Histogram and cumulative probability plot of porosity values for drill hole samples from (a) all stratigraphic units and (b) unit CHn only.

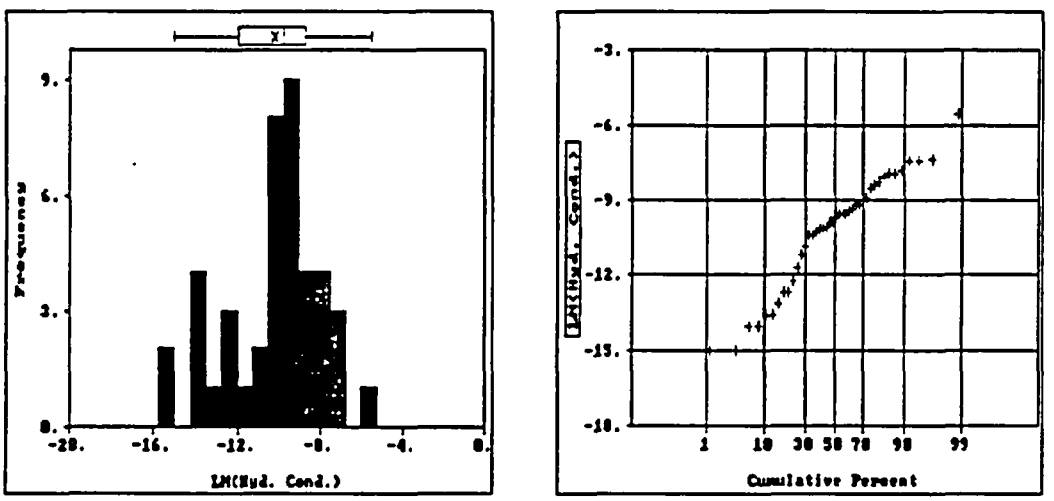

Figure 9. Histogram and cumulative probability plot of saturated hydraulic conductivity values for drill hole samples from all stratigraphic units.

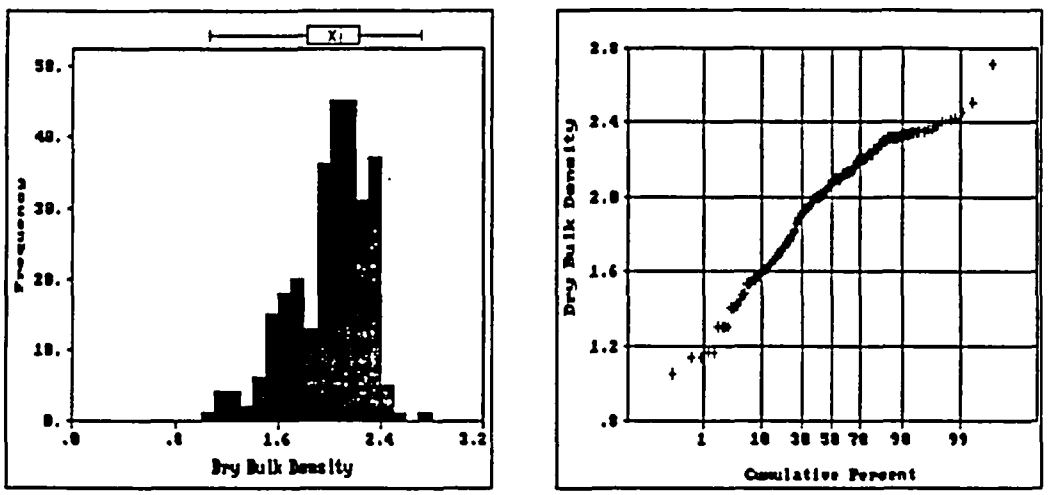

(a)

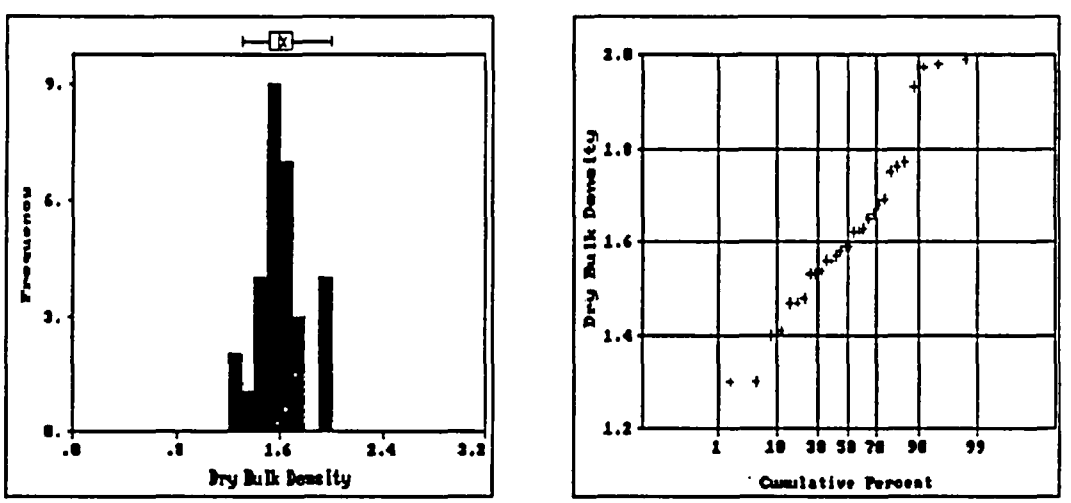

(b)

Figure 10. Histogram and cumulative probability plot of dry bulk density values for drill hole samples from (a) all stratigraphic units and (b) unit CHn only.

Table 3. Descriptive Statistics for Drill Hole Samples of Calico Hills

Statistic	Porosity (%)	Dry B.D. (Mg/m^3)
No. of Values	32.00	30.00
Maximum	46.10	1.99
Minimum	12.31	1.30
Mean	31.34	1.62
Median	31.95	1.59
Std.Dev.	7.67	0.18
Coef.Var.	0.24	0.11
Skewness	-0.27	0.49
Kurtosis	3.19	2.91

Note: No hydraulic conductivity data exist for the tuffs of Calico Hills

Drill hole porosity data appear approximately normally distributed in Figure 8, although a formal test rejects the normal hypothesis at the 0.05 significance level for the entire data set. A test of the Calico Hills subset of porosity values fails to reject the hypothesis of normality. A weak bimodality is present in the combined data set, reflecting commingling of samples from nonwelded units with more densely welded ash-flow tuffs (compare the modes of Figure 8a with 8b).

Hydraulic conductivity data taken without regard for stratigraphic unit again appear approximately log-normal (Figure 9), although a formal test of log-normality rejects the hypothesis at the 0.05 level of significance. There are insufficient samples of the Calico Hills unit to break these out as a subset. For comparison with the air permeability data presented for the surface samples, the hydraulic conductivity data shown in Table 2 vary from 4.48×10^{-6} md to 3.35×10^{-10} md.

Dry bulk density data are obviously not normally distributed (Figure 10). However, the degree of non-normality probably does not pose significant difficulties in applying standard geostatistical techniques. The subset of

values from the Calico Hills unit is sufficiently small that the formal test fails to reject the hypothesis of normality. Again, weak bimodality in the overall histogram (Figure 10a) reflects the commingling of welded and non-welded samples (compare with Figure 10b).

Spatial Description

Porosity

The observed values for porosity are plotted against traverse distance for the several profiles in Figure 11. In general, the porosity of the sampled unit(s) appears to vary relatively continuously, with some local erratic variability. This is particularly noticeable near the southern end of the main Prow Pass traverse. This small degree of variability implies a fairly high degree of spatial correlation.

Porosity values are plotted against depth in the drill hole in Figures 12 to 15. Crude segregation of the values into clusters corresponding to different stratigraphic units is obvious in some of the drill holes, notably UE-25 a#1, USW GU-3, and USW G-4. In other holes, exemplified by USW G-3, the variation in porosity tends to be more continuous. The vertical extent of the CHn thermal/mechanical unit identified by Ortiz and others (1984) is shown on the applicable figures.

Air Permeability

Air permeability values are plotted against traverse distance in Figure 16. As expected for air permeability, the degree of continuity is much less (see Prow Pass north traverse), suggesting that this variable is less correlated spatially.

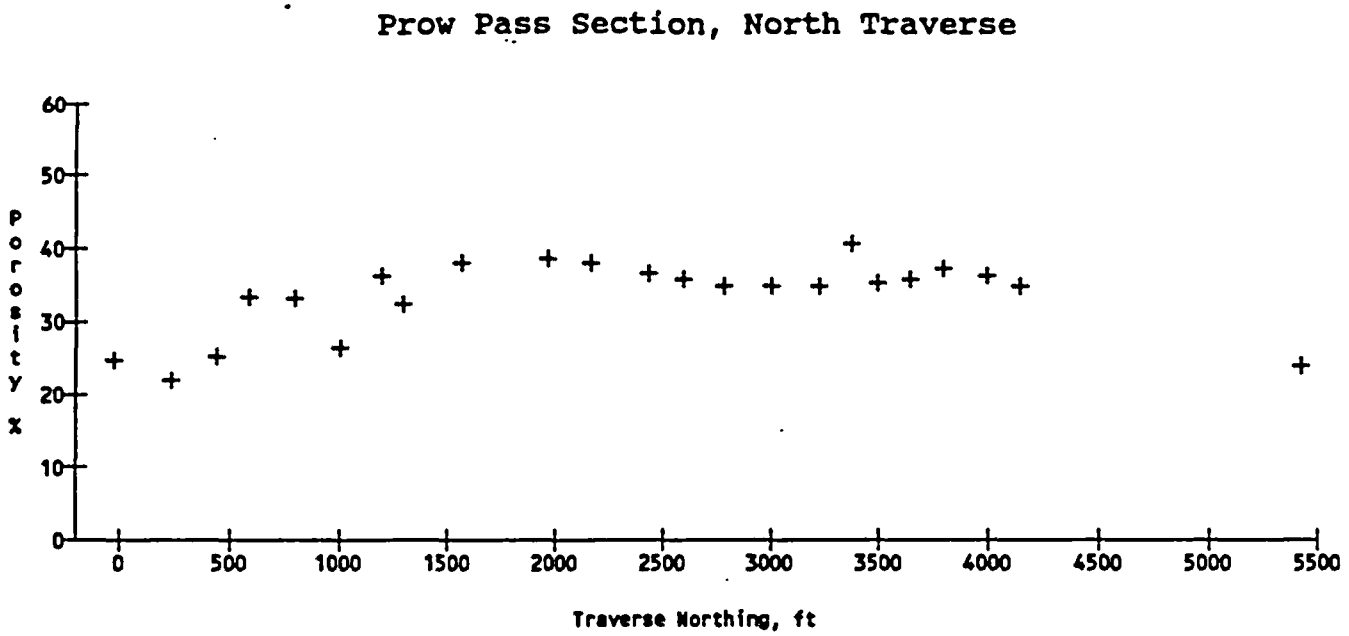

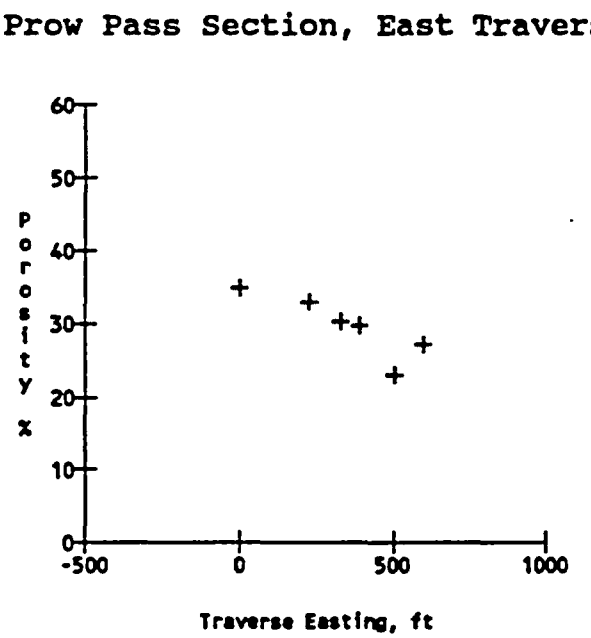

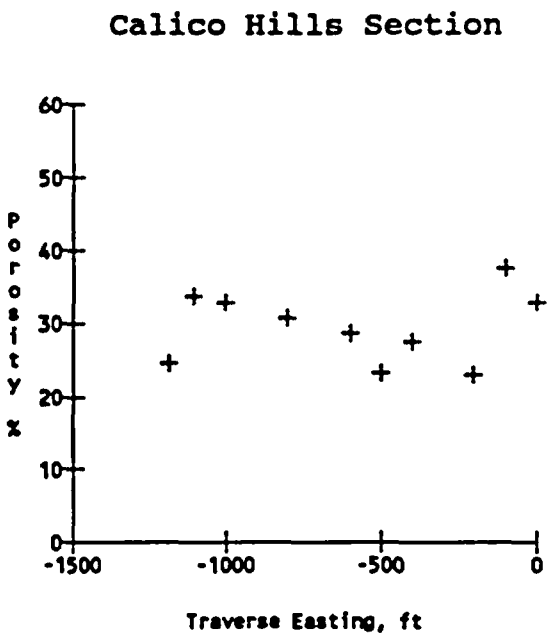

Figure 11. Porosity values plotted against traverse distance. (a) Prow Pass section, main (north) traverse; (b) Prow Pass section, supplementary (east) traverse; (c) Calico Hills section.

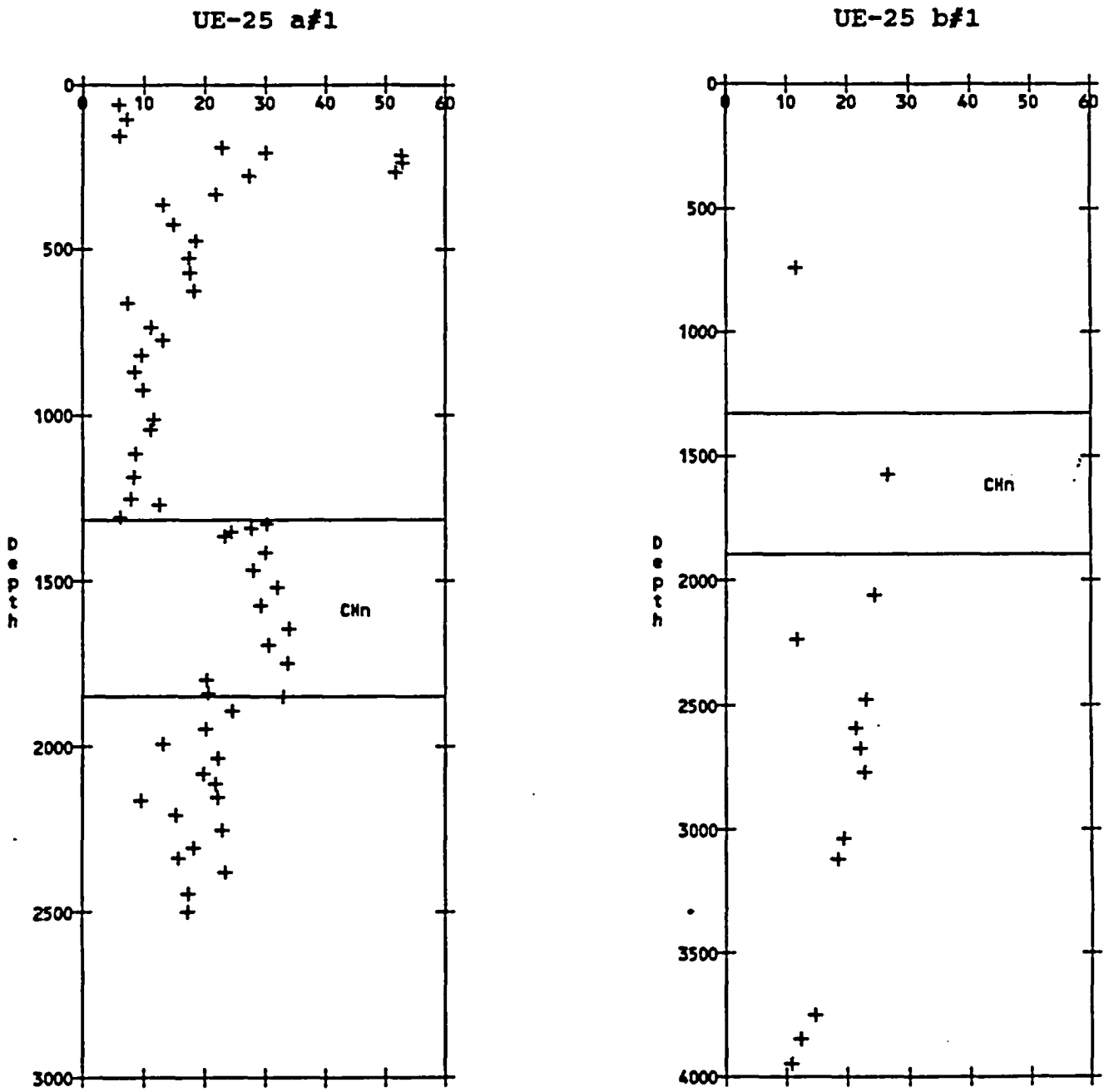

Figure 12. Porosity in drill holes UE-25 a#1 and UE-25 b#1. Porosity in percent, depth in feet.

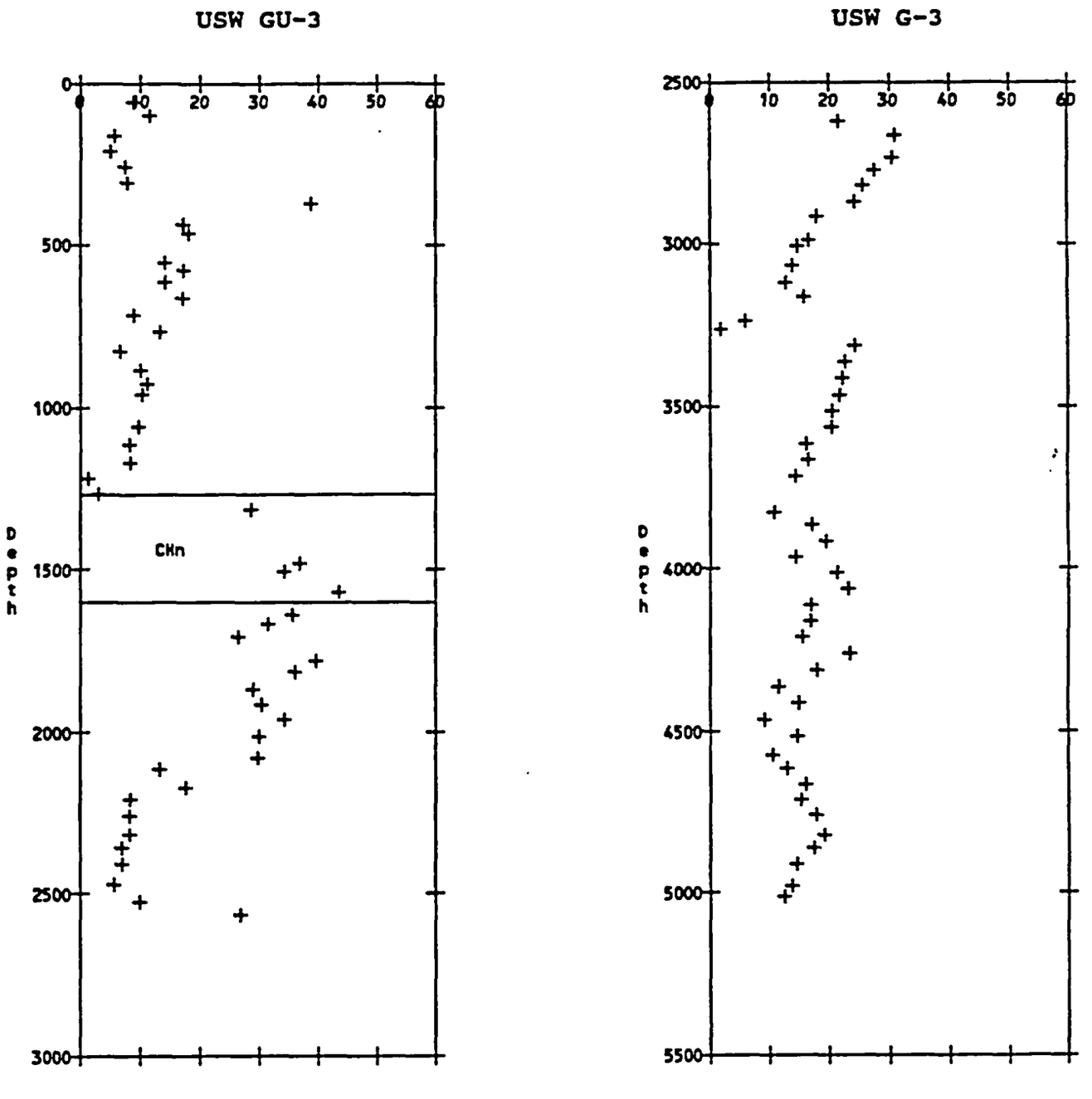

Figure 13. Porosity in drill holes USW GU-3 and USW G-3. Porosity in percent, depth in feet.

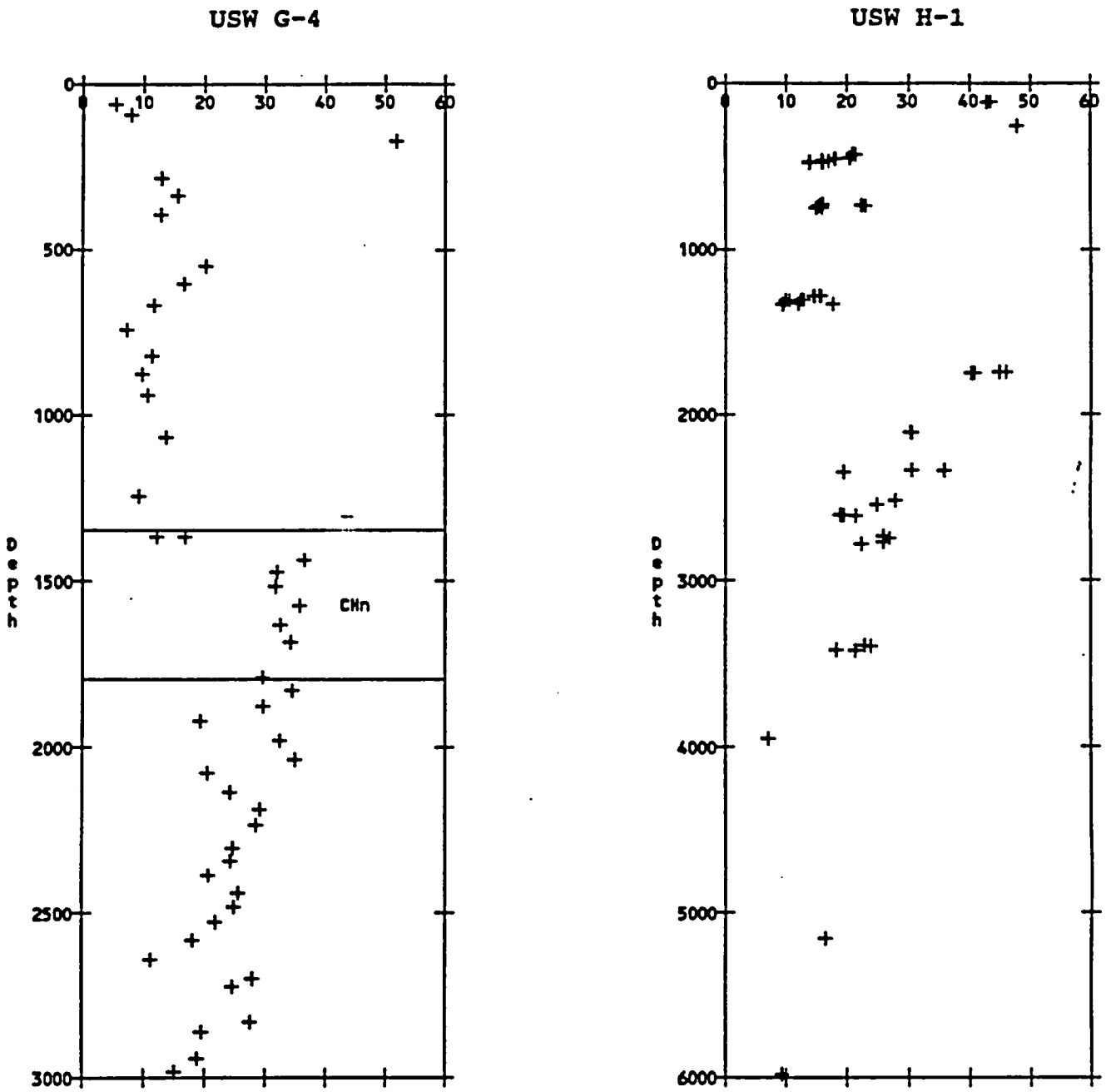

Figure 14. Porosity in drill holes USW G-4 and USW H-1. Porosity in percent, depth in feet. CHn unit not recognized by Ortiz and others (1984) in USW H-1.

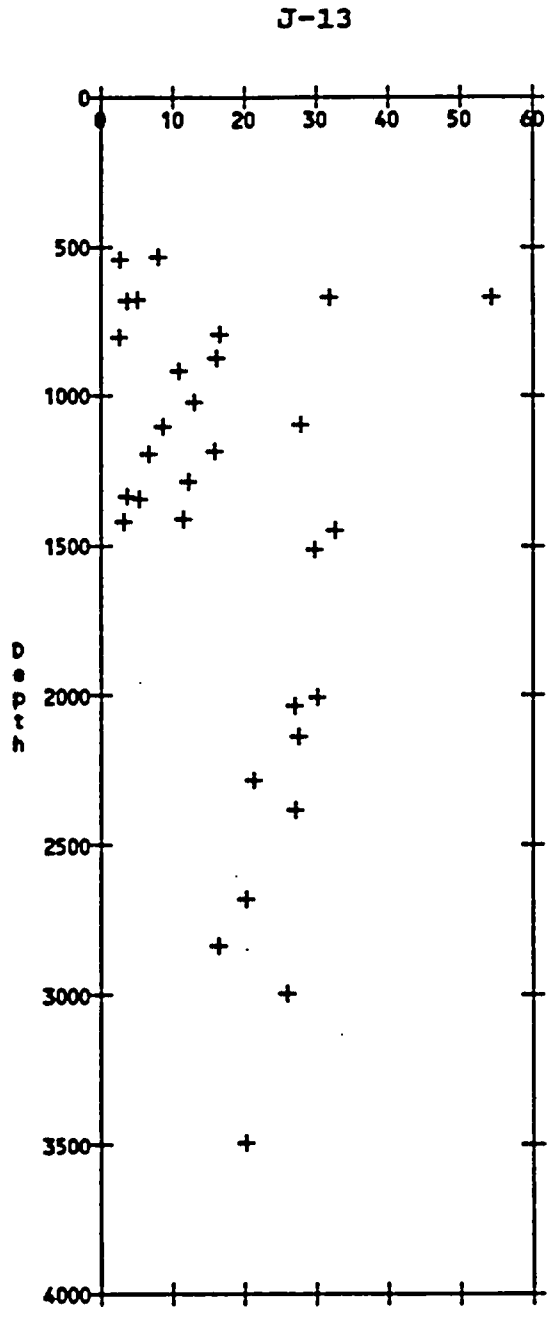

Figure 15. Porosity in drill hole J-13. Porosity in percent, depth in feet. No thermal/mechanical units recognized by Ortiz and others (1984).

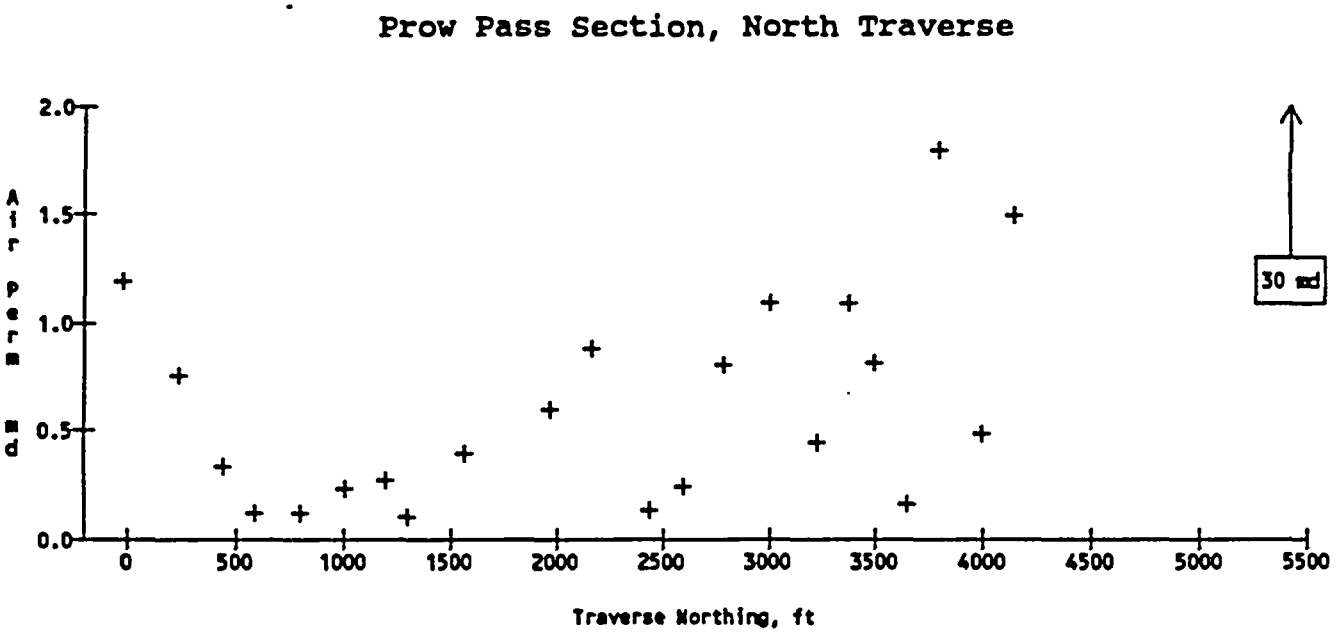

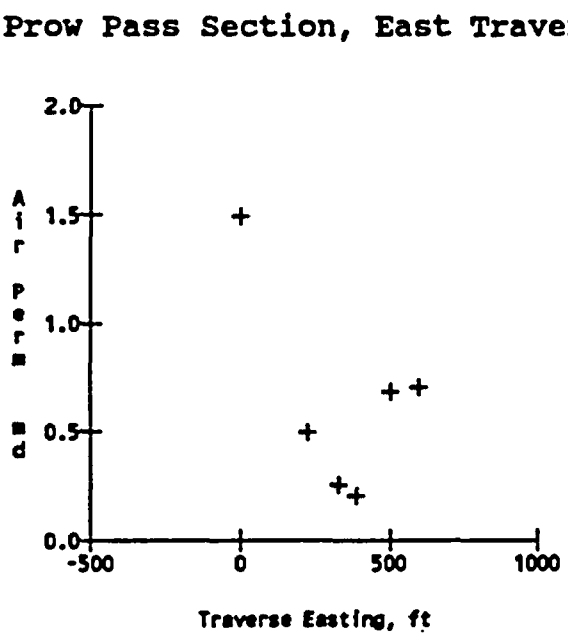

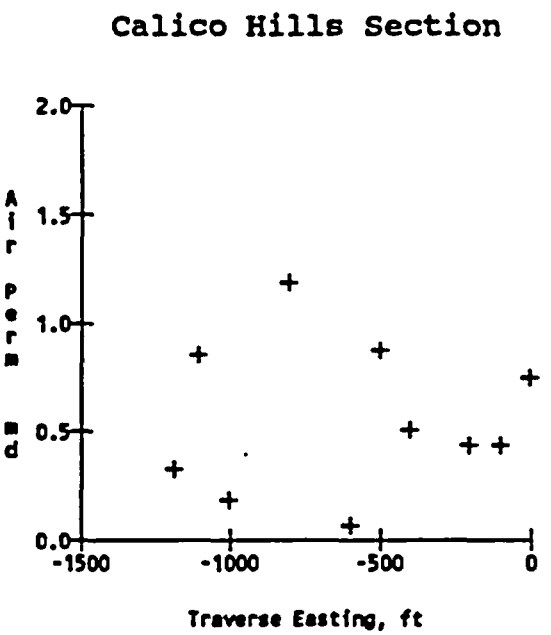

Figure 16. Air permeability values plotted against traverse distance. (a) Prow Pass section, main (north) traverse; (b) Prow Pass section, supplementary (east) traverse; (c) Calico Hills section.

Hydraulic Conductivity

The Site and Engineering Properties Data Base contains values for saturated hydraulic conductivity instead of air permeability. These values for drill hole samples are plotted against depth in Figures 17 and 18. Generally speaking, the data are somewhat sparse and the patterns exhibited are rather erratic.

Dry Bulk Density

Drill hole values of dry bulk density are plotted against depth in Figures 19 thru 22. Certain holes exhibit pronounced clustering of values corresponding to stratigraphic units of some type. Other holes appear to exhibit more continuously varying values of bulk density.

Geostatistical Analysis

Variograms

The principal type of geostatistical analysis undertaken by this study was to construct sample variograms for the variables of interest and to develop a mathematical representation of those variograms if possible. The mathematical or "theoretical" variogram is what would be used to interpolate between sampled locations to construct a representation of a rock property of interest. A useful introductory discussion of variogram analysis and geostatistics is given by Clark (1979). Figure 23 shows theoretical variograms corresponding to several frequently used models.

The classical sample variogram is constructed by taking all pairs of measurements separated by a given distance in space and obtaining one-half the average squared difference of those pairs.[1] The value thus obtained, gamma,

[1]Geostatistical terminology frequently appears rather abstruse to the non-practitioner, and indeed, there often is disagreement among professionals. The

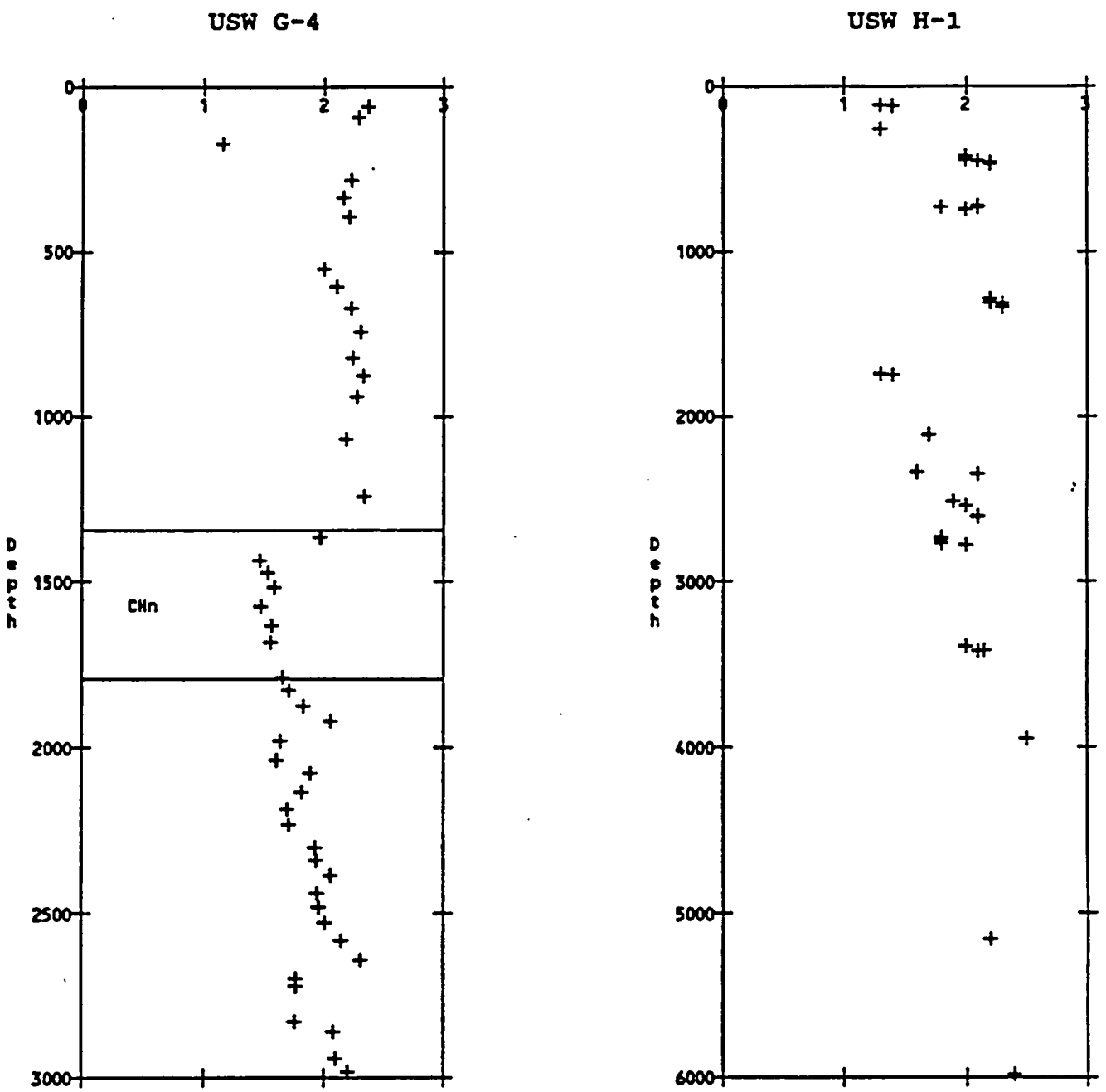

Figure 21. Dry bulk density in drill holes USW G-4 and USW H-1. Density in Mg/m**3, depth in feet. CHn unit not recognized by Ortiz and others (1984) in hole USW H-1.

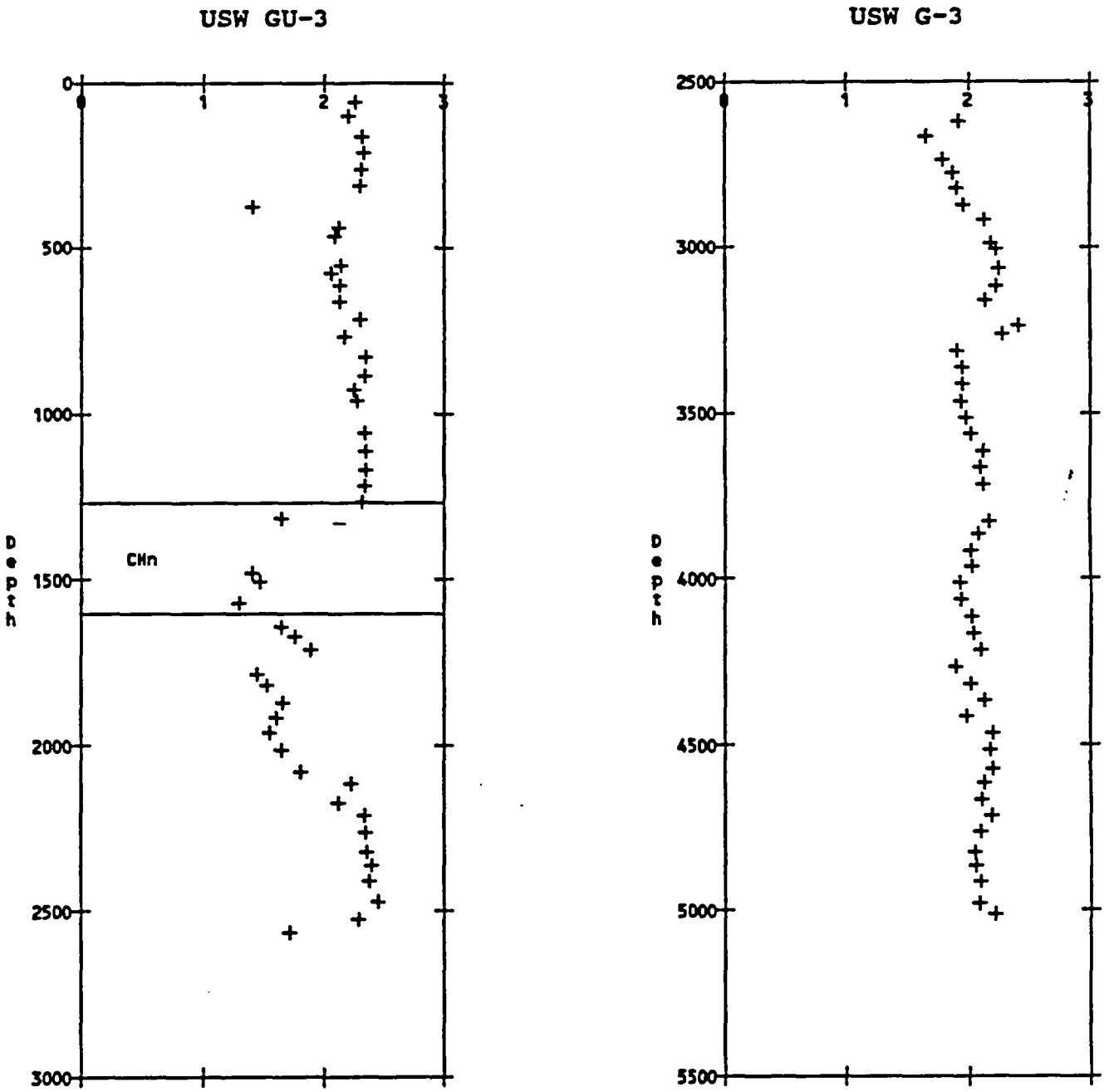

Figure 20. Dry bulk density in drill holes USW GU-3 and USW G-3. Density in Mg/m**3, depth in feet. CHn unit not sampled in USW G-3.

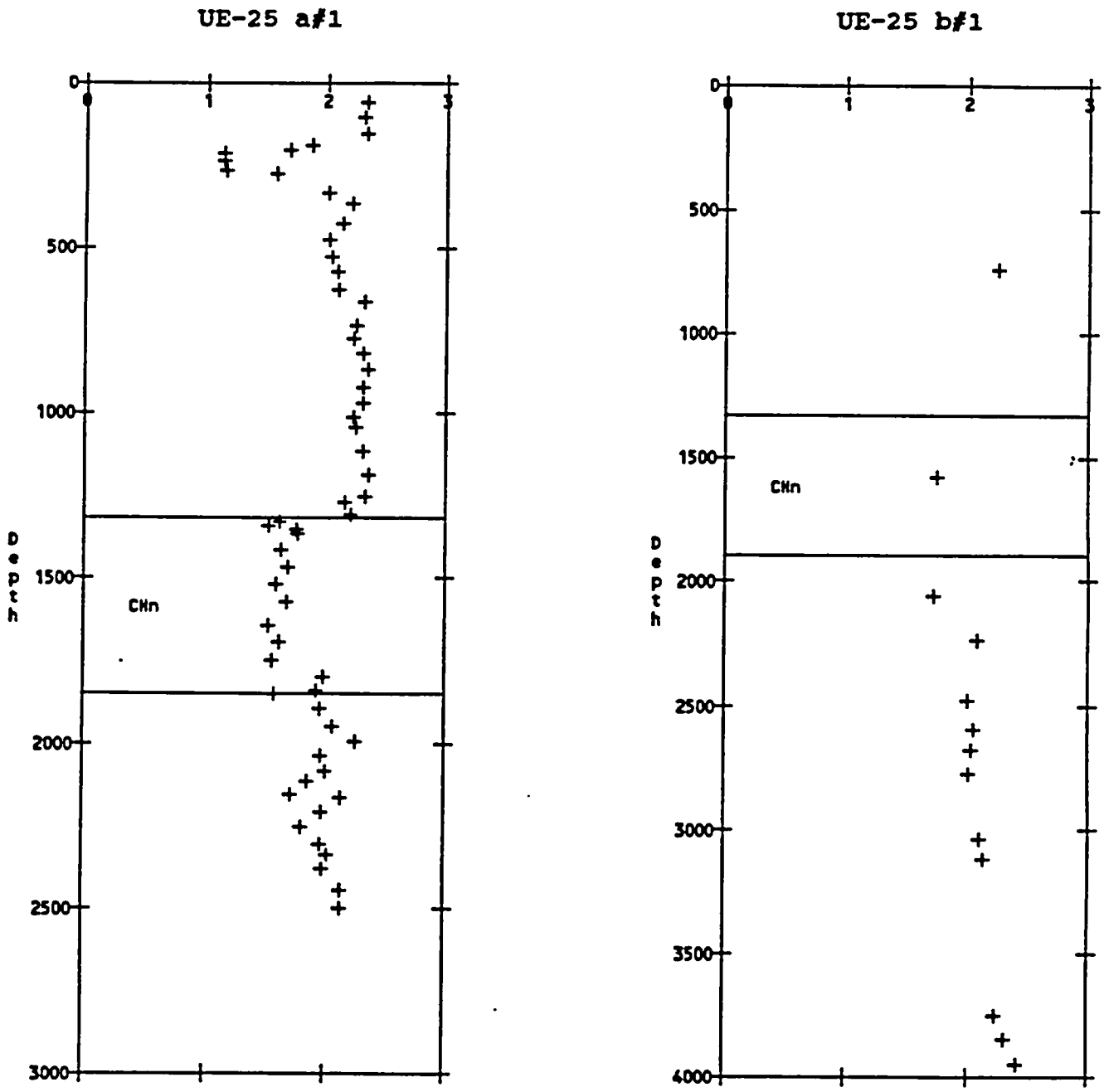

Figure 19. Dry bulk density in drill holes UE-25 a#1 and UE-25 b#1. Density in Mg/m**3, depth in feet.

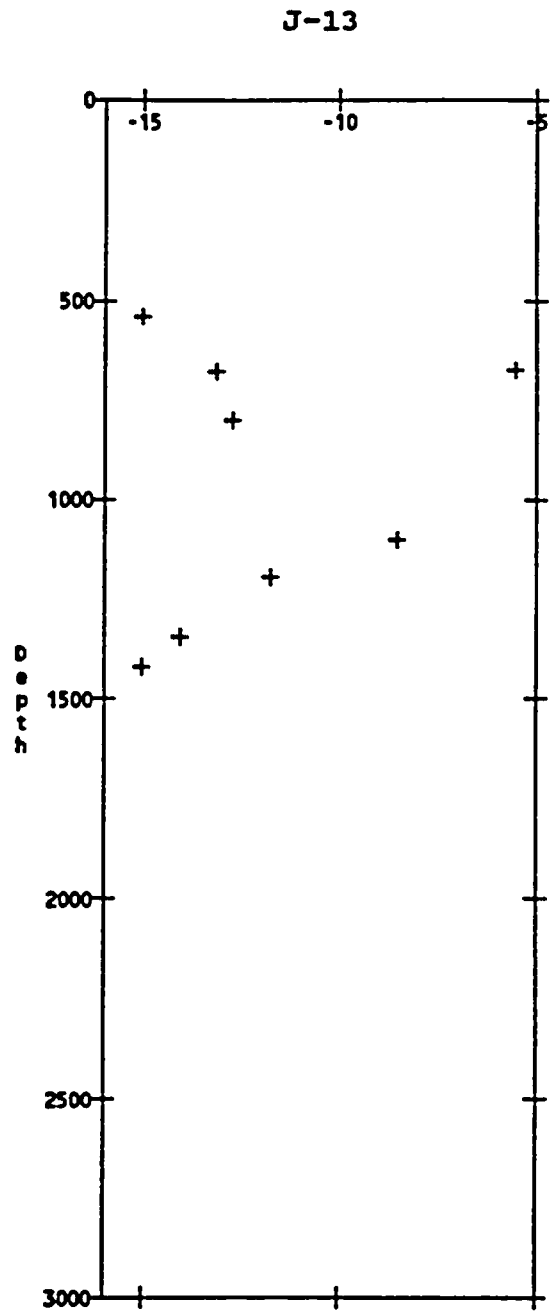

Figure 18. Natural log values of hydraulic conductivity in drill hole J-13. Conductivity in ln(meters/day), depth in feet. No thermal/mechanical units recognized by Ortiz and others (1984).

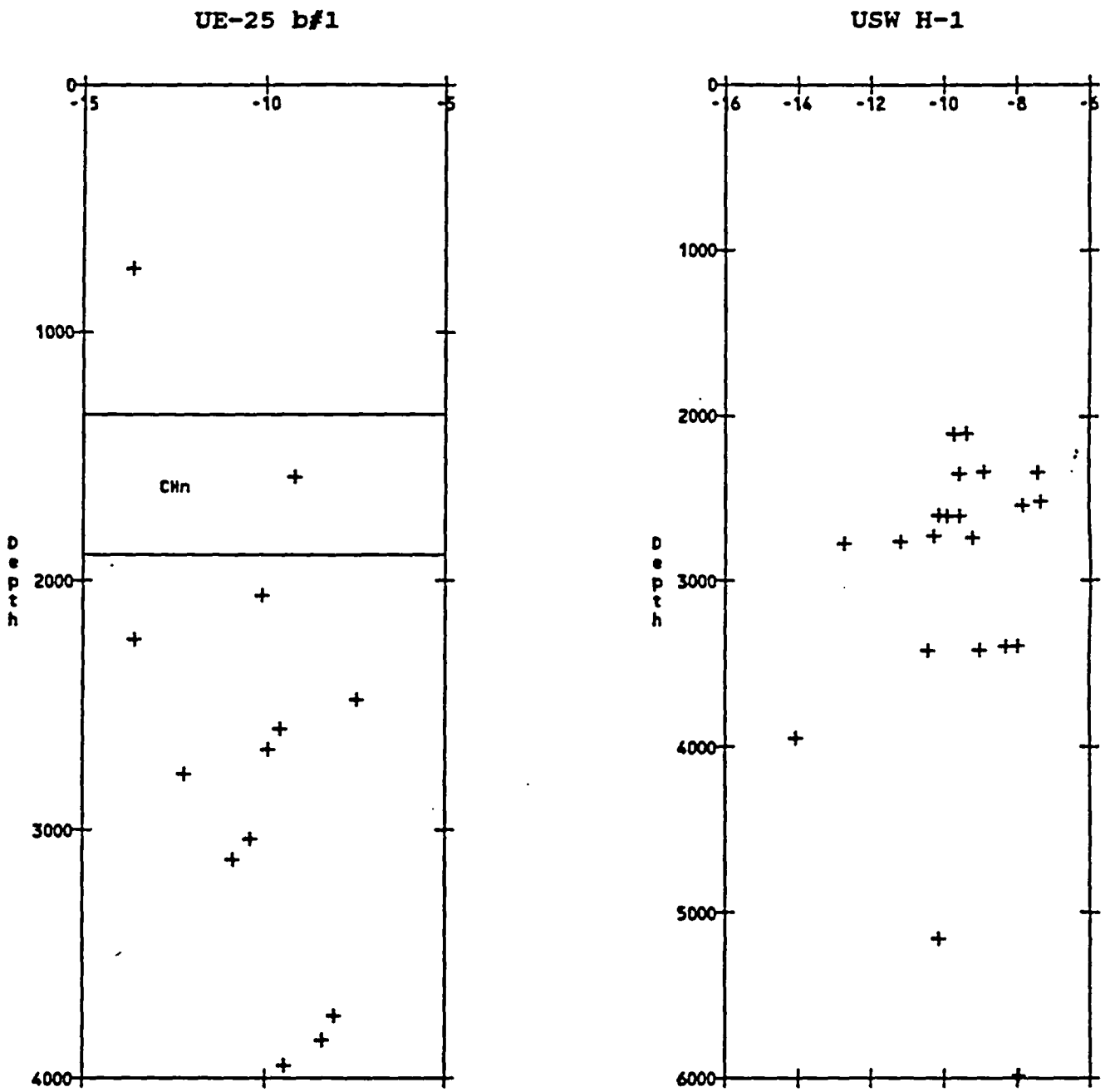

Figure 17. Natural log values of hydraulic conductivity in drill holes UE-25 b#1 and USW H-1. Conductivity in ln(meters/day), depth in feet. CHn unit not recognized by Ortiz and others, (1984) in USW H-1.

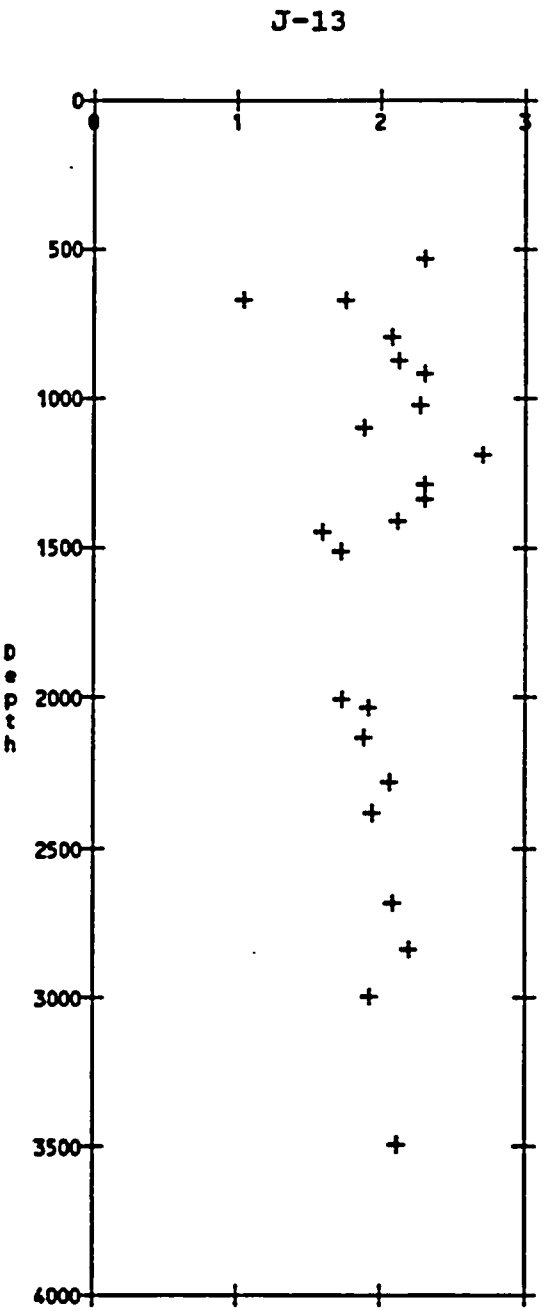

Figure 22. Dry bulk density in drill hole J-13. Density in Mg/m**3, depth in feet. No thermal/mechanical units recognized by Ortiz and others (1984) in hole J-13.

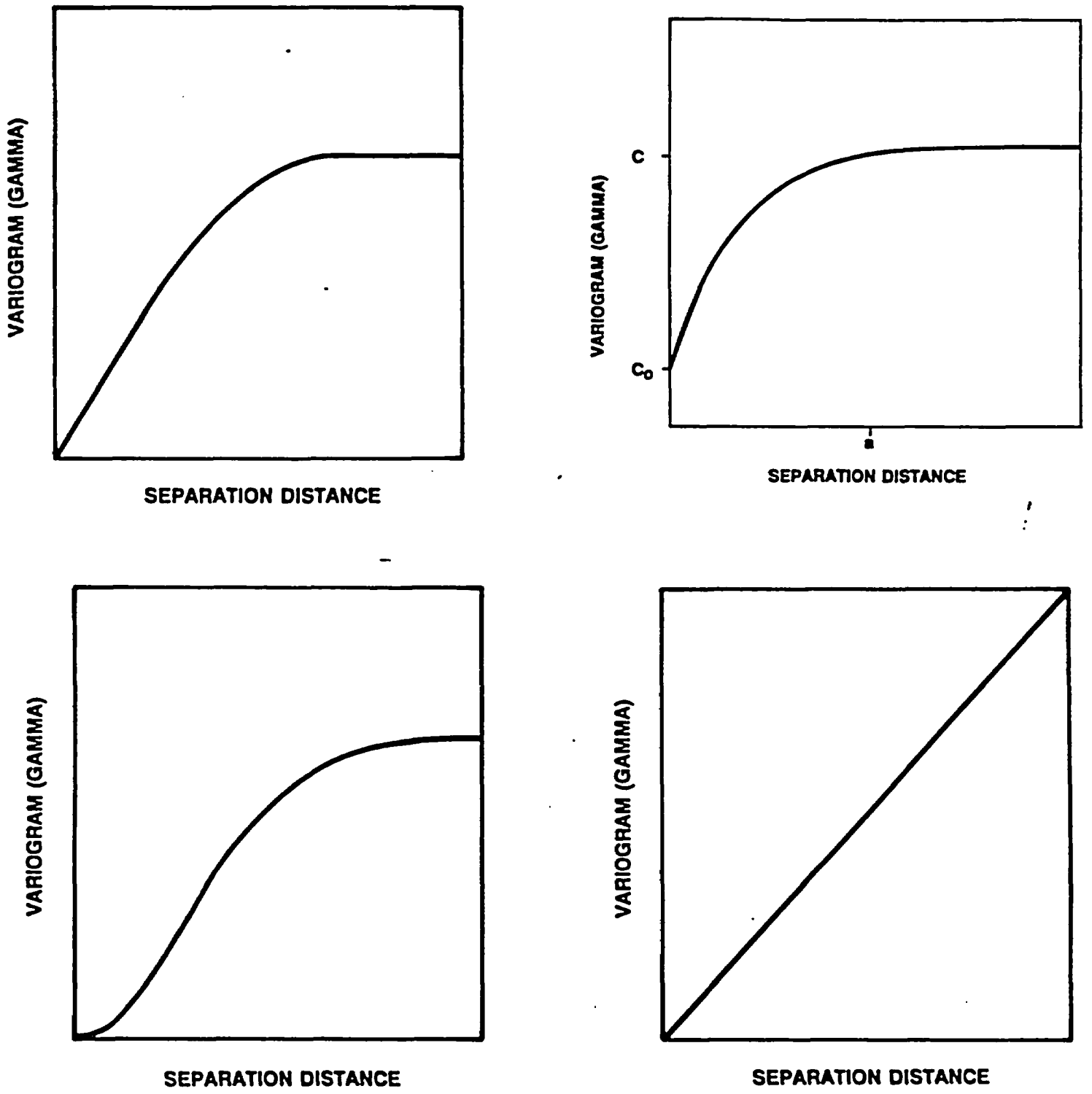

Figure 23. Commonly used theoretical variogram models. (a) spherical; (b) exponential (showing nugget [C_o], sill [C], and range [a]); (c) gaussian; (d) linear.

is plotted as a function of h, the separation distance. This process is repeated for all possible separation distances. Because the measured values rarely fall on an exactly uniform spacing, the usual practice is to consider h as a separation-distance class. All pairs whose separations fall within this class interval are plotted at the average separation distance, h. The conventional rule of thumb is that the desired number of pairs composing each point should exceed thirty, although interpretive discretion is allowed.

What the variogram represents is the "variance" anticipated for samples separated by a specified distance, h. In the variograms represented by Figure 23, it may be seen that for samples separated by small distances the variance is small. For larger distances, the expected variability is greater. At still larger distances, the variance typically appears to reach some constant value, referred to as the "sill" and designated as C. This sill value typically approximates the variance of the population of data as a whole. What this implies is that there is no spatial correlation beyond the distance a, referred to as the range of the variogram. At shorter distances, the data are spatially correlated to a greater or lesser extent, depending upon the separation distance involved. Variability observed at extremely short separation distances is referred to as a "nugget" effect, indicated as C_0. The nugget effect incorporates several factors related to small scale variability, including analytical errors, structure unresolved by the chosen sampling interval(s), and

---

term *variogram* is a case in point, and the argument hinges on the factor of one half referred to in the text. Some papers on geostatistics define two times gamma (without the factor) as the "variogram" (for valid theoretical reasons) and then proceed to work with gamma, referring to it as the "semi-variogram." Most practitioners appear to have bowed to what has become common verbal usage, and refer simply to "the variogram," usually with a footnote apology to "conventional, though theoretically sloppy jargon" (Isaaks and Srivastava, 1989, p. 65; see also David, 1977, p. 94; Englund and Sparks, 1988, p. xvi). The loss of the modifier "semi-" is entirely understandable as the field of geostatistics has grown from a single type of "variogram" to include an entire family of techniques for examining the correlation of values in space.

"true" erratic behavior of the phenomonon under study. Addition of a nugget effect has the impact of raising the entire variogram along the vertical axis. Variogram models may be added together (or nested) if required to represent the experimental data adequately.

The classical variogram uses one-half the average squared difference as the basis for describing spatial structure. In more recent work, a number of other quantities have been used (see, for example Englund and Sparks, 1988; Isaaks and Srivastava, 1989). Other measures of sample similarity or difference include the mean *absolute* difference (or madogram), and the *relative* mean squared difference (or relative variogram; gamma divided by the square of the mean of the values). A recently introduced measure that attempts to compensate for local changes in the sample means and variances is the so-called nonergodic covariance estimator (Isaaks and Srivastava, 1988). This latter technique is especially useful if the data are noticeably skewed or in the case of clustered or preferential sampling. The traditional variogram is notoriously unstable and difficult to interpret under these conditions. The nonergodic covariance may be presented in the form of a variogram simply by subtracting the covariance estimator from the a priori or sample variance (Isaaks and Srivastava, 1988, p. 330-336).

Whatever mathematical quantity for representing the degree of sample similarity is chosen, the variogram calculation process can be conducted with regard to absolute orientation. By examining variograms consisting of pairs that are restricted to those whose separation vectors are in a particular compass direction, spatial anisotropy can be identified and preserved. The only anisotropy firmly identified in this study is the case of down-the-hole versus lateral correlation distances. The data are insufficient for identifying "true" three-dimensional anisotropy.

Cross-validation of Variograms

A cross-validation technique is frequently used to evaluate the "goodness" of variogram models. The most commonly used method is to delete each measurement of a data set in turn, and to use the model of spatial structure developed from that data set to predict the missing value. Because the true value of each measurement is in fact known, one can calculate the error of prediction and compute various types of error statistics. If the model of spatial structure is a good one, presumably the errors will be approximately normally distributed with a mean equal to zero and a "small" standard deviation. Other measures of the overall error of prediction are the mean squared error (MSE) and the mean absolute error (MAE). Because the magnitude of the error is at least partially a function of the magnitude of the original units, the error statistics may be presented as the mean squared percentage error (MSPE) or mean absolute percentage error (MAPE).

Cross-validation can serve a useful purpose in causing the analyst to think about the variogram models developed in different ways. It is a useful exploratory tool. However, cross-validation has also been significantly abused as a method of choosing the "best" variogram model. Davis (1987) provides an interesting discussion of "Uses and Abuses of Cross-validation in Geostatistics." According to Davis (p. 247) the most prevalent abuses are the testing of a limited number of alternative models and reporting the best performer as optimum or inferring that a given model will outperform all others in general application based solely upon cross-validation of a single data set.

The concept of "best" obviously depends upon the criteria chosen. The various error statistics described above frequently do not agree with one another. This phenomonon may be observed with regard to the variogram models discussed below. The limitation of cross-validating from a single data set is

crucial. Indeed, it is becoming known in mining circles that the variogram developed from one subset of drill holes may be rather different from that developed from another subset, *even when the two subsets are physically interspersed one with another*, for example on the same mining bench (R. M. Srivastava, FSS International, Vancouver, B.C., pers. comm. at No. Am. Council of Geostatistics conference, Cloquet, Minn., Aug. 10-13, 1989). Such observations have limited the usefulness of the so-called "variogram cross" (for example, David, 1977, p. 199-200) as a technique for uniquely determining close-order spatial structure. Whatever the criteria, cross-validation can only help choose the "best" of the compared models. In fact, there is an indeterminate number of models of spatial structure that could be considered.

Additionally, because the types of error statistics typically used in cross-validation are global in scope, it may be possible to develop models that are globally unbiased, i.e., which have a mean error near zero, but which are conditionally biased (Isaaks and Srivastava, 1989, p. 264). A model with a conditional bias will overestimate (or underestimate) the true low values and underestimate (overestimate) the true high values. Depending upon the purpose of the analysis, it may be preferable to have a greater global error (judged by some particular statistic) in favor of less conditional bias over some particular range of values. The reverse situation (greater global accuracy) may be preferable in other analyses.

Despite the many limitations of the cross-validation technique, the various error statistics are presented for each variogram developed in this study. Within limits, error analysis can be useful in evaluating sufficiency of data and the adequacy of the spatial model.

Results: Lateral Correlation (Surface Data Set)

Porosity -- Sample variograms have been plotted for various subsets of the Calico Hills tuff data. Separate variograms were examined for samples from the Prow Pass traverses, the Calico Hills traverse, and for both locations combined. Porosity exhibits relatively consistent behavior across locations. As a result, most analysis focused on the combined data set.

A variogram model developed for the spatial correlation structure of porosity in the Calico Hills data set is shown in Figure 24. A model described by the following parameters has been fitted to the sample points.

Model type:	Spherical
Nugget:	9.00
Sill:	29.50
Range:	3,000.00
Mean Error:	0.067
MSE: 15.5	MSPE: 200
MAE: 3.0	MAPE: 10

It should be noted that although a mathematical variogram model has been fitted to the experimental data points in Figure 24, the fit is more an attempt to quantify the range of correlation than to present a comprehensive description of spatial structure. The underlying data set is only marginally adequate for much more than preliminary statements about spatial correlation. For example, in Figure 24, each point represents a number of pairs of physical samples. If each class interval is made large enough to capture a sufficient number of pairs (typically 30 to 90 in Figure 24), the interval becomes so large that the variability of squared differences may be poorly represented by some measure of central tendency. Reducing the class interval can be shown to reduce the variability markedly, but only at the expense of reducing the number of pairs below that generally considered acceptable for variogram analysis (typically about 30). Although the exact values of the parameters may be subject to individual interpretation, the implication is that porosity appears to

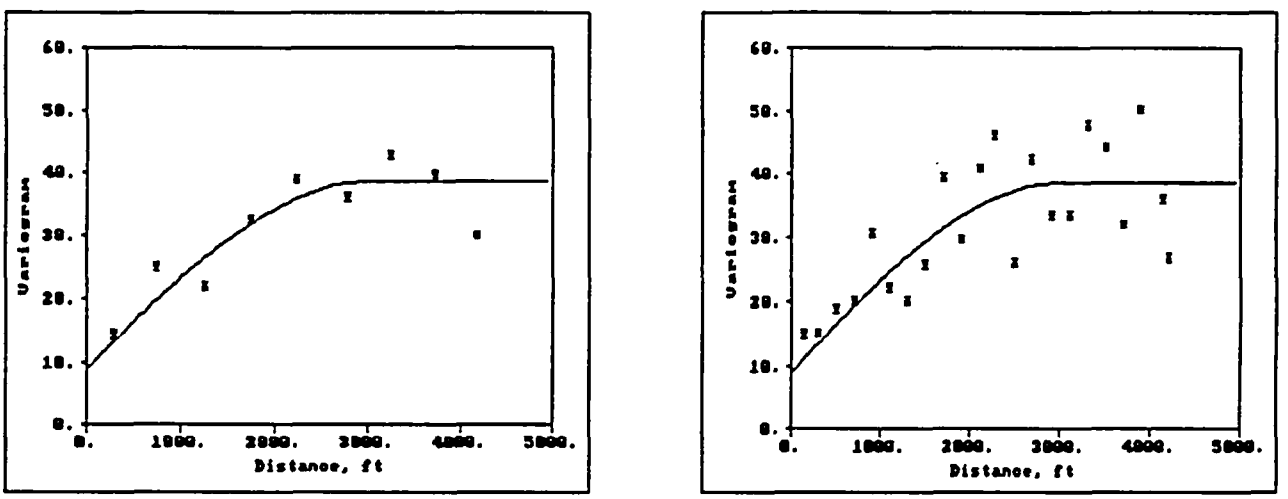

(a) (b)

Figure 24. Sample variogram and model for values of porosity from both surface localities. (a) Class interval 500 feet, total number of pairs (ΣN) = 421, number of pairs per point (N) typically = 30-90; (b) class interval 200 feet, ΣN = 419, N = 10-40.

exhibit a relatively well-defined spatial correlation structure for distances up to approximately 3,000 feet.

This variogram and its model are constructed under an assumption of isotropic structure; measurements are examined without regard for the orientation of the vector separating each pair of values. Because the majority of the outcrop data were obtained along a traverse oriented approximately north-south at Prow Pass (Figure 4), variograms were also constructed using only pairs whose separation vectors were along this direction. The resulting variogram together with virtually the same model (although with a smaller nugget) is shown in Figure 25. The sample variogram is somewhat better defined, although the number of pairs that constitute each point is below the limit generally considered acceptable (10 to 30 pairs per point).

Model type:	Spherical
Nugget:	3.00
Sill:	29.50
Range:	3,000.00
MSE: 15.6	MSPE: 200
MAE: 2.9	MAPE: 10

An observation of potential note in Figure 25 is the "flat" sequence of four data points at small separation distances. Such highly continuous behavior near the origin of a variogram is characteristic of a particular type of variogram model known as the Gaussian (Figure 23c). Such a model has been fitted to the identical sample data in Figure 26. The parameters are given as follows, and are otherwise identical to those of the spherical model presented in Figure 24.

Model type:	Gaussian
Nugget:	9.00
Sill:	29.50
Range:	3,000.00
Mean Error:	0.064
MSE: 16.8	MSPE: 216
MAE: 3.2	MAPE: 11

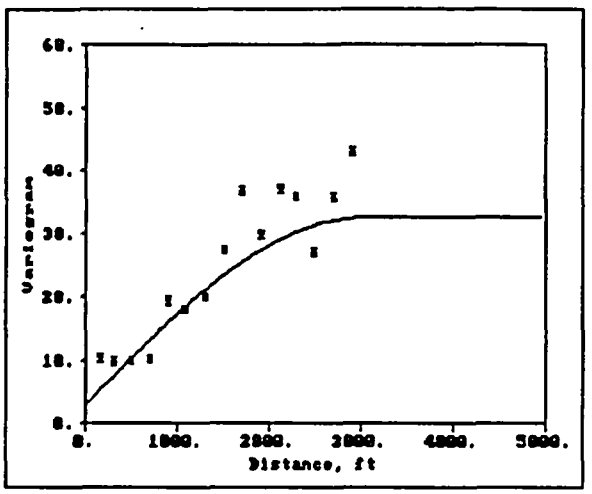

Figure 25. Sample variogram and model for values of porosity from north-south (Prow Pass) traverse only. Class interval 200 feet, ΣN = 374, N = 10-30.

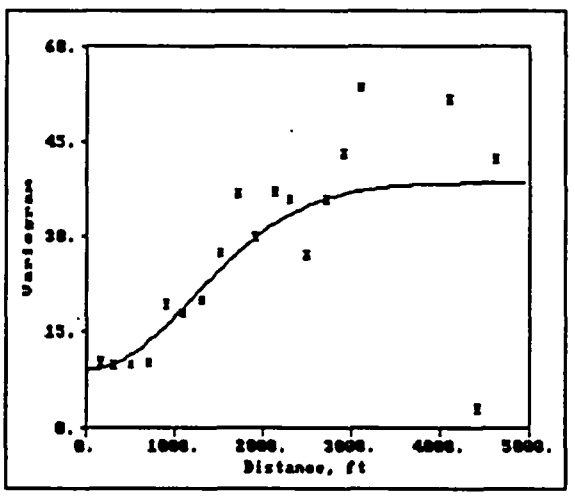

Figure 26. Sample variogram and alternative model for values of porosity from north-south (Prow Pass) traverse only. Class interval 200 feet, ΣN = 250, N = 10-20.

Use of the Gaussian model is typically restricted to those phenomena that are reasonably expected to be highly continuous at short distances. An example is the thickness of sedimentary units or the elevation of a stratigraphic contact in a flat-lying to only gently deformed terrane. Given that there is no particular reason to expect a rock property such as porosity to be highly continuous at short distances, one should most likely discount the model shown in Figure 26 as an artifact of the small data set available.

The restricted size of the Prow Pass and Calico Hills outcrop data set also limits the investigation of spatial anisotropy within the Calico Hills tuffs. Experimentation with variograms constructed in the north-south and east-west directions that correspond to the approximate orientation of the sample traverses (Figure 4) produced results that are a better illustration of techniques for dealing with anisotropy than of an actual description of Yucca Mountain. The resulting variograms could be interpreted to suggest that there may be a shorter range in the east-west direction (Figure 27). A potential model of the variogram shown in Figure 27 might be as follows.

Model type:	Exponential
Nugget:	3.00
Sill:	25.00
Range:	500.00

This model would not be usable directly in conjuction with one of the previously presented models for the north-south orientation (Figure 25) for estimation purposes, however. Variogram models incorporating anisotropy must be compatible with one another (see, for example Journel, 1978, p. 175-183). This implies that they must be of the same type (say, spherical) and with the same nugget and sill. In effect, the only difference allowed is the difference in range.

A congruent model of anisotropy is not presented here, because there are significant reasons for disbelieving the results obtained. First, the segmen-

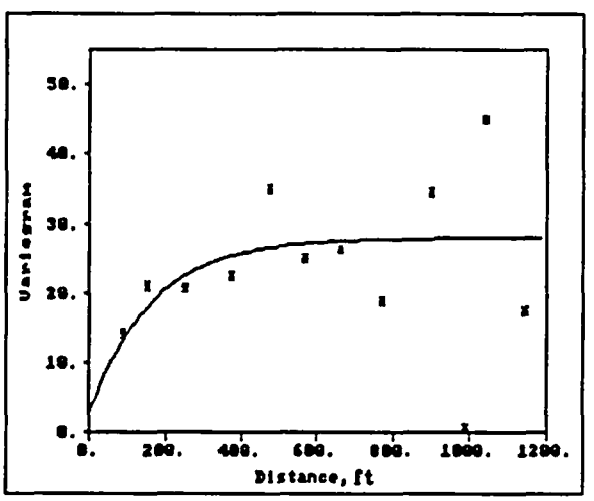

Figure 27. Sample variogram and model for values of porosity from east-west traverses. Class interval 100 feet, $\Sigma N = 60$, $N = 10$.

tation of the data set into the two directions produces east-west variograms whose sample points comprise far too few pairs to be considered reliable (Figure 27 comprises only about 10 pairs per point). Second, the longer (5,400-foot) north-south traverse provides a longer range than the two shorter (600- and 1,200-foot) east-west traverses. This correlation in particular suggests that the different observed ranges -- particularly in the east-west direction -- are an artifact resulting from insufficient sampling. A third cause of doubt in the reliability of the results is that there is no obvious geologic reason for a five- or six-to-one anisotropy ratio. Neither is there any particular evidence that suggests that the anisotropy is elongated exactly north-south as contrasted with some intermediate direction. Finally, in studies of spatial anisotropy, more than two directions should be investigated. This is not possible because of limited sampling in the current study (Figure 4).

Air Permeability -- In a similar fashion, variograms have been developed for the natural logarithms of air permeability. The examination has been restricted to only the samples from Prow Pass in an effort to eliminate one source of variability from the analysis. The behavior of air permeability data is much more erratic than that of porosity, as might be expected for this variable. A model described by the following parameters can be fitted to the sample variogram (Figure 28).

Model type:	Spherical
Nugget:	0.45
Sill:	0.30
Range:	1,200.00
Mean Error:	-0.030
MSE: 0.73	MSPE: 10^5
MAE: 0.71	MAPE: 204

A range of correlation of 1,200 feet seems excessively large for a vari-

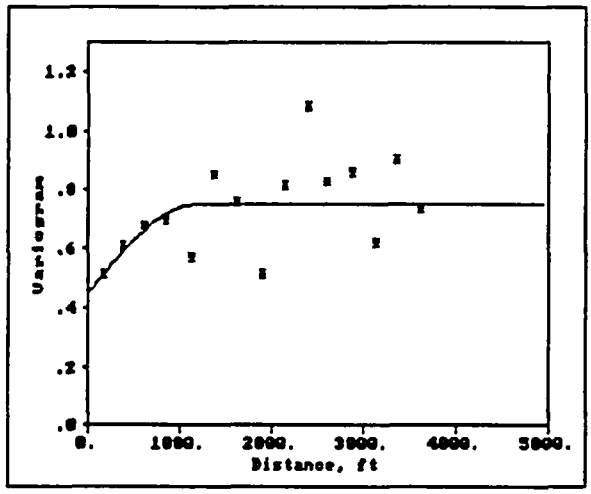

Figure 28. Sample variogram and model for natural log values of air permeability from Prow Pass sample locality. Class interval 250 feet, ΣN = 276, N = 10-30.

able such as air permeability. Additionally, the nugget effect identified is very large compared to the sill, suggesting that the class intervals used may be obscuring smaller scale detail. Efforts were made to examine the same data set at shorter separation intervals. However the existing data set is essentially inadequate for a rock property that varies over two orders of magnitude (Table 1).

Because of the significance of permeability-type rock properties to the Yucca Mountain Project, the issue of a large correlation range versus large nugget is of particular importance. Although the discussion that follows goes beyond the available numerical data, there are moderately compelling geologic interpretations that may be attached to the following speculation, which attempts to resolve smaller scale structure that simply may have been obscured by the class intervals chosen for Figure 28a.

Figure 29a presents a variogram developed for a class interval of 100 feet. This distribution of sample points might be represented by a nested model as follows.

Model types: Spherical (nested)
Nugget: 0.00
Sill: 0.47 0.28
Range: 400.00 1,200.00
Mean Error: -0.051
MSE: 1.16 MSPE: 10^5
MAE: 0.81 MAPE: 235

A simpler single term model of the identical data might use a different variogram form, the exponential model. This representation of the spatial structure of air permeability values has the following parameters (Figure 29b).

Model type: Exponential
Nugget: 0.00
Sill: 0.70
Range: 500.00
Mean Error: -0.048
MSE: 0.88 MSPE: 10^5
MAE: 0.75 MAPE: 219

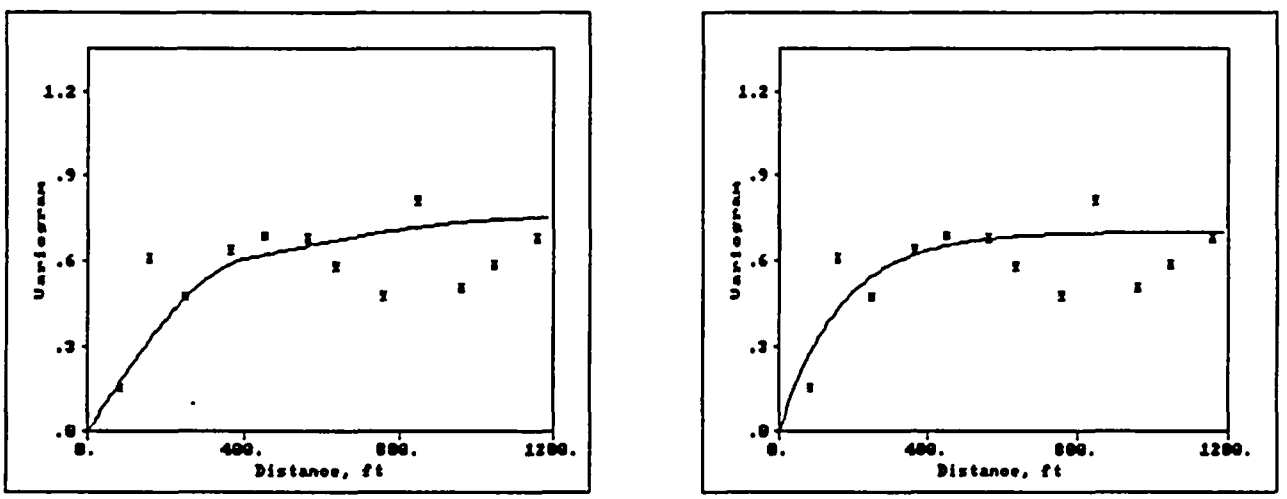

Figure 29. Sample variograms and alternative models for natural log values of air permeability from Prow Pass sample locality. Identical data resolved into (a) two nested spherical models, (b) exponential model. Class interval 100 feet, $\Sigma N = 249$, $N = 10\text{-}20$.

Neither representation is particularly convincing in itself. Overall variability is large as evidenced by the scatter of points. Additionally, the evidence for close-order structure is limited to the low-gamma point representing the shortest separation class. Because of limited data, there are only three pairs of samples represented in this class interval. However, two of the values are very small compared with the sill value, thus providing some evidence that samples separated by small distances are spatially correlated. A slight enlargement of the class size results in inclusion of six pairs. Three quarters of these closest pairs are valued at approximately half the sill value or less, again suggesting that there is some type of correlation underlying the otherwise quite messy data.

However extrapolated and dependent upon external geologic reasoning for validity, the nested variogram model of Figure 29b may yield the most intuitive interpretation of spatial correlation for air permeability. The relative sills and ranges of the two nested structures appear to indicate that a majority of the variability present -- that represented by the shorter range structure -- is achieved for separations of 400 feet (or less). In any event, the implication is that permeability is at least an order of magnitude less correlated spatially than porosity.

Results: Vertical Correlation (Drill Hole Data Set)

Porosity -- Variograms have been constructed for a number of subsets of the drill hole data from the Site and Engineering Properties Data Base. The general impression conveyed by these variograms is that expected from knowledge of stratigraphy. That is, that correlation distances are less in the vertical direction (across geologic units) than in the horizontal. The number of pairs of data composing each down-the-hole variogram is generally several hundred.

Figure 30a presents a vertical (down-the-hole) variogram for porosity from all stratigraphic units for 100-foot class intervals. The sample points are somewhat erratic, but they convey a distinct impression of increasing and then stabilizing variability with increasing separation distance. Figure 30b presents the nonergodic covariance in variogram format. The spatial structure revealed by this second presentation is much more evident and tightly defined. Both variograms are adequately represented by a single theoretical model as follows.

Model type: Exponential
Nugget: 45.00
Sill: 80.00
Range: 800.00
Mean Error: -0.055
MSE: 51.2 MSPE: 9990
MAE: 4.7 MAPE: 41

An alternative model for the same data might be as follows (Figure 31).

Model type: Spherical
Nugget: 55.00
Sill: 60.00
Range: 800.00
Mean Error: -0.065
MSE: 55.5 MSPE: 11454
MAE: 5.0 MAPE: 43

The distinction between the two mathematical models is not particularly significant, especially because the range is identical in both instances. Examination of the cross-validation statistics suggests that the exponential model may be a better representation -- at least for the existing set of data.

Because the vertical range of 800 feet intuitively seemed unlikely, some additional experimentation with variogram models was conducted. This work utilized the nonergodic variogram form exclusively because of the better definition of spatial continuity thereby obtained. This experimentation developed a three-term nested spherical model as follows (Figure 32).

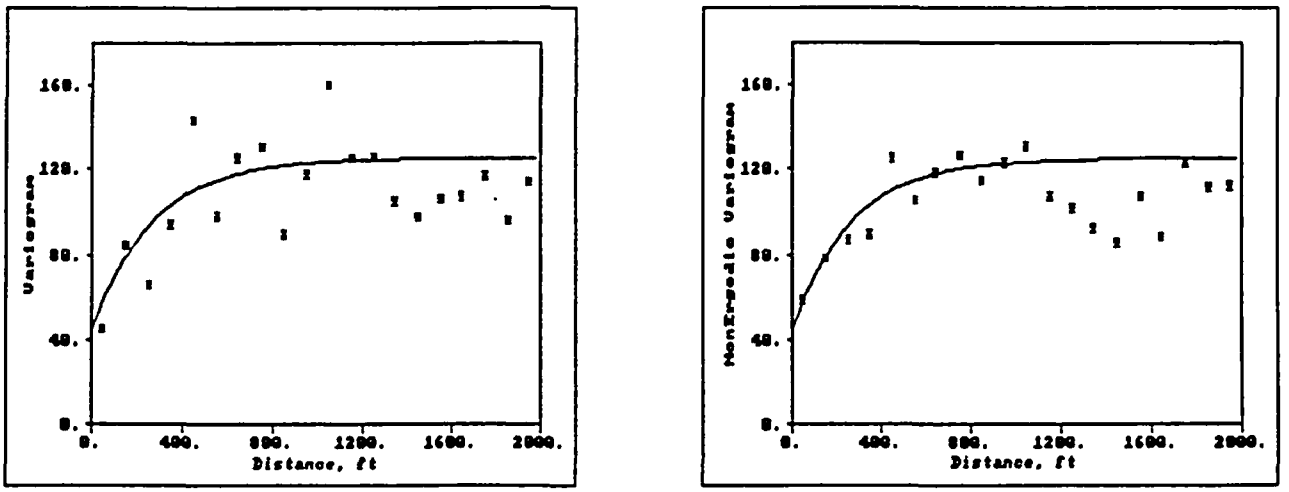

(a) (b)

Figure 30. Sample down-the-hole variograms and model for porosity values from all stratigraphic units. (a) Classical variogram, (b) nonergodic variogram. Class interval 100 feet, $\Sigma N = 6,543$, $N \approx 130$-550.

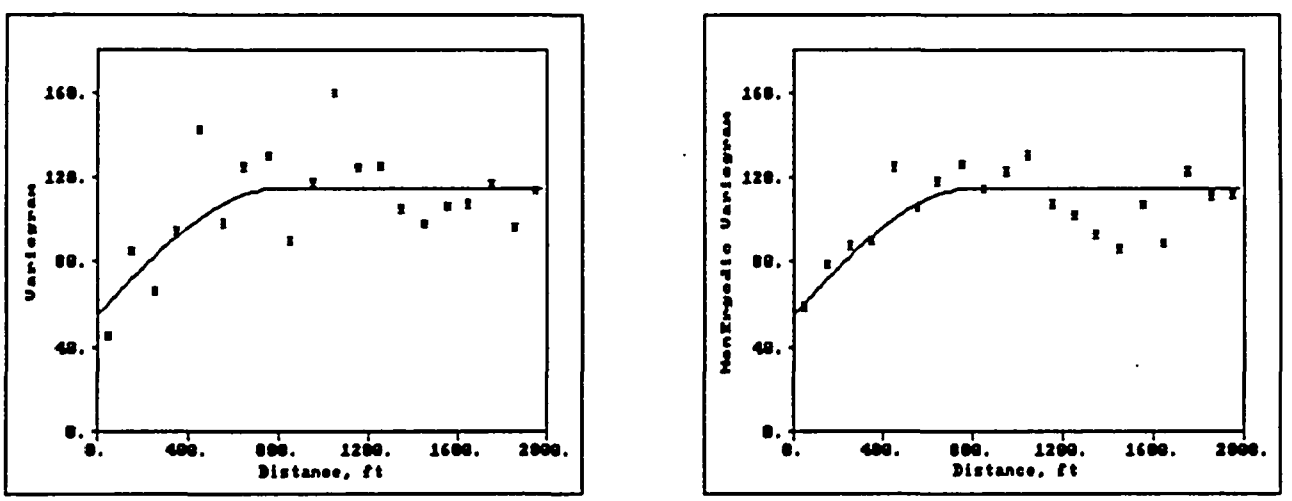

(a) (b)

Figure 31. Sample down-the-hole variograms and alternative model for porosity values from all stratigraphic units. (a) Classical variogram, (b) nonergodic variogram. Class interval 100 feet, $\Sigma N = 6,543$, $N \approx 130$-550.

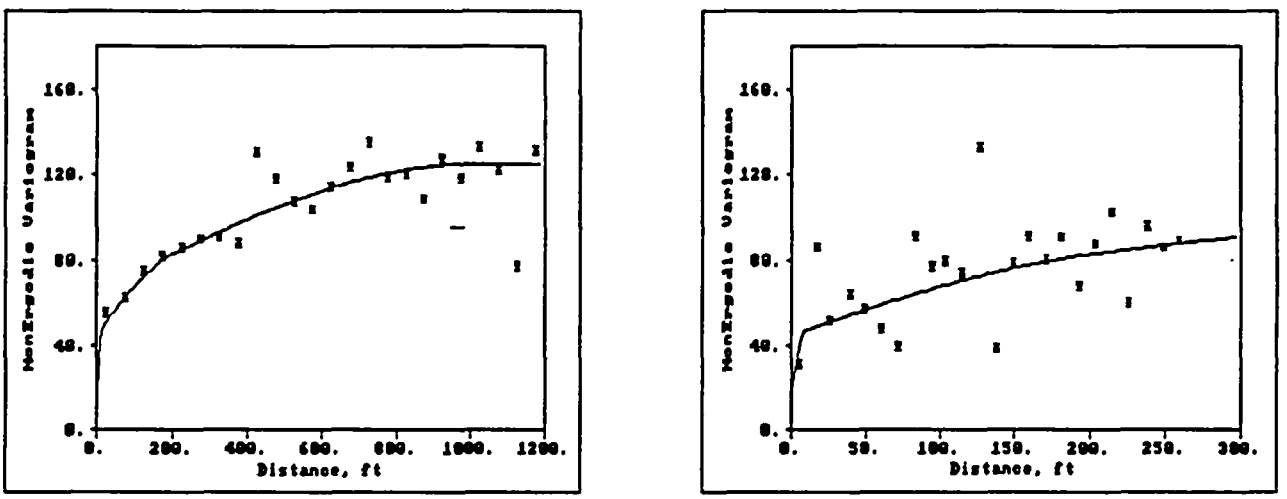

(a) (b)

Figure 32. Sample down-the-hole variograms and nested model for porosity values from all stratigraphic units. Nonergodic variogram, three-term nested model. (a) Class interval 50 feet, $\Sigma N = 4,838$, $N = 110-320$; (b) class interval 11 feet, $\Sigma N = 1,315$, $N = 20-120$.

Model types:	Spherical (nested)		
Nugget:	20.0		
Sill:	25.0	20.0	60.0
Range:	10.0	200.0	1,000.0

Mean Error: -0.017
MSE: 47.3 MSPE: 9407
MAE: 4.5 MAPE: 39

A physical interpretation of this nested structure might be as follows. The nugget, as usual, represents irresolvable, small-scale variability. The first structure with a = 10 feet represents continuity related to individual beds, particularly for the nonwelded units, or within subunits related to intra-ash flow eruptive pulses for the welded units. This data set is taken without regard for geologic stratigraphy. The larger-scale structure with a = 200 feet is most likely related to stratigraphic units themselves. The thousand-foot scale structure may again be reflecting stratigraphic units, or it may be indicating changes in porosity with gross position in the stratigraphic column. Such changes might reflect compaction related to overburden pressure or infilling of porosity by secondary minerals. There is a marked drop in gamma after about 1,200 feet (not shown) that suggests a stratigraphic-unit origin, in which the separation distance is such that one is comparing a nonwelded unit with the next nonwelded unit separated by a thick welded unit.

Obviously, such interpretations are highly speculative. Nevertheless, the identification of structure(s) with ranges smaller than 800 feet is "comforting," in that visual examination of the stratigraphic column at Yucca Mountain suggests quite a bit of vertical variability over much shorter distances.

The issue then arises as to the practical significance of the different models. Although the cross-validation error statistics of the three-term nested model are somewhat "better" than those for the simple, one-term exponential or spherical models, a simpler model may well be preferably for actual use. In particular, if kriging is to be conducted in two or three dimensions,

models chosen to represent anisotropy must be compatible. It will be significantly simpler to modify the one-term variogram model to account for anisotropy than to attempt the same task with a complex set of nested structures. Additionally, the sample set being used for estimation will influence the choice of models. If samples are spaced on the order of a few feet, the longer range structures will be completely unused in kriging; their effect will be screened out by nearby samples. Only if estimation is required for very wide sample spacings will the long-range structures prove important.

Because the variograms and models of Figures 30 though 32 were constructed without regard for stratigraphy, it is instructive also to consider spatial continuity within the Calico Hills unit only. Figures 33 and 34 present down-the-hole porosity variograms for samples of Calico Hills tuffs. Although this subdivision of the drill hole data eliminates the effects of comparing samples from different stratigraphic units, there are significantly fewer data to work with. The number of pairs in each separation class is generally less than desired, particularly at the shorter separations (some points are represented by as few as 15 pairs). The simple variogram is practically uninterpretable, whereas the nonergodic variogram reveals a rather clear pattern of spatial structure. The data may be represented by the following variogram model (Figure 33).

```
Model type: Spherical
Nugget:          15.0
Sill:            50.0
Range:          200.0
Mean Error: -0.168
MSE: 29.5  MSPE: 481
MAE:  4.3  MAPE:  15
```

An alternative variogram model for porosity may also be fitted to the Calico Hills data (Figure 34).

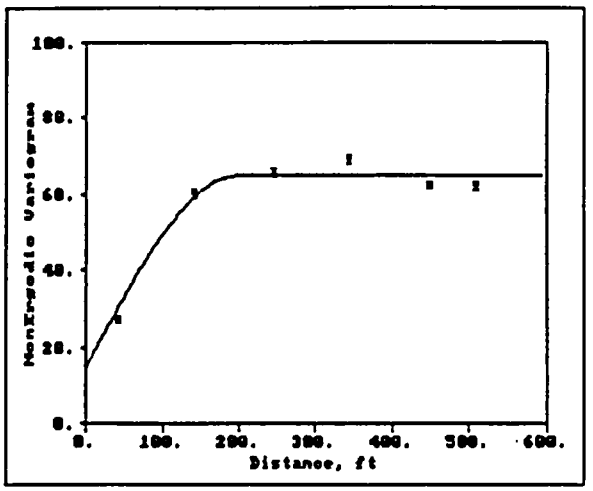

Figure 33. Sample down-the-hole variogram and model for porosity values from the tuffs of Calico Hills only. Nonergodic variogram. Class interval 100 feet, $\Sigma N = 139$, $N = 15\text{-}40$.

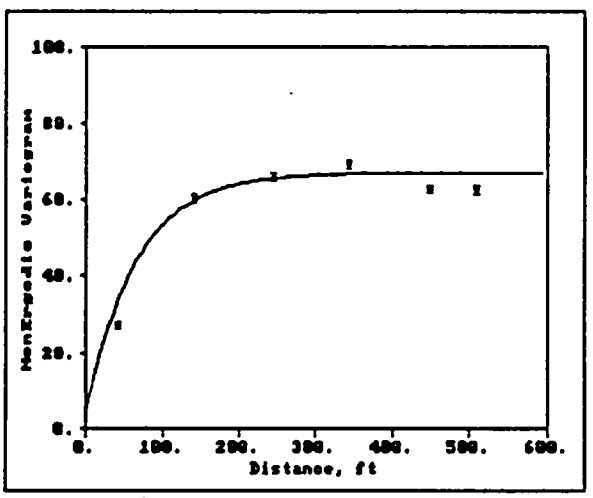

Figure 34. Sample down-the-hole variogram and alternative model for porosity values from the tuffs of Calico Hills only. Nonergodic variogram. Class interval 100 feet, $\Sigma N = 139$, $N = 15\text{-}40$.

Model type: Exponential
Nugget: 5.00
Sill: 62.00
Range: 200.00
Mean Error: -0.273
MSE: 24.8 MSPE: 370
MAE: 4.0 MAPE: 14

Although the variograms of both Figures 33 and 34 depend heavily upon the data point representing the shortest separation class, there is a more than sufficient number of pairs constituting this point (n = 39).

Comparing the data set representing the Calico Hills tuffs to that for all stratigraphic units, one notices several features. First, the total variability in porosity represented by the sill is smaller for the single stratigraphic unit, about one-half the value for all units. This is as expected for a relatively homogeneous stratigraphic unit compared with an aggregation of many different rock types (including both densely welded and nonwelded tuffs). Second, the range is shorter and better defined. This implication of more rapid vertical variability is compatible with knowledge that the Calico Hills sequence includes intercalated nonwelded and bedded units, which are compared with the overall data set, which includes welded tuffs that form cooling units many hundreds of feet thick.

Conductivity -- Similar variograms were constructed for the drill hole hydraulic conductivity data without regard for stratigraphic unit. The conductivity data are much fewer in number (n = 42, Table 3) than for porosity (over 300). Only one conductivity value from the Calico Hills tuffs appears in the Site and Engineering Properties Data Base; hence no analysis was attempted for the Calico Hills unit.

Figure 35 presents simple and nonergodic variograms for hydraulic conduc-

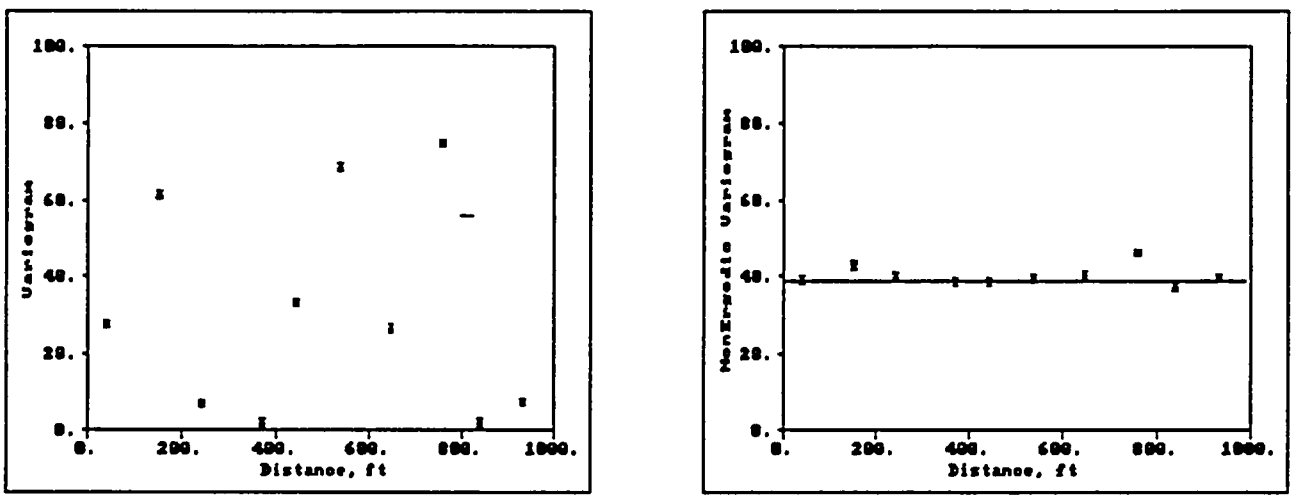

(a) (b)

Figure 35. Sample down-the-hole variograms for values of hydraulic conductivity. (a) Classical variogram, (b) nonergodic variogram. Class interval 100 feet, $\Sigma N = 283$, $N \approx 10$-30.

tivity (multiplied by 10^4 as a rescaling factor). The classical variogram (Figure 35a) appears to be pure noise, with sample values plotting all over the diagram. The nonergodic version of the variogram (Figure 35b) is much more coherent, but the interpretation is much the same. The only model that can be fitted to the hydraulic conductivity data is a pure nugget effect, here shown equal to the variance of the data set. The nugget effect reveals itself clearly on all scales examined, varying from 200-foot class intervals to 10-foot class intervals.

Both the classical and nonergodic variograms contain squared or product terms in their formulation. If the raw values vary over several orders of magnitude (hydraulic conductivity varies from 10^{-3} to 10^{-7}; Table 2), the effect of the squared term becomes overwhelming. Journel (1983, p. 445) states that when dealing with "highly variant phenomona, ... raw variograms become extremely sensitive to high-valued data, and are basically useless." In this case with a four-order of magnitude variability, even the nonergodic covariance estimator is unable to reveal underlying structure. Indeed, the appearance of what seems to be a well-defined pure nugget effect may argue against the existence of structure.

Because of the extreme variability of the conductivity data, it is possible that spatial correlation is obscured by artifacts of the calculational process. There are several techniques for attempting to reduce the distorting effect of multiplying widely differing values or squaring very large differences. First, one can examine the so-called madogram, which uses the mean absolute difference instead of the squared difference. Second, one can transform the data to reduce the variability and apply the variogram operator to the transformed values. The log transform historically is a commonly used technique, but the reverse transformation from log space to normal space creates

difficulties in estimation. A less commonly used transformation is the rank-order transform. This transform substitutes the relative order of each value (1, 2, 3, ..., N) for the absolute magnitude of the measurements. The technique has the same effect of "compressing" the variability of the data as taking the logarithms. Still another transform that extinguishes all variability except "highs" and "lows" is the indicator transform developed by Journel (1983). This technique recodes all samples to 1 if the sample value is below some particular cut-off value and to zero otherwise. In effect, one examines whether the "higher-than" samples cluster separately from the "lower-than" samples, or if the two classes are interspersed.

Applying these methods to the drill hole conductivity values yields mixed, but intriguing results. The madogram is as uninterpretable as the simple variogram of Figure 35a. However, the three transformed data sets contain indications of spatial correlation that cannot simply be ignored. The data are presented in Figure 36. The number of pairs comprising each point on the variograms is generally considered adequate, especially for the ones with 200-foot class intervals. These variograms may be modeled as follows.

log Variogram		Rank-Order Variogram	
Model type:	Spherical	Model type:	Exponential
Nugget:	2.50	Nugget:	0.00
Sill:	2.20	Sill:	160.00
Range:	500.00	Range:	300.00
Mean Error:	0.12	Mean Error:	1.18
MSE: 5.0	MSPE: 793	MSE: 160	MSPE: 10^4
MAE: 1.6	MAPE: 17	MAE: 10	MAPE: 113

Median Indicator Variogram	
Model type:	Spherical
Nugget:	0.20
Sill:	0.12
Range:	800.00
Mean Error:	0.0041
MSE: 0.23	MSPE: 10^3
MAE: 0.40	MAPE: 20

Nonergodic variograms of the rank-order transformed values were examined

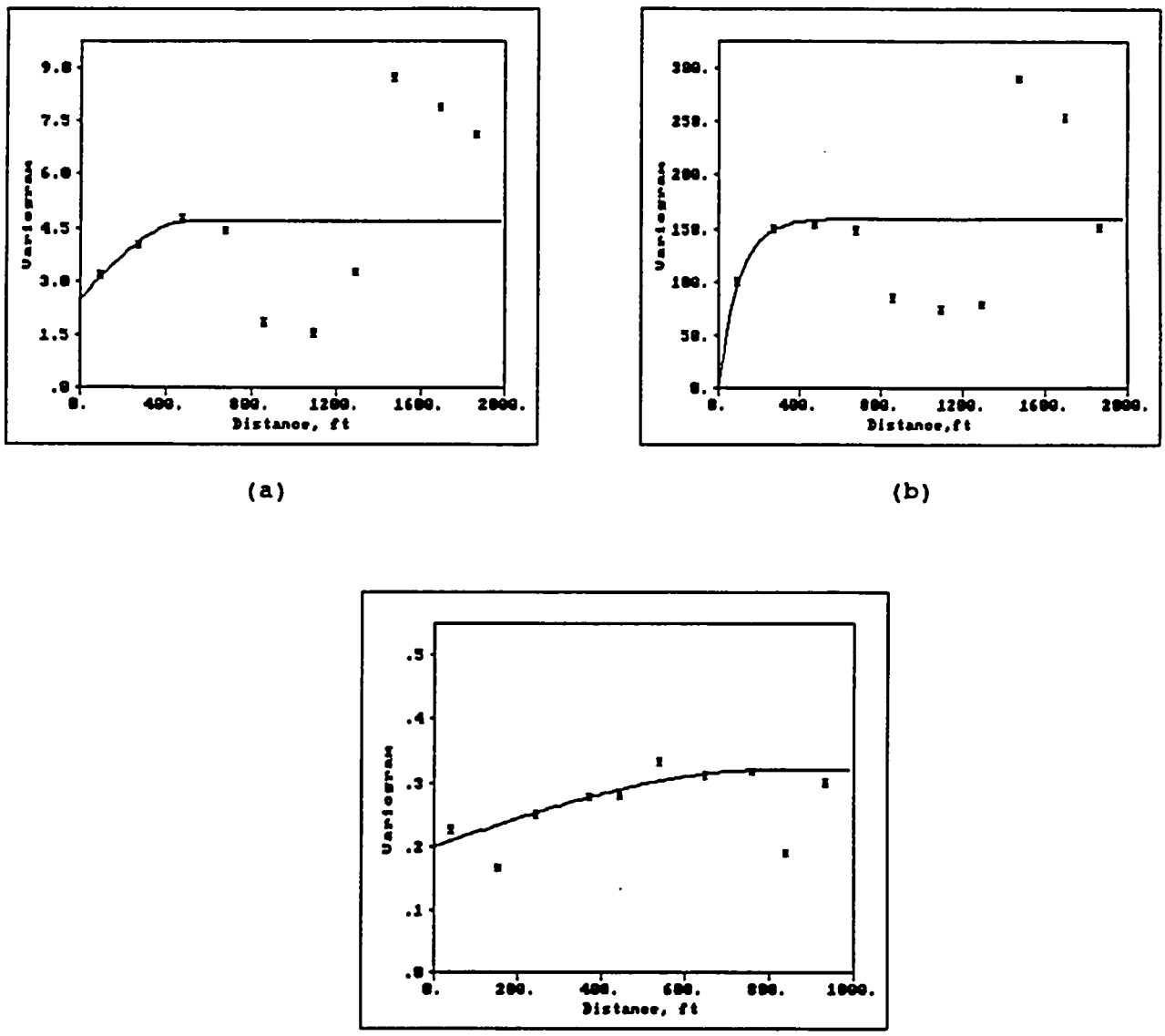

Figure 36. Sample down-the-hole variograms and models for (a) natural log transform, (b) rank-order transform, and (c) median-indicator transform of values of hydraulic conductivity. (a) and (b) Class interval 200 feet, $\Sigma N = 274$, $N \approx 20$-60; (c) class interval 100 feet, $\Sigma N = 283$, $N \approx$ 10-30.

in an effort to refine close-order spatial structure because it seemed unlikely that a nugget of zero was warranted for hydraulic conductivity (Figure 36b). Figure 37 shows the results of this exercise for two different groupings of the data: 100-foot and 22-foot class intervals. The same model has been fitted to both figures.

Model type:	Spherical
Nugget:	15.00
Sill:	85.00
Range:	500.00
Mean Error:	0.57
MSE: 150.3	MSPE: 10^4
MAE: 9.4	MAPE: 105

Although the number of pairs for each sample point in Figure 37b is below that considered acceptable for a valid variogram (maximum of 12 pairs per point), the consistency of the pattern throughout the analysis suggests that there is in fact some spatial structure with approximately a 300- to 500-foot range. Both the rank-order and indicator analyses are saying that high values tend to be clustered with other high values, whereas low values tend to cluster with other low values.

The indicator variogram presented in Figure 36c utilized the median conductivity value as the cut-off, or threshold value. Use of the median value causes one-half the sample data to become zeros while the other half become ones. This equal division will produce the most stable results. It is possible to code the data to any other desired threshold as well. However, the number of values above cut-off will become markedly greater or smaller than the number of values below as the extremes of the distribution are approached. Clearly, this approach is not possible with the current small data set. Journel and Alabert (1989) have identified instances wherein the spatial structure of high values as revealed by indicator coding of the 90th percentile is vastly different from that portrayed by indicator coding of the median or

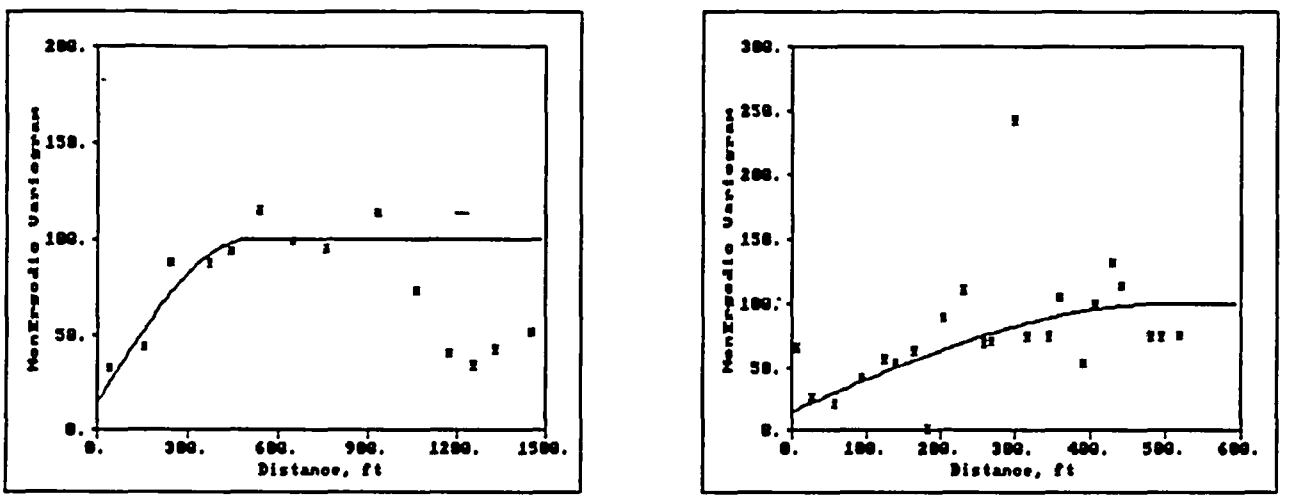

Figure 37. Nonergodic sample down-the-hole variogram and model for rank-order values of hydraulic conductivity. (a) Class interval 100-feet, $\Sigma N = 274$, $N \approx 10$-30; (b) class interval 22 feet, $\Sigma N = 129$, $N \approx 12$ or less.

lower percentiles. Given the confounding effect of extreme values, it is likely that an analysis technique that simply lumps all data together could fail to reveal actual structure (cf. the "pure nugget" structure of Figure 35). Significantly, Journel and Alabert (1989) illustrate their spatial structure-absolute magnitude dependence with permeability data!

The pronounced decrease in variogram values associated with separations of greater than 800 feet in Figures 36 and 37 demands some comment. The progressive increase and later decrease in variability with increasing vertical separation distance suggests that the conductivity values are reflecting some type of periodicity in the hole, such as less-welded to nonwelded tops and bottoms of thick ash flow units (approximately 800 to 1,000 feet thick). This phenomonon is frequently referred to as a "hole effect." If one examines the actual spatial distribution of conductivity values, it is possible to observe such a periodicity of values, particularly in Figure 18.

A final caveat should be applied to the foregoing discussion of correlation for hydraulic conductivity. It turns out that the majority of conductivity data available in the Project Site and Engineering Properties Data Base are from rock units below the repository horizon. The relevance of the conclusions of this section to the actual repository units is thus somewhat indirect.

Dry Bulk Density -- Because it initially seemed unlikely that hydraulic conductivity values would exhibit such large spatial correlation, particularly in a vertical (cross-stratigraphy) direction, drill hole data for a third rock property were examined. Dry bulk density generally exhibits very little variability in comparison to hydraulic conductivity. The coefficient of variation across all stratigraphic units is only 14 percent (Table 2). Because of this

low univariate variability, it was anticipated that this rock property would be relatively well-behaved spatially as well. Figure 38 presents a well-defined variogram for bulk density. The data are modeled as follows.

Model type: Exponential
Nugget: 0.010
Sill: 0.095
Range: 600.000
Mean Error: -0.0026
MSE: 0.03 MSPE: 140
MAE: 0.12 MAPE: 7

An alternative model might employ a spherical variogram model instead of an exponential (Figure 39).

Model type: Spherical
Nugget: 0.035
Sill: 0.075
Range: 800.000
Mean Error: -0.0019
MSE: 0.04 MSPE: 169
MAE: 0.13 MAPE: 7

A somewhat different model is suggested by the nonergodic variogram shown in Figure 40. The sample data are much more tightly organized by this direct estimate of the spatial covariance. However, the model that follows suggests a much higher nugget-to-sill ratio than does the classical variogram.

Model type: Exponential
Nugget: 0.320
Sill: 0.085
Range: 700.000
Mean Error: 0.0001
MSE: 0.05 MSPE: 203
MAE: 0.15 MAPE: 8

If the analysis is restricted to only samples of the Calico Hills, the result is a variogram model with a much lower sill, approximately 25 percent of that for the model that results for samples of all stratigraphic units. This difference in variance is as expected for a relatively homogeneous unit compared to a mix of welded and nonwelded rocks. A more important difference is that the range of spatial correlation within the Calico Hills unit is less,

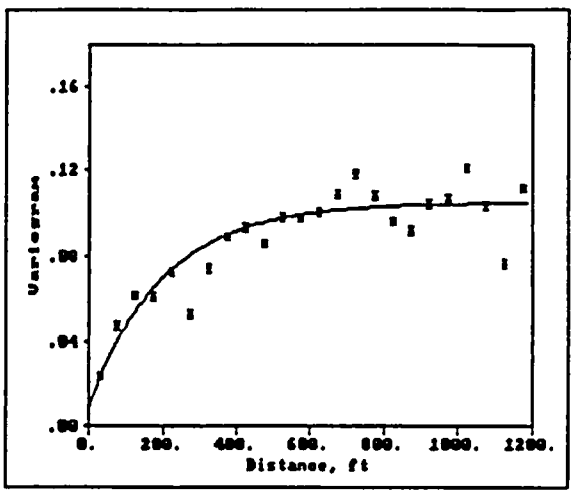

Figure 38. Sample down-the-hole variogram and model for values of dry bulk density from all stratigraphic units. Class interval 50 feet, ΣN = 4,188, N ≈ 120-220.

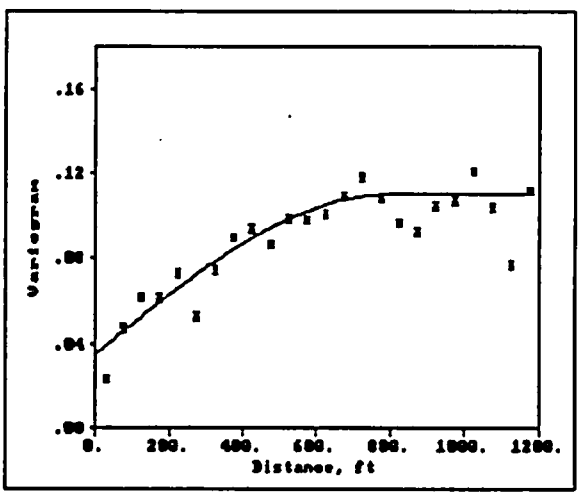

Figure 39. Sample down-the-hole variogram and alternative model for values of dry bulk density from all stratigraphic units. Class interval 50 feet, ΣN = 4,188, N ≈ 120-220.

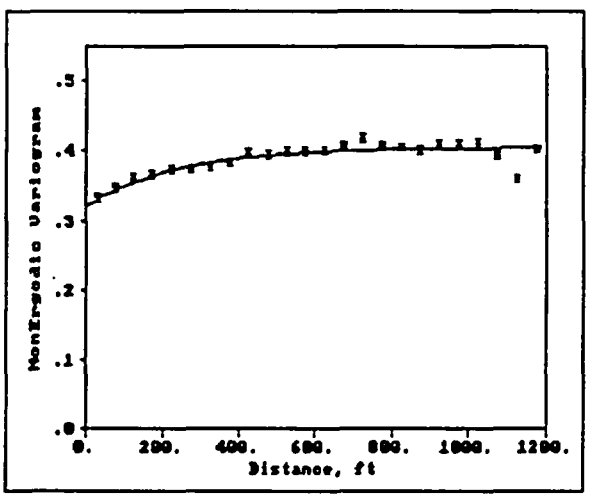

Figure 40. Sample down-the-hole variogram and model for values of dry bulk density from all stratigraphic units. Nonergodic variogram. Class interval 50 feet, ΣN = 4,188, N = 120-220.

roughly 200 feet compared with 600 to 800 feet for all units. This too, is as expected. The Calico Hills is an intercalated sequence of bedded and nonwelded tuffs, whereas a dominant portion of the entire stratigraphic column is massively welded units. A satisfactory model is presented in Figure 41 as follows.

Model type: Spherical
Nugget: 0.008
Sill: 0.020
Range: 200.00
Mean Error: 0.0004
MSE: 0.02 MSPE: 83
MAE: 0.12 MAPE: 7

Efforts to "clean up" the variogram by using the nonergodic formulation produced a more tightly defined sample pattern (Figure 42). As with bulk density taken without regard for stratigraphy (Figure 40), the nugget-to-sill ratio is much higher. Additionally, the range of correlation is even shorter: a mere 80 feet. The model for the nonergodic variogram is as follows.

Model type: Exponential
Nugget: 0.140
Sill: 0.055
Range: 80.00
Mean Error: -0.0043
MSE: 0.02 MSPE: 84
MAE: 0.13 MAPE: 8

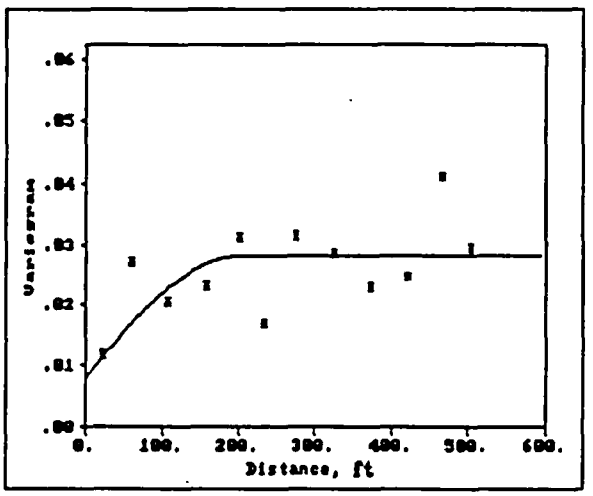

Figure 41. Sample down-the-hole variogram and model for values of dry bulk density from Calico Hills tuffs. Class interval 44 feet, ΣN = 134, N = 10-20.

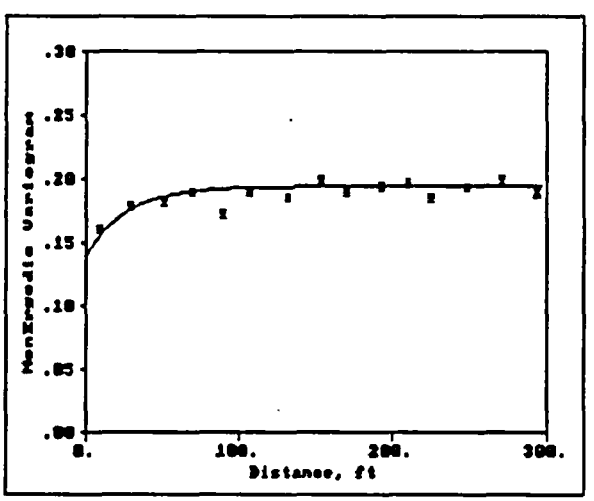

Figure 42. Sample down-the-hole variogram and model for values of dry bulk density from Calico Hills tuffs. Nonergodic variogram. Class interval 20 feet, ΣN = 127, N = 15 or less.

DISCUSSION AND IMPLICATIONS

Summary of Findings

This study employed geostatistical techniques to examine the spatial correlation characteristics of physical properties measured on outcrop and subsurface samples of volcanic tuffs from Yucca Mountain, Nevada. Rock properties examined include porosity, air permeability, saturated hydraulic conductivity, and dry bulk density, although not all properties have been measured on all samples. A number of possible variogram models have been fitted to the sample data as summarized in Table 4.

The data obtained from outcrop samples of the Calico Hills tuffs suggest that porosity is spatially correlated for lateral distances of up to approximately 3,000 feet. Similar porosity data obtained from core samples of Calico Hills tuffs suggest that the range of vertical correlation is approximately an order of magnitude less, perhaps up to 200 feet or so. A ratio of anisotropy of 10- or 15-to-1, as suggested by the data in Table 4, is not unexpected for a stratified lithologic unit, such as the Calico Hills. The unit is well layered in outcrop.

If porosity values are examined vertically, across stratigraphy, but without regard for lithologic unit, a longer range correlation structure with range of 800 to 1,000 feet can be identified. The nugget effect associated with this larger correlation structure is significantly larger than that associated with the single-unit stratigraphic subset of the data. A single model consisting of three nested structures can be developed that rationalizes both scales of spatial correlation.

For the interpretive purposes of this study, air permeability and saturated conductivity are viewed by this study as (poor?) substitutes for each other. This "equivalence" is more of necessity than of desire: the air permea-

Table 4. Summary of Variograms Modeled by this Study.

Property	Unit	Type	C_o	C	a	M.E.	MAE	Remarks
Porosity								
horiz.	CHn	Sph.	9.0	29.5	3000	.067	3.0	pref.
	CHn	Sph.	3.0	29.5	3000	.047	2.9	N-S
	CHn	Exp.	3.0	25.0	500	--	--	quest.
	CHn	Gaus.	9.0	29.5	3000	.064	3.2	
vertical	all	Exp.	45.0	80.0	800	-.055	4.7	pref.
	all	Sph.	55.0	60.0	800	-.065	5.0	
	all	Sph.	20.0	25.0	10			
		"	nested	20.0	200			
		"	nested	60.0	1000	-.017	4.5	
	CHn	Sph.	15.0	50.0	200	-.168	4.3	pref.
	CHn	Exp.	5.0	62.0	200	-.273	4.0	
ln(Air Perm)								
horiz.	CHn	Sph.	.45	.30	1200	-.030	.71	
	CHn	Sph	0.0	.47	400			
		"	nested	.28	1200	-.051	.81	
	CHn	Exp.	0.0	.70	500	-.048	.75	pref.
Hyd. Cond.								
vertical	all	nugget	38.7					
(ln)	all	Sph.	2.5	2.2	500	.12	9.4	pref.
(R/O)	all	Exp.	0.0	160.0	300	1.18	10.0	
(R/O)	all	Sph.	15.0	85.0	500	.57	9.4	
(ind.)	all	Sph.	0.2	0.12	800	0.004	0.4	
Dry Bulk Density								
vertical	all	Exp.	.010	.095	600	-.0026	.12	pref.
	all	Sph.	.035	.075	800	-.0019	.13	
	all	Exp.	.320	.085	700	.0001	.15	
	CHn	Sph.	.008	.020	200	.0004	.12	pref.
	CHn	Exp.	.140	.055	80	-.0043	.13	

Note: M.E. = mean error; MAE = mean absolute error; Sph. = spherical model; Exp. = exponential model; Gaus. = gaussian model; ln = natural log transform; R/O = rank-order transform; ind. = median indicator transform; pref. = preferred model for this rock property; C_o = nugget; C = sill; a = range of correlation.

bility data are available only in a lateral orientation, and only conductivity data are available vertically. Both types of data are potentially correlated for distances of up to 400 or 500 feet (Table 4), although this conclusion definitely stretches the limitations of the existing data. No particular anisotropy can be identified using the preferred models of spatial variability.

However, there may be a longer-range lateral structure with correlation distances of up to 1,200 feet (a 2-to-1 ratio). The cause of spatial correlation of such magnitude in a rock property as highly variable (in a univariate sense) as permeability is uncertain. Cross-validation errors for both air permeability and hydraulic conductivity are quite large. There is some evidence suggesting that evaluation of spatial structure for permeability-type data may be obscured by value-related anisotropy such as that described by Journel and Alabert (1989). Additional closely spaced data are required to resolve these issues.

Drill hole data for bulk density were examined briefly as well. The stratigraphic subset of data for the Calico Hills tuffs indicates that this rock property is correlated vertically for distances of up to 200 feet (Table 4). This magnitude of spatial correlation is the same as that observed for down-the-hole porosity values. If the density data are examined without regard for stratigraphy, the range of correlation expands to approximately 600 or 700 feet (Table 4). In similar fashion to porosity, the nugget effect associated with the lumping together of stratigraphic units is larger than in the single-unit Calico Hills case. No density data are available for determination of lateral correlation structure.

Application of Spatial Structure Findings to Site Characterization

One of the principal concerns involved in the nuclear waste repository program at Yucca Mountain is the determination of the adequacy of geologic and engineering characterization of the site. However, there are different criteria for "adequate" depending upon how one views the purpose of site characterization. End-member views of site characterization may be described as (1) "representative" value characterization, here taken as a mean-plus-or-

minus-standard deviation formula, or (2) sampling for identification of extreme values. Regardless of the perspective desired, spatial correlation of rock properties has implications for characterization efforts, in that application of classical statistical techniques to spatially dependent samples without adjusting for that dependence will produce overly confident results.

The Yucca Mountain Project Site Characterization Plan (DOE, 1988) describes plans for surface-based drilling and testing activities. The implication of the geostatistical analysis presented here is that initial sampling of the site under these site characterization activities should take place on a scale that is well within the range of correlation for the rock properties of interest. For porosity -- and by extension, any rock property that is correlated with porosity -- drill holes should be located no more than one to two thousand feet apart. A sample spacing of more than 85 percent of the range of correlation is described as sparse by Yfantis and others (1987, p. 203). Eighty-five percent of 3,000 feet is 2,250 feet. For hydraulic conductivity and any other rock properties correlated therewith, the implication is that sample locations should be no more than a few hundred feet apart horizontally; 85 percent of 500 feet is 425 feet. The 500-foot horizontal range for permeability identified by this study appears to be a maximum value, in that the model sill value of approximately 0.7 $[\ln(md)]^2$ is reached for separations of this magnitude (Figure 29). The actual range may be shorter, as is suggested by the empirical points in Figure 29. The 1,200-foot structure modeled by Figure 28 is largely discounted, because the very large nugget effect exhibited (some 60-plus percent) suggests that the inferred relationship is very weak at this scale. More closely spaced data must be obtained to confirm the structure of air permeability.

The range of vertical correlations obtained by this study suggests that

some rock properties may be more highly correlated spatially than previously believed. Accordingly, fewer samples may be required in each drill hole than initially planned. Sampling and testing of different rock properties most likely can be conducted on different scales because of larger or smaller ranges of correlation. However, because existing data for hydraulic conductivity are somewhat limited, the correlation structure developed for this potentially critical rock property is moderately suspect. Additional sampling, either from the underground workings of the Exploratory Shaft Facility or from outcrops, should be used to confirm the close-order variability of all rock properties of interest. Initial sampling and testing of site characterization drill holes should be at a fairly close interval to confirm these interpretations.

After site characterization activities are underway, knowledge of the degree of spatial correlation may be used to evaluate the adequacy of the results of those activities under either major purpose of characterization. If one adheres to the representative value philosophy, one must temper the classical confidence limits (Equation 1) inferred for the mean value by the realization that physical samples taken within the correlation distance of other samples do not count as "full" independent samples for statistical purposes. Calculation of the number of equivalent independent samples, N_{eq}, can utilize the method presented by Barnes (1988). Alternatively, if one ascribes to the extreme-value sampling objective presented originally by Barnes (1988) and reviewed in the earlier sections of this paper, the liklihood that a given level of sampling has detected at least one value exceeding the ß-percentile of that property's distribution of values will be affected by the degree of spatial correlation that exists for that rock property.

For example, applying Barnes' method for calculating the number of equivalent samples to the outcrop locations (N = 38) sampled for this report yields

N_{eq} = 13.3 for porosity and N_{eq} = 18.4 for air permeability using the "preferred" spatial models summarized in Table 4. The different values arise because of the longer range for porosity. With greater spatial correlation, each physical sample contributes less additional information, thus resulting in a lower N_{eq}. If we apply Equation 2 using these values of N_{eq}, we obtain the probabilities shown in Table 5 of having sampled an extreme value corresponding to the indicated percentile of the rock property's underlying distribution.

Table 5. Probability of Sampling an Extreme Value

Variable	Percentile	Probability
Porosity, horiz.	.50	0.9999
Porosity, horiz.	.75	0.9780
Porosity, horiz.	.90	0.7529
Porosity, horiz.	.95	0.4937
Porosity, horiz.	.99	0.1248
Air Perm., horiz.	.50	1.0000
Air Perm., horiz.	.75	0.9949
Air Perm., horiz.	.90	0.8553
Air Perm., horiz.	.95	0.6098
Air Perm., horiz.	.99	0.1684

The conclusions regarding sample spacing presented in this section suggest that vertical sampling of site characterization drill holes will be more than adequate for modeling needs. In an otherwise unconstrained setting, it would appear desirable to increase the number of drill holes while limiting vertical sample densities to the level actually required. However, the Yucca Mountain Project is constrained by regulatory requirements to limit penetrations of the site. Thus, it is not necessarily a simple matter of transferring resources from sampling and analytical efforts focused on a few sites to drilling additional holes.

A possible approach to resolving to this dilemma of being unable to sample enough lateral locations may lie in geostatistical simulation. In simulation,

a number of equally likely "realizations" of rock properties may be generated, all of which exhibit the same spatial correlation structure. In effect, the same geostatistical model that is used in kriging can also be used to generate a series of potential "Yucca Mountains." These multiple images of a true but unknown reality may then be examined to see if the conclusions of performance assessment or design analyses are sensitive to the type of uncertainty that results from inadequate horizontal sampling. If the final results *are* sensitive to the uncertainty implied by the multiple simulations, then additional data must be required to reduce that uncertainty.

Journel and Alabert (1989) note other advantages of simulation, or "data expansion" in their words, over a more deterministic kriged estimate. The kriging process is well known to "smooth" the variability of a field of data. Although a kriged model will always respect known data points (the process is an exact interpolator), the overall effect is to smear out a certain degree of the variability expected on geologic grounds. Simulation, on the other hand, can preserve a "sharpness" of image, even though repeated simulations will vary in detail according to the degree of uncertainty in sampling the site. Journel and Alabert provide an excellent illustration of the differences between the two techniques (their Figures 1 and 2).

Speculation on the Origin of Spatial Correlation

The existence of large-scale spatial correlation in volcanic tuffs such as identified through the variograms presented in this report is somewhat unexpected. Although the data for the lateral correlation portion of this work are more limited than desirable, the number of samples available from vertical drill holes is large. Confidence in the large vertical ranges is relatively high, particularly for porosity and bulk density.

Although a specific mechanism for the origin of such correlation is unknown, it may be instructive to examine the mode of emplacement of tuffs at Yucca Mountain. Figure 43 is a schematic representation of an ash flow eruption patterned after the general setting of the Southwestern Nevada Volcanic Field (Figure 5). Plinian-type eruptions associated with collapse of a major caldera 8 to 15 miles across (Timber Mountain-Oasis Valley complex; Carr, 1988, Figure 4.1) can easily produce eruption clouds extending to altitudes of 25 to 50 miles, based upon historical data (Bezymianny Volcano; Krakatoa) cited by MacDonald (1972, p. 133, 238, 303). In southern Nevada, multiple caldera collapse events have produced ash flow deposits in excess of 1,000 feet thick (near the caldera) which extend for distances in excess of 25 miles from the caldera margin. Such a deposit is shown without vertical exaggeration as the solid pattern in Figure 43.

Clearly, an area such as the proposed Yucca Mountain repository is a tiny feature by comparison. Within such a small portion of the ash flow environment -- which includes the eruption column, the collapsing ash flow itself, and the resulting deposit -- one may easily imagine that conditions are relatively uniform. Turbulent mixing of material will occur within the Plinian column. Collapse of the column produces the fluidized ash flow which disperses over great distances. Although fluidized high-density flows are not particularly well known for producing good particle-size sorting, any sorting which does occur will take place over the length of the flow. In southern Nevada, this dimension is well in excess of the preserved volcanic deposits -- some 25 miles. The repository site at slightly over a mile from north to south represents only a few percent of this distance.

Following deposition of the ash flow material, the hot debris cooled and welded in place. Again, compared with the total environment of an emplaced ash

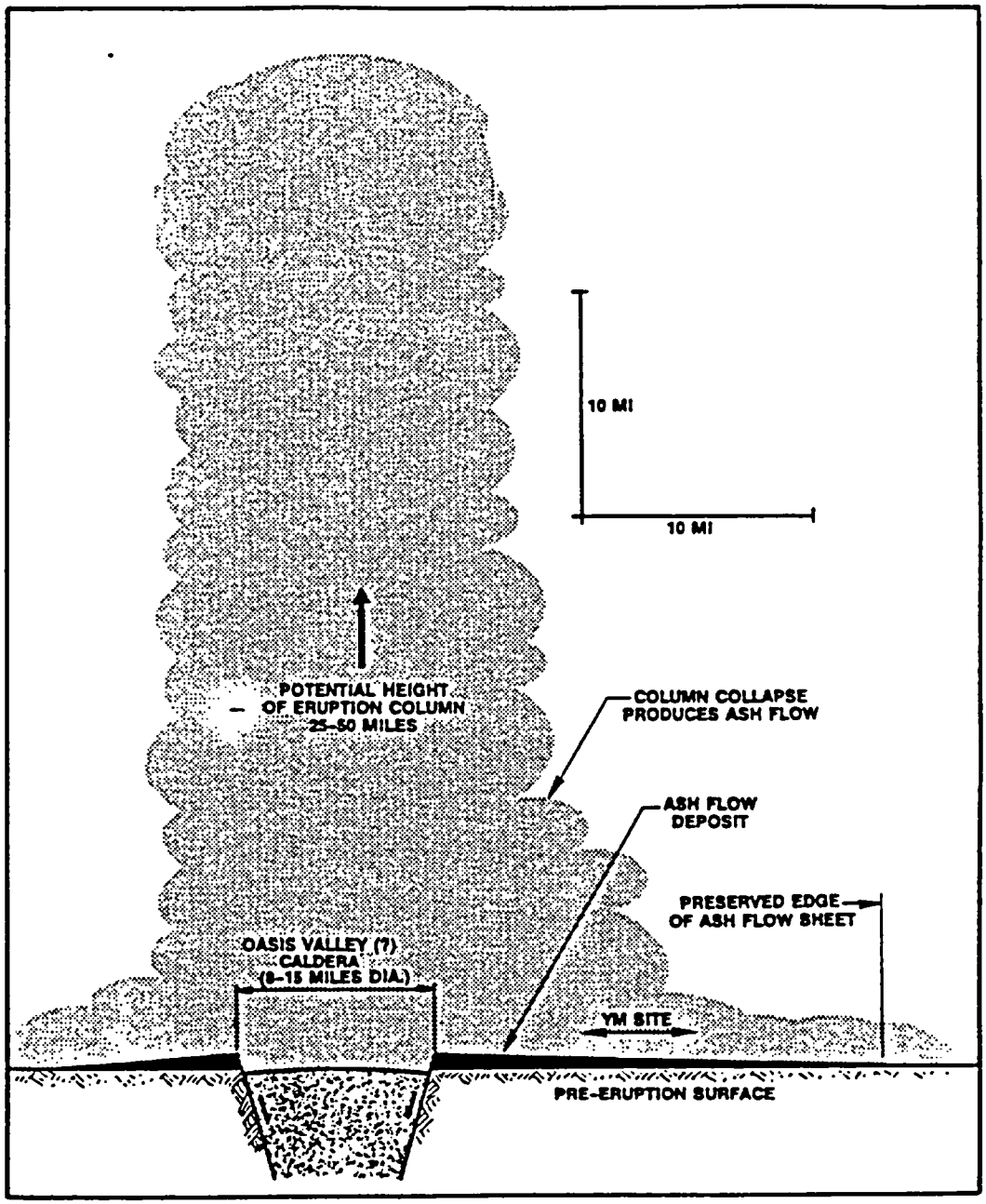

Figure 43. Schematic illustration of a major caldera-collapse event producing ash flows and a thick welded tuff unit. No vertical exaggeration. Adapted from numerous sources, principally MacDonald (1972).

flow sheet, the portion represented by the Yucca Mountain site is minuscule. Perhaps as no small surprise, the extent of vertical spatial correlation observed in this study, 300 to 1,200 feet, approximates the vertical dimensions of individual cooling units such as the Topopah Spring, the Tiva Canyon, and others.

The tuffs of Calico Hills represent a much less energetic and less extensive environment. Much of the Calico contains ashflow material. However, these flows are not welded, and a portion of the interval is represented by air fall and bedded (i.e., reworked) material. Thus Figure 43 is no longer an adequate illustration; the scale of events must be reduced by at least one to two orders of magnitude. Nevertheless, even smaller Vulcanian or Peléean eruptions can send eruption clouds to several tens of thousands of feet elevation. The existence of the tuffs of Calico Hills at Prow Pass and at the repository site is mute evidence that lateral transport of material from such eruptions can exceed 10 miles (Figure 5). This may be visualized by replacing the broad caldera source shown in Figure 43 by a more localized vent or vents at about the location of the caldera-margin fault nearest to Yucca Mountain, and by reducing the (cumulative) thickness of the resulting deposits by about one-third. The lateral distances remain roughly the same. Thus although the extent of spatial correlation identified at Yucca Mountain may appear significant by comparison with an engineered structure such as a repository, the scale must be viewed within the context of the massive natural system of which that correlation is a part.

REFERENCES

Barnes, R. L., 1988, Bounding the required sample size for geologic site characterization: Mathematical Geology, v. 20, p. 477-490. (NNA.891114.0345)

Borgman, L. E., 1988, New advances in methodology for statistical tests useful in geostatistical studies: Mathematical Geology, v. 20, p. 383-403. (NNA.891208.0049)

Carr, W. J., 1988, Volcano-tectonic setting of Yucca Mountain and Crater Flat, southwestern Nevada: U.S. Geol. Survey Bull. 1790, p. 35-49. (NN1.881128.0011)

Clark, I., 1979, Practical geostatistics, London: Elsevier Applied Science Publishers, 141 p. (NNA.890906.0194)

David, M., 1977, Geostatistical ore reserve estimation: Developments in Geomathematics 2, New York: Elsevier Scientific Publishing Co., 385 p. (NNA.891222.0026)

Davis, B. M., 1987, Uses and abuses of cross-validation in geostatistics: Mathematical Geology, v. 19, p. 241-248. (NNA.891114.0347)

DOE (U.S. Dept. of Energy), 1988, Site Characterization Plan, Yucca Mountain Site, Nevada Research and Development Area, Nevada: U. S. Dept. of Energy, Office of Civilian Radioactive Waste Management, Report DOE/RW-0199. (HQO.881201.0002)

Englund, E., and A. Sparks, 1988, Geo-EAS (geostatistical environmental assessment software) user's guide: U. S. EPA Report EPA600/4-88/033, U. S. Environmental Protection Agency, Environmental Monitoring Systems Laboratory, Las Vegas, Nevada. (NNA.891208.0050)

Isaaks, E. H., and R. M. Srivastava, 1988, Spatial continuity measures for probabilistic and deterministic geostatistics: Mathematical Geology, v. 20, p. 313-341. (NNA.891114.0348)

Isaaks, E. H., and Srivastava, R. M., 1989, [An introduction to] applied geostatistics: Oxford University Press, 578 p. (NNA.900420.0087)

Journel, A. G., 1983, Non-parametric estimation of spatial distributions: Mathematical Geology, v. 15, p. 445-468. (NNA.891114.0349)

Journel, A. G., and C. J. Huijbregts, 1978, Mining geostatistics, New York: Academic Press, 611 p. (NNA.890906.0246)

Journel, A. G., and F. Alabert, 1989, Non-gaussian data expansion in the earth sciences: Terra Nova, v. 1, p. 123-134. (NNA.891208.0051)

MacDonald, G. A., 1972, Volcanoes, Englewood Cliffs (NJ): Prentice-Hall, Inc., 510 p. (NNA.900727.0309)

Ortiz, T. S., R. L. Williams, F. B. Nimick, B. C. Whittet, and D. L. South , 1985, A three-dimensional model of reference thermal-mechanical and hydrological stratigraphy at Yucca Mountain, southern Nevada: Sandia Report SAND84-1076, Sandia National Laboratories, Albuquerque, New Mexico, 79 p. (NNA.890315.0013; HQS.880517.1691)

Scott, R. B., and J. Bonk, 1984, Preliminary geologic map of Yucca Mountain, Nye County, Nevada, with geologic sections: U.S. Geol. Survey Open-File Report 84-494. (HQS.880517.1443)

SEPDB, 1989, Yucca Mountain Project Site and Engineering Properties Data Base Product SEP0061, Sandia National Laboratories, Albuquerque, New Mexico.

Spengler, R. W., and M. P. Chornak, 1984, Stratigraphic and structural characteristics of volcanic rocks in core hole USW G-4, Yucca Mountain, Nye County, Nevada, with a section on Geophysical Logs by D. C. Muller and J. E. Kibler: U. S. Geol. Survey Open-File Report 84-789, 82 p. (NNA.870519.0105; HQS.880517.1489)

Yfantis, E. A., G. T. Flatman, and J. V. Behar, 1987, Efficiency of kriging estimation for square, triangular, and hexagonal grids: Mathematical Geology, v. 19, p. 183-205. (NNA.891114.0350)

APPENDIX A

DESCRIPTION OF DATA USED IN THIS REPORT

Collection and Laboratory Measurement, Surface Samples

This appendix contains a description of the outcrop sampling program and laboratory procedures used to determine the values of porosity and air permeability for surface samples reported in this document. Laboratory work was performed by Litton Core Lab, P. O. Box 152053, Irving, Texas 75015. A copy of the final laboratory report is included.

Location -- Forty-one samples were collected from two broad exposures of Calico Hills tuffs. One section, located immediately south of Prow Pass (main text, Figure 4), is the principal focus of this study because of interpreted similarities to the rocks underlying the repository site. The other section is located within the Calico Hills (main text, Figure 4); its similarity to the subsurface units of concern is somewhat less direct. Outcrop appearance of the two units is similar.

Basis for Sampling -- Because the focus of this portion of the study is on estimating spatial correlation in a lateral dimension, the sampling was restricted to as limited a stratigraphic interval as possible. The intent was to minimize effects of vertical variability. This was accomplished by maintaining approximately the same position in the section relative to some identifiable marker horizon. This effort was easily accomplished at the Calico Hills locality; the unit is well bedded and nearly flat-lying. The Prow Pass section is much more extensive and is marked by several covered intervals. Fortunately, the section is exposed on a moderately steep hillside that allows easy identification of the distinctive basal vitrophyre of the overlying Topopah Spring Member of the Paintbrush Tuff. Within limits, the sampling traverse maintained a nearly uniform distance below this obvious marker unit.

Sampling near the north end of the traverse is less well controlled, as the Topopah Spring Member has been removed by erosion between The Prow and Prow Pass proper.

Sampling Technique -- The sampling scheme attempted to obtain a large hand sample every 100 or 200 feet along the chosen traverse. Samples were collected from a locally representative outcrop using a chisel and small hand sledge. No strict definition of "representative" is possible. Efforts were made to avoid obviously weathered, stained, or otherwise altered zones that were not typical of the majority of rock near a given station. Distances were measured from an identifiable starting location with a "topofil" measured-string device or hand tape. Where an even hundred feet along the traverse occurred in a covered area or where no sample could be obtained for any of several reasons, the nearest suitable outcrop was selected. Sample identifications and the traverse distances are given in Table A-1.

Laboratory Techniques -- The samples thus obtained were analyzed for porosity and air permeability by Litton Core Lab (P. O. Box 152053, Irving, Texas 75015). Subsamples in the form of a right-circular cylinder were subcored from each suitable hand specimen. Of the 41 samples collected, three specimens proved inadequate for sample preparation (Table A-1).

Porosity was calculated from the bulk volume and grain volume of the sample using API (American Petroleum Institute) standard procedure RP40. Bulk volume was determined by mercury displacement and the grain volume by Boyle's Law gas pressure measurement. The permeability of the same sample to air was determined using a technique that incorporates Darcy's Law and measures the pressure drop in air flowing through the sample. Permeability measurements follow API standard procedure RP40. Porosity and air permeability data are given in Table A-1.

The air permeability and porosity data obtained for this study are believed to be measured with accuracy and precision typical of the petroleum industry. No representation is made regarding the quality assurance level of the data other than that associated with good scientific and engineering practice. Because of the preliminary nature of this study and the need to conduct the study at minimum cost and in a reasonable time frame, the intent was to obtain a suite of samples and rock properties measurements suitable for the analysis at hand, rather than to "characterize" the Yucca Mountain site. If the set of data is internally consistent -- as opposed to necessarily accurate in the absolute sense -- they are useful for purposes of applying geostatistical techniques. Determination of spatial correlation structure is based upon *differences between pairs of data,* not upon the specific values obtained. The use of industry standards in the analytical technique provides more than sufficient accuracy for the current purpose.

Table A-1. Porosity and Air Permeability, Tuffs of Calico Hills

Sample Number	Traverse North	Traverse East	Nevada State Plane Northing	Nevada State Plane Easting	Porosity (percent)	Air Perm. (md)
			Prow Pass Section			
CRPP-1-SNL	-20	0	783540	550696	24.9	1.200
CRPP-2-SNL	240	0	783795	550747	22.2	0.760
CRPP-3-SNL	445	0	783996	550787	25.4	0.340
CRPP-4-SNL	590	0	784138	550816	33.6	0.130
CRPP-5-SNL	800	0	784344	550857	33.4	0.130
CRPP-6-SNL	1010	0	784550	550898	26.7	0.240
CRPP-7-SNL	1200	0	784737	550935	36.5	0.280
CRPP-8-SNL	1300	0	784835	550955	32.6	0.110
CRPP-9-SNL	1400	0	784933	550975	--	--
CRPP-10-SNL	1570	0	785099	551008	38.3	0.400
CRPP-11-SNL	1970	0	785492	551086	38.9	0.600
CRPP-12-SNL	2170	0	785688	551126	38.3	0.890
CRPP-13-SNL	2440	0	785953	551179	36.9	0.140
CRPP-14-SNL	2600	0	786110	551210	36.1	0.250
CRPP-15-SNL	2790	0	786296	551247	35.1	0.810
CRPP-16-SNL	3010	0	786512	551290	35.1	1.100
CRPP-17-SNL	3230	0	786727	551333	35.1	0.450
CRPP-18-SNL	3380	0	786874	551363	40.9	1.100
CRPP-19-SNL	3500	0	786992	551386	35.5	0.820
CRPP-20-SNL	3650	0	787139	551416	36.1	0.170
CRPP-21-SNL	3800	0	787286	551445	37.6	1.800
CRPP-22-SNL	4000	0	787483	551485	36.5	0.490
CRPP-25-SNL	4150	0	787650	551500	35.1	1.500
CRPP-26-SNL	4150	100	787596	551584	--	--
CRPP-27-SNL	4150	225	787527	551689	33.2	0.500
CRPP-28-SNL	4150	330	787470	551777	30.4	0.260
CRPP-29-SNL	4150	390	787437	551827	29.9	0.210
CRPP-30-SNL	4150	505	787375	551923	23.2	0.690
CRPP-31-SNL	4150	600	787323	552003	27.4	0.710
CRPP-23-SNL	4200	0	787678	551524	--	--
CRPP-24-SNL	5430	0	788885	551765	24.2	30.000

Table A-1. Porosity and Air Permeability, Tuffs of Calico Hills (concluded)

Sample Number	Traverse North	Traverse East	Nevada State Plane Northing	Nevada State Plane Easting	Porosity (percent)	Air Perm. (md)
			Calico Hills Section			
CRCH-1-SNL	20000	0	775300	591800	33.1	0.750
CRCH-2-SNL	20000	-100	775300	591700	37.7	0.440
CRCH-3-SNL	20000	-205	775300	591595	23.2	0.440
CRCH-4-SNL	20000	-400	775300	591400	27.7	0.510
CRCH-5-SNL	20000	-500	775300	591300	23.5	0.880
CRCH-6-SNL	20000	-597	775300	591203	28.9	0.073
CRCH-7-SNL	20000	-800	775300	591000	30.9	1.200
CRCH-8-SNL	20000	-1000	775300	590800	33.1	0.190
CRCH-9-SNL	20000	-1105	775300	590695	34.0	0.860
CRCH-10-SNL	20000	-1185	775300	590615	24.8	0.330

Note: Coordinates in feet. Missing values (--) indicate no plug sample could be prepared. "Northing" of 20,000 feet is arbitrary.

Laboratory Procedures and Laboratory Report Provided by Litton Core Lab

The description of the procedures used to measure porosity and air permeability on the surface samples collected for this study and the laboratory report are provided as received from Litton Core Lab. The description of the procedures used reference API (American Petroleum Institute) procedure RP-40, entitled "Recommended Practice for Core-Analysis Procedure," which is dated August 1960.

DRAFT

Litton
Core Lab

May 8, 1987

Sandia National Laboratories
Division 6315
Sandia Base
Albuquerque, New Mexico 87185

Attention: C. A. Rautman

Subject: Permeability to Air and Porosity Measurements
Rock Samples
Sandia National Laboratories Work Order Number 23-8111
File Number: SCAL-308-87033

Gentlemen:

On March 25, 1987, the Special Core Analysis Department of Core Laboratories, Inc., at Irving, Texas, received the 41 subject rock samples. On April 3, 1987, Sandia National Laboratories work order number 23-8111 was received, and authorized the performance of Permeability to Air and Porosity Determinations on plug-sized samples to be obtained from the rock samples. The requested tests have now been completed and the results are presented herein in final form. A preliminary report concerning the progress of this study was issued on April 23, 1987. All rock sample remnants and plug samples obtained for use in this study are being returned to the Albuquerque, New Mexico facilities of Sandia National Laboratories under separate cover.

In preparation for testing, attempts were made to drill a 1-inch diameter, cylindrical plug sample from each of the 41 submitted rock samples using a diamond core drill with water as the bit coolant and lubricant. Unfortunately, no plug sample could be obtained from rock samples CRPP-7-SNL, CRPP-22-SNL, And CRPP-26-SNL due to sample fracturing during the drilling process. The core plugs were dried in a vacuum oven at 220°F, and allowed to cool in a moisture-free environment before permeability to air and Boyle's law porosity (using helium as the gaseous medium) determinations were performed on each.

A brief lithological description of each of the plug samples obtained for use in this study, along with identification as to sample number, is presented on Pages 1 and 2. Permeability to air and porosity data are presented in tabular form on Pages 3 and 4, and in graphic form on Page 5.

DRAFT

Litton
Core Lab

Sandia National Laboratories
File Number: SCAL-308-87033
Page Two

It has been a pleasure to be of service by performing this study on behalf of Sandia National Laboratories. Should there be any questions, or if we could be of any further assistance, please do not hesitate to contact us.

Very truly yours,

CORE LABORATORIES, INC.

Laura G. Kelsoe, Laboratory Supervisor
Special Core Analysis

LGK:DLM:jf

7 cc. - addressee

IDENTIFICATION AND LITHOLOGICAL DESCRIPTION OF SAMPLES

Sandia National Laboratories — Rock Samples

Rock Sample Identification	Plug Number	Lithological Description
CRPP-1-SNL	1	Tf; pk-brn, mod ind, lit frag, ash Mtrx, ves
CRPP-2-SNL	2	Tf; pk-brn, mod ind, lit frag, ash Mtrx, ves
CRPP-3-SNL	3	Tf; pk-brn, mod ind, lit frag, ash Mtrx, ves
CRPP-4-SNL	4	Tf; pk-tn, mod ind, lit frag, ash Mtrx, ves
CRPP-5-SNL	5	Tf; tn, mod ind, lit frag, ash Mtrx, ves
CRPP-6-SNL	6	Tf; tn, mod ind, lit-vit frag, ash Mtrx, ves
CRPP-7-SNL	7	Tf; tn-lt gn, mod ind, lit-vit frag, ash Mtrx, ves
CRPP-8-SNL	8	Tf; tn-lt gn, mod ind, lit frag, ash Mtrx, slily ves
CRPP-9-SNL		Plug-sized sample could not be obtained
CRPP-10-SNL	10	Tf; tn-lt gn, mod ind, lit frag, ash Mtrx, slily ves
CRPP-11-SNL	11	Tf; pk-tn, mod ind, lit frag, ash Mtrx, slily ves
CRPP-12-SNL	12	Tf; pk-tn, mod ind, lit frag, ash Mtrx, slily ves
CRPP-13-SNL	13	Tf; pk, mod ind, lit frag, ash Mtrx, ves
CRPP-14-SNL	14	Tf; pk, mod ind, lit frag, ash Mtrx, ves
CRPP-15-SNL	15	Tf; pk, mod ind, lit frag, ash Mtrx, ves
CRPP-16-SNL	16	Tf; pk, mod ind, lit frag, ash Mtrx, ves
CRPP-17-SNL	17	Tf; pk, mod ind, lit frag, ash Mtrx, ves
CRPP-18-SNL	18	Tf; pk, mod ind, lit frag, ash Mtrx, ves
CRPP-19-SNL	19	Tf; pk, mod ind, lit frag, ash Mtrx, ves
CRPP-20-SNL	20	Tf; pk, mod ind, lit frag, ash Mtrx, ves
CRPP-21-SNL	21	Tf; pk, mod ind, lit frag, ash Mtrx, ves
CRPP-22-SNL	22	Tf; pk-tn, mod ind, lit frag, ash Mtrx, ves
CRPP-23-SNL		Plug-sized sample could not be obtained
CRPP-24-SNL	24	Tf; tn-lt gn, mod ind, lit-vit frag, ash Mtrx, ves, frac
CRPP-25-SNL	25	Tf; tn, mod ind, lit-vit frag, ash Mtrx, ves
CRPP-26-SNL		Plug-sized sample could not be obtained
CRPP-27-SNL	27	Tf; tn-lt gn, mod ind, lit frag, ash Mtrx, ves
CRPP-28-SNL	28	Tf; tn-lt gn, mod ind, lit frag, ash Mtrx, ves
CRPP-29-SNL	29	Tf; tn, mod ind, lit-vit frag, ash Mtrx, ves
CRPP-30-SNL	30	Tf; tn, mod ind, lit-vit frag, ash Mtrx, ves
CRPP-31-SNL	31	Tf; tn, mod ind, lit frag, ash Mtrx, ves

IDENTIFICATION AND LITHOLOGICAL DESCRIPTION OF SAMPLES

Sandia National Laboratories — Rock Samples

Rock Sample Identification	Plug Number	Lithological Description
CRCH-1-SNL	32	Tf; gn, mod ind, lit frag, ash Mtrx, ves
CRCH-2-SNL	33	Tf; pk-gn, mod ind, lit frag, ash Mtrx, v ves
CRCH-3-SNL	34	Tf; pk-gn, mod ind, lit frag, ash Mtrx, ves
CRCH-4-SNL	35	Tf; gn-pk, mod ind, lit frag, ash Mtrx, ves
CRCH-5-SNL	36	Tf; gn, mod ind, lit frag, ash Mtrx, ves, frac
CRCH-6-SNL	37	Tf; gn, mod ind, lit frag, ash Mtrx, ves
CRCH-7-SNL	38	Tf; rd, mod ind, lit frag, ash Mtrx, v ves
CRCH-8-SNL	39	Tf; tn, mod ind, ht-vit frag, ash Mtrx, ves
CRCH-9-SNL	40	Tf; gn, mod ind, lit frag, ash Mtrx, ves
CRCH-10-SNL	41	Tf; gn, mod ind, lit frag, ash Mtrx, ves

PERMEABILITY TO AIR AND POROSITY

Sandia National Laboratories — Rock Samples

Rock Sample Identification	Plug Number	Permeability to Air, millidarcys	Porosity, percent
CRPP-1-SNL	1	1.2	24.9
CRPP-2-SNL	2	0.76	22.2
CRPP-3-SNL	3	0.34	25.4
CRPP-4-SNL	4	0.13	33.6
CRPP-5-SNL	5	0.13	33.4
CRPP-6-SNL	6	0.24	26.7
CRPP-7-SNL	7	0.28	36.5
CRPP-8-SNL	8	0.11	32.6
CRPP-9-SNL		*	*
CRPP-10-SNL	10	0.40	38.3
CRPP-11-SNL	11	0.60	38.9
CRPP-12-SNL	12	0.89	38.3
CRPP-13-SNL	13	0.14	36.9
CRPP-14-SNL	14	0.25	36.1
CRPP-15-SNL	15	0.81	35.1
CRPP-16-SNL	16	1.1	35.1
CRPP-17-SNL	17	0.45	35.1
CRPP-18-SNL	18	1.1	40.9
CRPP-19-SNL	19	0.82	35.5
CRPP-20-SNL	20	0.17	36.1
CRPP-21-SNL	21	1.8	37.6
CRPP-22-SNL	22	0.49	36.5
CRPP-23-SNL		*	*
CRPP-24-SNL	24	30**	24.2
CRPP-25-SNL	25	1.5	35.1
CRPP-26-SNL		*	*
CRPP-27-SNL	27	0.50	33.2
CRPP-28-SNL	28	0.26	30.4
CRPP-29-SNL	29	0.21	29.9
CRPP-30-SNL	30	0.69	23.2
CRPP-31-SNL	31	0.71	27.4

*Plug-size sample could not be obtained
**Plug is fractured vertically

PERMEABILITY TO AIR AND POROSITY

Sandia National Laboratories — Rock Samples

Rock Sample Identification	Plug Number	Permeability to Air, millidarcys	Porosity, percent
CRCH-1-SNL	32	0.75	33.1
CRCH-2-SNL	33	0.44	37.7
CRCH-3-SNL	34	0.44	23.2
CRCH-4-SNL	35	0.51	27.7
CRCH-5-SNL	36	0.88	23.5
CRCH-6-SNL	37	0.073	28.9
CRCH-7-SNL	38	1.2	30.9
CRCH-8-SNL	39	0.19	33.1
CRCH-9-SNL	40	0.86	34.0
CRCH-10-SNL	41	0.33	24.8

PERMEABILITY TO AIR VERSUS POROSITY

Sandia National Laboratories — Rock Samples

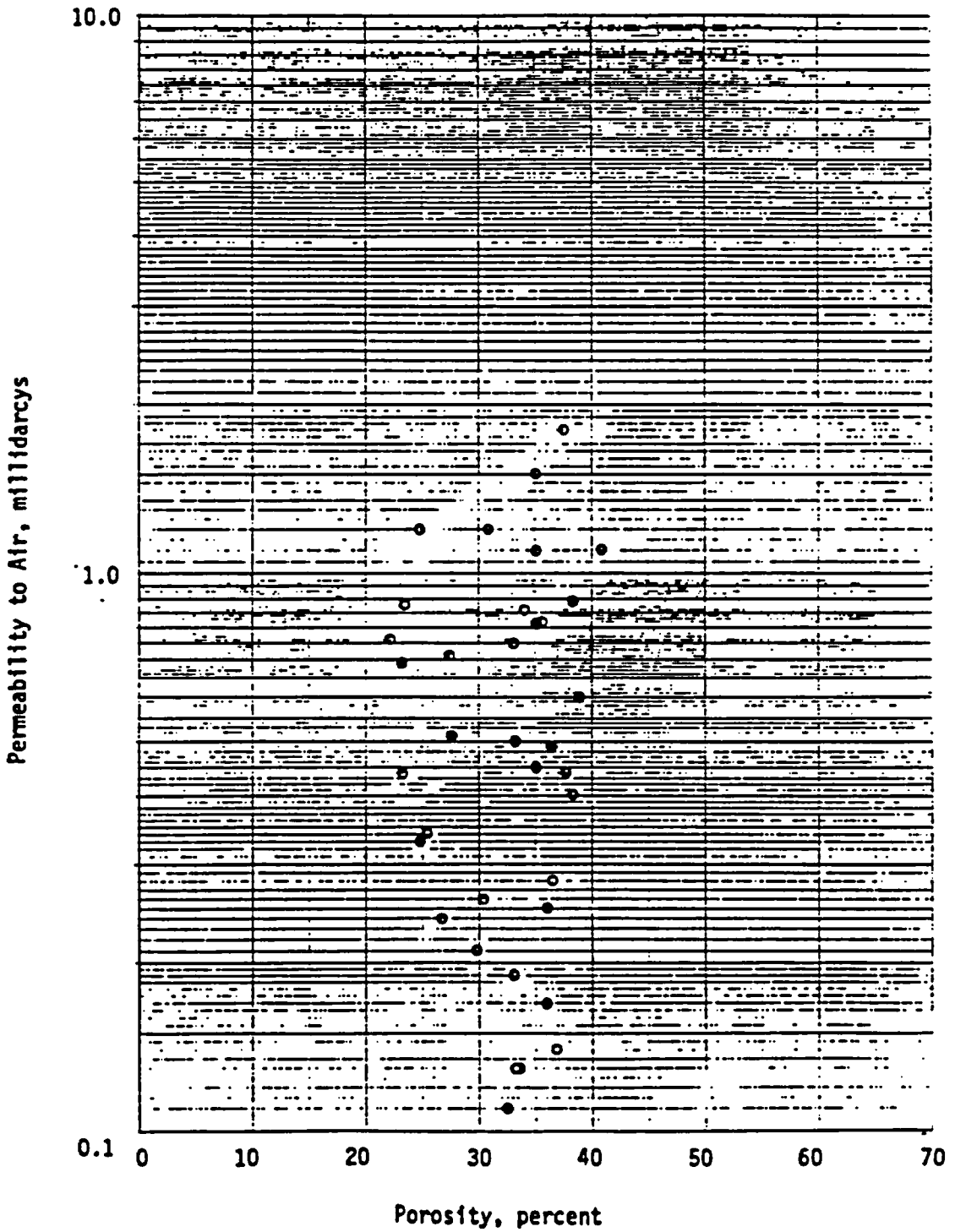

DRAFT

Litton
Core Lab

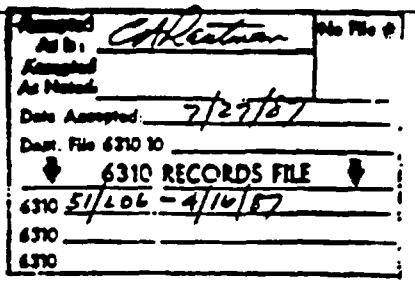

July 20, 1987

Sandia National Laboratories
P.O. Box 5800
Albuquerque, New Mexico 87185

Attention: C. A. Rautman

Subject: Test Procedures
File Number:SCAL-308-87033

Gentlemen:

Enclosed please find a description of test methods used in the performance of permeability to air and porosity measurements on core samples from the subject project.

If you should have any questions regarding these procedures, please do not hesitate to contact us.

Very truly yours,

Core Laboratories, Inc.

Laura G. Kelsoe
Laboratory Supervisor
Special Core Analysis Department

Boyle's Law Porosity Measurement

Porosity may be measured using a number of different techniques, however the following description applies to the subject project.

Two properties are measured for determination of porosity. They are bulk volume and grain volume. A detailed description of each determination follows.

Bulk Volume-Mercury pump method

The mercury pump used by Core Laboratories, Inc. is a volumetric pump in which displacement is accomplished by a screw-actuated plunger which operates through a packing gland into a cylinder. The plunger and a micrometer scale attached to its actuating screw are precisely machined, allowing the displacement of the plunger to be read very accurately, the micrometer scale being graduated in units of 0.01 cubic centimeter. A linear scale past which the plunger moves is graduated in cubic centimeters. The sample chamber is closed by a lucite cap which has a machined capillary and two scribe marks for observing mercury level. Merury is used as the liquid medium because it has a high surface tension and will not, in most cases, penetrate or be absorbed into the pores of reservoir samples under the mercury.

To measure the bulk volume, the level of mercury is lowered by retracting the plunger from the cylinder until a volume of mercury has been removed from the chamber that is approximately 10 cc's greater than the estimated bulk volume of the sample. The sample is then placed in the chamber and the plunger displaced to the left until mercury is observed in the capillary (machined in the lucite cap) and aligned to the two scribe marks. The linear scale and inside micrometer scale are read as one reading. This is the observed bulk volume of the sample in cubic centimeters

Grain Volume

The principle of gas expansion described by Boyle's Law where P1V1=P2V2 if temperature is constant, is the theory behind the technique used by Core Laboratories, Inc.. A known (reference) volume of gas at a known preset pressure is expanded isothermally into an unknown volume. The resultant measured equilibrium pressure after expansion will be dependent upon the unknown volume which can be calculated using Boyle's Law.

The Core Lab porosimeter consists of a matrix cup,(which accomodates the sample and stainless steel dead volume cylinders), a pressure transducer with a digital panel voltmeter readout, and various small volume and large volume reference cells.

The four stainless steel right cylinders have been exactly calibrated and are used to determine dead volume of the system and to calibrate the porosimeter. The dead volume is first determined with all the stainless steel plugs in the matrix cup. Then one or more of them is left out and a void space is determined exactly as if a sample were present. A ratio of observed to measured volume should be within the limits of 0.999-1.001.

The following equations are used to obtain the porosity value:

Bulk Volume-Grain Volume = Pore Volume

Porosity= Pore Volume / Bulk Volume

Core Laboratories follows the API RP40 standard procedure for porosity determination.

PERMEABILITY TO AIR

The Core Laboratories micropermeameter can be used to measure permeabilities to air from as low as 0.01 millidarcies to more than 10 darcies. The linear form of Darcy's Law is used in the determination of permeability on a core plug sample.

$$k_G = \frac{C\, Q_g\, L}{A}$$

where : k_G= Gas permeability (millidarcies)

Q_g= Volume flow rate of air at barometric pressure and room temperature

and $C = \frac{(1000)(2)(\mu_G)(P_b)}{(p1 + p2)(P)}$

(μ_G = Dry air viscosity, = 0.0183 centipoise at 72 F)

Two parameters relating to the test sample are measured; these are: the pressure drop across the core sample and the flow rate through the sample. Dry air flows through the core sample and orifice (downstream of the sample) in proportion to the applied differential air pressure. The differential pressure developed across the calibrated orifice is used to determine the air volume flow rate. The pressure drop across the sample is indicated on the instrument by the "C" value reading of the mercury manometer, the middle (upstream) water manometer, or the extended "C" value pressure gauge used for low permeability tests. "C" is inversely proportional to the pressure drop across the core. The pressure drop is the absolute pressure of the "upstream" or high pressure side of the sample minus the absolute pressure of the "downstream" or low pressure side using atmospheres as the unit of measure.

Flow rate through the sample is measured on the low pressure side by reading the water manometer height obtained in conjunction with a calibrated orifice, but is corrected back to the flow at mean pressure in the sample automatically in the value of "C". "C" also includes a correction for the mean pressure in the sample, since the volume of air flowing through the high pressure side of the sample is less than the volume of air flowing through the low pressure side due to the expansion of the air at decreased pressure. A factor of 1000 is used in the permeability equation so that the reported units are millidarcy's.

Core Laboratories follows the standards for permeability measurement given in API RP40.

Data Collection and Laboratory Measurement, Drill Hole Data

Data for the (stratigraphically) vertical-correlation portion of this study were obtained from the Yucca Mountain Project Site and Engineering Properties Data Base (SEPDB, 1989), Product SEP0061, which contains values for porosity, hydraulic conductivity, and dry bulk density. These values have been obtained by various investigators at various times and for various purposes. Accordingly, all measurements may not be exactly comparable. However, the data are believed useful for a "first look" at spatial correlation. A rigorous evaluation of the laboratory procedures used to obtain these measurements, as well as any discussion of their accuracy and precision could be conducted by tracing the individual values to their original source via the documentation log maintained by the SEPDB for Produce SEP0061.

The Site and Engineering Properties Data Base contains data collected throughout the entire drilled interval without regard for stratigraphic unit. Rock properties corresponding to samples of tuffs of Calico Hills were extracted from this larger data set using the depth intervals corresponding to the three-dimensional thermal/mechanical model of Ortiz et al. (1985, Appendix B).

Table A-2. Values of Porosity, Dry Bulk Density, and Saturated Hydraulic Conductivity from SEPDB Product SEP0061

Depth (ft)	Porosity (%)	Bulk Density (Mg/m^3)	Hydraulic Conductivity (m/day)
Drill Hole UE-25 a#1	N: 566349.9	E: 764900.2	elev: 3934.4
58.000	6.000	2.330	—
102.000	7.300	2.310	—
153.000	6.140	2.330	—
187.000	22.900	1.870	—
202.000	30.100	1.690	—
212.000	52.700	1.140	—
234.000	52.900	1.140	—

Table A-2. Values of Porosity, Density and Conductivity (continued)

Depth (ft)	Porosity (%)	Density (Mg/m^3)	Bulk Conductivity (m/day)	Hydraulic
263.000	51.700	1.160	—	
273.000	27.400	1.580	—	
328.000	21.900	2.010	—	
360.000	13.300	2.210	—	
421.000	15.000	2.130	—	
471.000	18.600	2.020	—	
524.000	17.600	2.040	—	
569.000	17.700	2.090	—	
623.000	18.400	2.100	—	
660.000	7.500	2.320	—	
733.000	11.300	2.250	—	
772.000	13.300	2.230	—	
816.000	9.800	2.310	—	
866.000	8.650	2.350	—	
921.000	10.000	2.310	—	
969.000	—	2.310	—	
1010.000	11.800	2.230	—	
1040.000	11.200	2.250	—	
1112.000	8.700	2.310	—	
1183.000	8.500	2.360	—	
1249.000	8.030	2.330	—	
1266.000	12.700	2.160	—	
1304.000	6.280	2.210	—	
1324.000	30.300	1.620	—	
1338.000	27.700	1.530	—	
1349.000	24.400	1.760	—	
1361.000	23.400	1.770	—	
1411.000	30.100	1.630	—	
1464.000	28.100	1.690	—	
1516.000	32.100	1.590	—	
1568.000	29.300	1.680	—	
1638.000	34.100	1.530	—	
1686.000	30.700	1.620	—	
1741.000	33.800	1.560	—	
1791.000	20.400	1.990	—	
1833.000	20.700	1.930	—	
1842.000	33.100	1.580	—	
1888.000	24.700	1.960	—	
1942.000	20.300	2.070	—	
1988.000	13.300	2.260	—	
2032.000	22.300	1.970	—	
2078.000	20.000	2.010	—	
2108.000	21.900	1.860	—	
2148.000	22.300	—	—	
2149.000	—	1.720	—	
2159.000	9.680	2.140	—	
2201.000	15.400	1.980	—	
2247.000	23.000	1.810	—	
2300.000	18.400	1.970	—	

Table A-2. Values of Porosity, Density and Conductivity (continued)

Depth (ft)	Porosity (%)	Density (Mg/m^3)	Bulk Conductivity (m/day)	Hydraulic
2331.000	15.900	2.030	—	
2377.000	23.500	1.990	—	
2440.000	17.500	2.140	—	
2495.000	17.400	2.140	—	
Drill Hole UE-25 b#1	N: 566416.4	E: 765243.4	elev: 3939.0	
740.747	11.700	2.250	1.215e-06	
1573.063	26.650	1.750	1.035e-04	
2053.876	24.500	1.730	4.200e-05	
2230.119	11.850	2.090	1.265e-06	
2470.361	23.150	2.010	5.800e-04	
2589.170	21.450	2.060	6.950e-05	
2671.876	22.200	2.040	5.000e-05	
2768.367	22.900	2.020	5.000e-06	
3032.240	19.400	2.110	3.050e-05	
3113.962	18.550	2.140	1.900e-05	
3746.075	14.800	2.240	3.100e-04	
3843.222	12.400	2.320	2.250e-04	
3944.308	10.850	2.420	7.850e-05	
Drill Hole USW G-1	N: 561000.5	E: 770500.2	elev: 4348.6	
1223.700	8.400	2.305	—	
1232.200	6.540	2.357	—	
Drill Hole USW GU-3	N: 558501.3	E: 752690.1	elev: 4856.6	
54.200	9.000	2.260	—	
96.300	11.700	2.200	—	
158.800	5.800	2.320	—	
207.500	5.100	2.330	—	
257.000	7.600	2.310	—	
305.700	7.900	2.300	—	
370.900	38.800	1.410	—	
435.200	17.300	2.120	—	
461.100	18.200	2.090	—	
552.300	14.200	2.140	—	
576.000	17.300	2.060	—	
610.300	14.300	2.130	—	
660.300	17.200	2.130	—	
713.800	9.000	2.300	—	
765.000	13.400	2.170	—	
825.600	6.800	2.350	—	
884.100	10.200	2.340	—	
925.000	11.200	2.250	—	
957.700	10.400	2.280	—	
1055.800	9.800	2.340	—	
1108.900	8.300	2.350	—	

Table A-2. Values of Porosity, Density and Conductivity (continued)

Depth (ft)	Porosity (%)	Density (Mg/m^3)	Bulk Conductivity (m/day)	Hydraulic
1165.900	8.500	2.350	—	
1213.200	1.400	2.340	—	
1261.800	3.100	2.320	—	
1310.900	28.700	1.650	—	
1477.200	36.900	1.410	—	
1501.800	34.300	1.470	—	
1566.000	43.600	1.300	—	
1637.700	35.700	1.650	—	
1666.700	31.600	1.760	—	
1706.600	26.600	1.890	—	
1779.600	39.700	1.450	—	
1813.500	36.100	1.530	—	
1866.900	29.100	1.660	—	
1912.700	30.500	1.610	—	
1958.400	34.300	1.550	—	
2008.400	30.000	1.650	—	
2075.000	29.900	1.810	—	
2110.000	13.400	2.230	—	
2167.500	17.700	2.120	—	
2204.900	8.500	2.340	—	
2256.800	8.400	2.350	—	
2315.000	8.400	2.360	—	
2356.700	7.000	2.400	—	
2407.200	7.100	2.380	—	
2468.500	5.800	2.450	—	
2521.500	10.100	2.290	—	
2562.400	26.900	1.720	—	
Drill Hole USW G-3	N: 558483.1	E: 752779.8	elev: 4856.5	
2617.500	21.700	1.920	—	
2660.500	31.100	1.660	—	
2730.900	30.700	1.790	—	
2771.700	27.700	1.870	—	
2817.700	25.800	1.910	—	
2868.200	24.300	1.960	—	
2913.600	18.000	2.130	—	
2986.100	16.700	2.190	—	
3004.100	14.800	2.230	—	
3062.000	13.900	2.250	—	
3115.400	12.800	2.230	—	
3159.600	15.900	2.140	—	
3235.000	6.000	2.410	—	
3259.300	1.800	2.280	—	
3310.700	24.400	1.910	—	
3360.300	22.700	1.950	—	
3411.200	22.300	1.950	—	
3463.900	21.800	1.940	—	
3511.200	20.600	1.980	—	

Table A-2. Values of Porosity, Density and Conductivity (continued)

Depth	Porosity (ft)	Density (%)	Bulk Conductivity (Mg/m^3)	Hydraulic (m/day)
	3560.200	20.500	2.020	—
	3611.300	16.200	2.120	—
	3659.300	16.600	2.100	—
	3709.900	14.400	2.120	—
	3822.700	10.900	2.170	—
	3861.200	17.200	2.080	—
	3912.300	19.500	2.020	—
	3960.500	14.400	2.030	—
	4008.900	21.400	1.930	—
	4058.700	23.300	1.940	—
	4110.600	17.000	2.030	—
	4159.400	16.900	2.040	—
	4209.500	15.600	2.100	—
	4261.000	23.500	1.900	—
	4311.800	18.000	2.020	—
	4361.000	11.600	2.130	—
	4409.900	15.000	1.990	—
	4461.100	9.200	2.200	—
	4510.80-	14.700	2.180	—
	4567.800	10.600	2.200	—
	4609.600	13.000	2.130	—
	4659.900	16.100	2.110	—
	4707.900	15.300	2.190	—
	4755.900	17.900	2.100	—
	4818.600	19.300	2.050	—
	4860.800	17.500	2.060	—
	4910.700	14.600	2.100	—
	4977.900	13.800	2.090	—
	5009.800	12.600	2.220	—
Drill Hole USW G-4		N: 563081.6	E: 765807.1	elev: 4166.9
	59.000	5.500	2.370	—
	90.800	8.000	2.290	—
	169.600	51.900	1.160	—
	280.400	13.000	2.230	—
	332.300	15.700	2.160	—
	390.300	12.900	2.210	—
	548.400	20.300	2.000	—
	602.600	16.800	2.110	—
	668.600	11.900	2.230	—
	742.500	7.400	2.310	—
	821.200	11.500	2.240	—
	875.500	9.900	2.330	—
	937.600	10.800	2.280	—
	1064.500	13.800	2.190	—
	1239.200	9.400	2.340	—
	1361.500	16.900	1.970	—
	1362.100	12.310	1.980	—

Table A-2. Values of Porosity, Density and Conductivity (continued)

Depth (ft)	Porosity (%)	Density (Mg/m^3)	Bulk Conductivity (m/day)	Hydraulic
1431.500	36.600	1.470	—	
1468.200	32.100	1.540	—	
1511.400	31.800	1.590	—	
1570.300	35.800	1.480	—	
1627.200	32.600	1.570	—	
1678.400	34.300	1.560	—	
1784.300	29.700	1.660	—	
1822.800	34.600	1.710	—	
1870.700	29.800	1.830	—	
1915.800	19.400	2.060	—	
1976.000	32.500	1.640	—	
2032.400	35.000	1.610	—	
2072.900	20.600	1.890	—	
2131.200	24.300	1.820	—	
2181.800	29.200	1.700	—	
2228.500	28.600	1.710	—	
2298.000	24.800	1.930	—	
2336.800	24.400	1.940	—	
2381.600	20.800	2.060	—	
2436.100	25.700	1.950	—	
2478.000	25.000	1.960	—	
2523.700	21.900	2.010	—	
2577.700	18.200	2.150	—	
2637.500	11.300	2.310	—	
2694.600	28.000	1.770	—	
2719.500	24.700	1.770	—	
2826.200	27.600	1.760	—	
2856.800	19.600	2.080	—	
2938.600	18.900	2.100	—	
2979.800	15.200	2.200	—	
Drill Hole USW H-1	N: 62388.0	E: 770254.3	elev: 4274.4	
109.947	43.600	1.300	—	
111.916	43.000	1.400	—	
252.386	48.000	1.300	—	
420.096	21.000	2.000	—	
423.378	21.500	2.000	—	
423.706	21.450	—	—	
442.742	20.550	—	—	
443.070	20.500	2.000	—	
448.321	18.150	—	—	
449.634	18.000	2.100	—	
459.480	16.000	2.200	—	
462.762	17.000	2.200	—	
466.044	16.000	2.200	—	
467.685	16.150	—	—	
469.326	14.000	2.200	—	
470.311	13.950	—	—	

Table A-2. Values of Porosity, Density and Conductivity (continued)

Depth	Porosity (ft)	Density (%)	Bulk Conductivity (Mg/m^3)	Hydraulic (m/day)
	718.758	16.000	2.100	—
	719.414	16.100	—	—
	725.322	22.500	1.800	—
	726.635	23.050	—	—
	728.604	15.500	2.100	—
	728.932	15.950	—	—
	740.419	15.100	—	—
	741.732	16.000	2.000	—
	1279.980	15.500	2.200	—
	1281.293	15.750	—	—
	1281.949	14.750	—	—
	1283.262	14.500	2.200	—
	1305.908	12.900	—	—
	1306.236	12.500	2.200	—
	1308.533	10.600	—	—
	1309.518	10.000	2.300	—
	1329.210	12.000	2.300	—
	1330.523	17.700	—	—
	1331.836	9.500	—	—
	1332.492	9.450	2.300	—
	1741.757	46.100	—	—
	1742.742	45.000	1.300	—
	1748.650	40.900	—	—
	1749.306	40.500	1.400	—
	2100.480	30.500	1.700	8.500e-05
	2103.762	30.667	1.700	6.000e-05
	2326.938	30.667	1.600	1.375e-04
	2330.220	36.000	1.600	6.000e-04
	2340.066	19.500	2.100	7.000e-05
	2507.448	28.000	1.900	6.500e-04
	2533.704	25.000	2.000	4.000e-04
	2592.780	19.000	2.100	4.000e-05
	2596.062	19.500	2.100	7.000e-05
	2599.344	21.500	2.100	5.000e-05
	2724.060	26.000	1.800	3.500e-05
	2733.906	27.000	1.800	1.000e-04
	2756.880	26.000	1.800	1.400e-05
	2770.008	22.500	2.000	3.000e-06
	3383.742	23.000	2.000	3.500e-04
	3387.024	24.000	2.000	2.500e-04
	3409.998	18.333	2.150	1.233e-04
	3413.280	21.500	2.100	3.000e-05
	3941.682	7.150	2.500	8.000e-07
	5149.458	16.500	2.200	4.000e-05
	5973.240	9.400	2.400	3.500e-04
Drill Hole J-13		N: 579651.0	E: 749209.0	elev: 3318.0
	530.699	8.100	2.310	—

Table A-2. Values of Porosity, Density and Conductivity (continued)

Depth (ft)	Porosity (%)	Density (Mg/m^3)	Bulk Conductivity (m/day)	Hydraulic
539.233	2.800	—	3.000e-07	
666.574	54.400	1.050	—	
669.200	31.900	1.760	—	
675.107	5.200	—	4.000e-03	
680.359	3.700	—	2.000e-06	
792.603	16.700	2.080	—	
801.136	2.700	—	3.000e-06	
873.012	16.200	2.130	—	
915.350	11.000	2.310	—	
1020.374	13.100	2.280	—	
1094.219	27.900	1.890	—	
1100.455	8.700	—	2.000e-04	
1184.146	16.000	2.710	—	
1193.335	6.800	—	8.000e-06	
1283.918	12.300	2.310	—	
1334.461	3.700	2.310	—	
1342.338	5.400	—	8.000e-07	
1407.978	11.600	2.120	—	
1416.511	3.300	—	3.000e-07	
1446.049	32.700	1.600	—	
1509.392	29.900	1.730	—	
2002.020	30.200	1.740	—	
2028.276	27.100	1.920	—	
2128.705	27.600	1.890	—	
2276.723	21.400	2.070	—	
2377.809	27.200	1.950	—	
2675.815	20.300	2.090	—	
2832.038	16.500	2.200	—	
2989.902	26.000	1.930	—	
3488.110	20.300	2.120	—	

APPENDIX B

Reference Information Base Site & Engineering Properties Data

This report contains no data from the Reference Information Base.

This report contains no candidate information for the Reference Information Base.

The data contained in Table A-1 of this report are candidate information for the Yucca Mountain Site and Engineering Properties Data Base. This information consists of values of porosity and air permeability from hand specimens of Calico Hills tuffs.